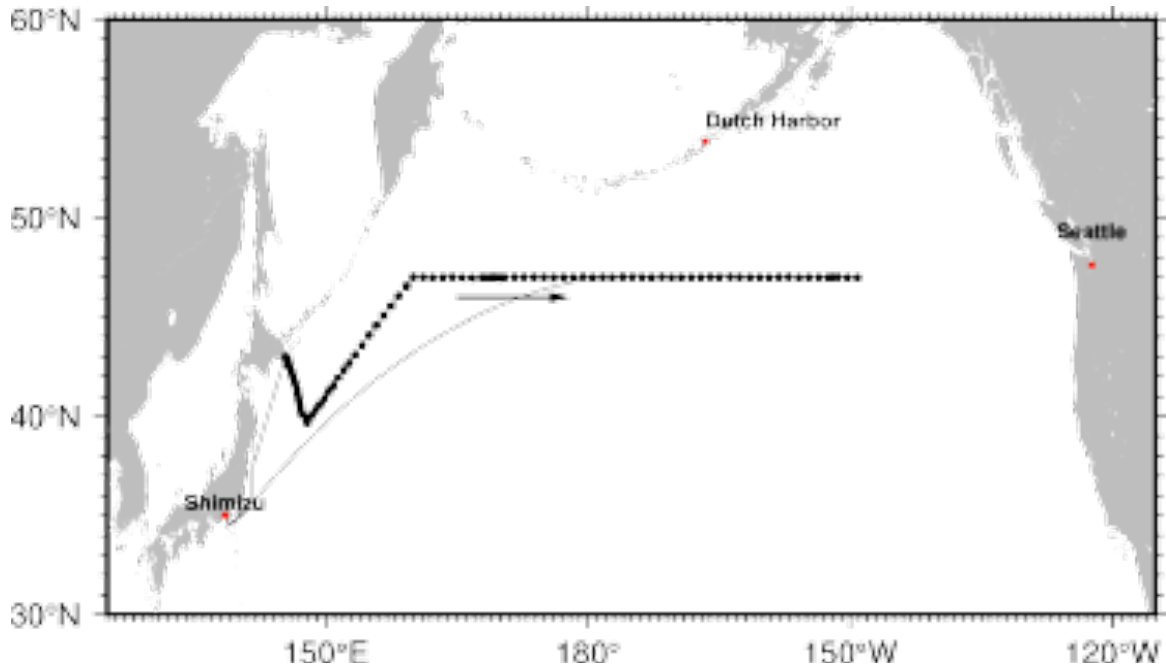


# CRUISE REPORT: P01

(Updated JAN 2022)



## Highlights

### Cruise Summary Information

Section Designation	<b>P01 (MR21-04)</b>	
Expedition designation (ExpoCodes)	<b>49NZ20210713</b>	
Chief Scientists	<b>Shinya Kouketsu</b>	
Dates	2021 JUL 13 – 2021 AUG 26	
Ship	R/V <i>Mirai</i>	
Ports of call		
Geographic Boundaries	145.25.3 E	47.42.02 N 149.8.54 W 39.42.02 N
Stations	62	
Floats and drifters deployed	2 Core Argo, 2 Deep Argo floats deployed 2 drifters deployed	
Moorings deployed or recovered		

### Contact Information:

Shinya Kouketsu (JAMSTEC)  
skoukestu[at]jamstec.go.jp

R/V *Mirai* Cruise Report  
MR21-04

GO-SHIP Observation

– decadal/bi-decadal changes in the North Pacific Ocean –

North Pacific/P1

Jul. 13, 2021 - Aug. 26, 2021

Japan Agency for Marine-Earth Science and Technology  
(JAMSTEC)



## Contents

1. Cruise Information.....	5
1.1 Basic information.....	5
2. Science Party .....	6
2.1 Participants for MR21-04 .....	6
2.2 Principal investigators.....	7
3. Underway Measurements .....	8
3.1 Navigation.....	8
3.2 Swath Bathymetry.....	9
3.3 Surface Meteorological Observation .....	10
3.4 Thermo-Salinograph and Related Properties .....	19
3.5. Shipboard ADCP.....	19
3.6 Ceilometer observation .....	21
3.7 Optical Disdrometer.....	23
3.8 Micro Rain Radar.....	25
3.9 C-band weather radar.....	26
3.10 GNSS precipitable water.....	27
3.11 Lidar.....	28
3.12 Microwave Radiometer.....	28
3.13 Satellite image acquisition .....	29
3.14 Aerosol optical characteristics measured by Shipborne Sky radiometer.....	30
3.15 Atmospheric CO <sub>2</sub> and CH <sub>4</sub> .....	31
3.16 Atmospheric and surface seawater pCO <sub>2</sub> .....	31
3.17 Sea Surface Gravity .....	33
3.18 Sea Surface Magnetic Field .....	33
4. Hydrographic Measurement .....	35
4.1 CTDO2 .....	35
4.2 Bottle Salinity .....	35
4.3 Density and Refractive Index.....	46
4.4 Lowered Acoustic Doppler Current Profiler.....	50
4.5 Microstructure in Temperature and Conductivity .....	50
4.6 Underway-CTD (UCTD).....	52
4.7 Vertical Microstructure Profiler (VMP).....	54
4.8 Oxygen.....	55
4.9 Nutrients .....	60
4.10 CFCs and SF <sub>6</sub> .....	60
4.11 Carbon properties.....	90
4.12 Chlorophyll <i>a</i> .....	94
4.13 Carbon isotopes.....	98

4.14 Dissolved organic carbon (DOC) and Total Dissolved Nitrogen (TDN) .....	98
4.15 Fluorescent dissolved organic matter (FDOM).....	99
4.16 Absorption coefficients of Chromophoric Dissolved Organic Matter (CDOM).....	101
4.17 Iodine isotopes .....	105
4.18 Spatial patterns of prokaryotic abundance, activity and community composition.....	108
4.19. NORPAC/Ring nets/VMPS/Surf. Water sampling.....	109
4.20 Radiocesium .....	113
4.21 XCTD .....	113
4.22 In situ calibration of the Compact-TDs.....	115
5. Float, Drifter and Mooring.....	118
5.1 Core/Deep Argo Floats .....	118
5.2 Deep Argo float.....	121
5.3 Subsurface Drifter.....	122
6. Notice on Using .....	122

# 1. Cruise Information

## 1.1 Basic information

Cruise ID	MR21-04
Name of vessel	R/V <i>Mirai</i>
Title of cruise	GO-SHIP Observation –decadal/bi-decadal changes in the North Pacific Ocean –
GO-SHIP section designation	P01
Chief Scientist	Shinya Kouketsu
Cruise date	13 <sup>th</sup> July, 2021 – 26 <sup>th</sup> August, 2021
Research area	North Pacific
Research map	

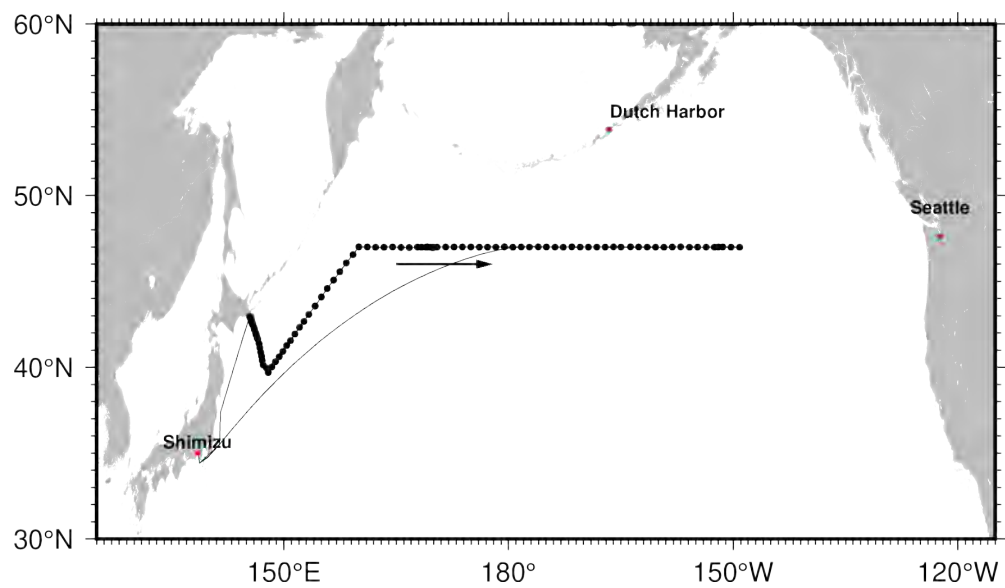


Fig. 1.1 Cruise map of MR21-04.

## 2. Science Party

### 2.1 Participants for MR21-04

Name	Responsibility	Affiliation
Shinya Kouketsu	CTD/Microrider/LADCP/Water sampling	RIGC/JAMSTEC
Katsuro Katsumata	CTD/Microrider/LADCP/Water sampling	RIGC/JAMSTEC
Sayaka Yasunaka	CTD/Microrider/LADCP/Water sampling	RIGC/JAMSTEC
Yuichiro Kumamoto	CFCs/DO/Cs/ <sup>14</sup> C/ <sup>13</sup> C	RIGC/JAMSTEC
Hiroshi Uchida	Salinity/Density	RIGC/JAMSTEC
Masahito Shigemitsu	CFCs/FDOM/DOC	RIGC/JAMSTEC
Kosei Sasaoka	CDOM/Chl-a	RIGC/JAMSTEC
Kei Kondo	Water sampling	RIGC/JAMSTEC
Koki Miyakawa	FDOM	RIGC/JAMSTEC
Ayaka Tanaka	FDOM	RIGC/JAMSTEC
Atsushi Yamaguchi	Plankton Net	Hokkaido Univ.
Daiki Kojima	Plankton Net	Hokkaido Univ.
Takumi Teraoka	Plankton Net/Water sampling	Hokkaido Univ.
Yuanzhi Qi	Iodine isotopes /Water sampling	Univ. of Tokyo
Sasaki Yusuke	Microridar/AFP07/VMP/UCTD	Univ. of Tokyo
Taku NIINUMA	VMP/UCTD/Water sampling	Univ. of Tokyo
Ryosuke Oyabu	VMP/UCTD/Water sampling	Univ. of Tokyo
Masanori Murakami	Meteorology/Geophysics/ADCP	NME
Wataru Tokunaga	Meteorology/Geophysics/ADCP	NME
Fumine Okada	Meteorology/Geophysics/ADCP	NME
Katsunori Sagishima	Water sampling	MWJ
Hiroaki Sako	DO/TSG/Chla	MWJ
Misato Kuwahara	DO/TSG/Chla	MWJ
Shiori Ariga	DO/TSG/Chla	MWJ
Rei Ito	CTD/Argo	MWJ
Ko Morita	CTD/Argo	MWJ
Takayuki Hashimukai	CTD/Argo	MWJ
Tomokazu Chiba	CTD/Water sampling /Salinity	MWJ
Nagisa Fujiki	DIC/TA	MWJ
Hiroshi Hoshino	DIC/TA	MWJ
Minori Kamikawa	DIC/TA	MWJ
Aine Yoda	CFCs	MWJ
Haruka Sato	CFCs	MWJ
Yasuhiro Arii	Nutrients	MWJ
Yuko Miyoshi	Nutrients	MWJ
Yuta Oda	Nutrients	MWJ
Hiroyuiki Nakajima	Water sampling/CTD	MWJ
Kaihe Yamazaki	Water sampling	MWJ
Yumi Abe	Water sampling	MWJ
Gakuto Murata	Water sampling	MWJ

RIGC: Research Institute for Global Change, JAMSTEC: Japan Agency for Marine-Earth Science and Technology

MWJ: Marine Works Japan, NME: Nippon Marine Enterprises

## 2.2 Principal investigators

Measurements	Name	Affiliation
Navigation, Bathymetry, Surf. Met., SADCP, Ceilometer, Satellite image, Gravity, Magnetic Field, LADCP	Shinya Kouketsu	RIGC/JAMSTEC
TSG, CTDO <sub>2</sub> , Salinity, Density, CompactTDs	Hiroshi Uchida	RIGC/JAMSTEC
Disdrometer, Rain Radar, C-band radar, GNSS, Lidar	Masaki Katsumata	RIGC/JAMSTEC
Microwave Radiometer	Mikiko Fujita	RIGC/JAMSTEC
Aerosol optical characteristics	Aoki	Toyama Univ.
Atmospheric CO <sub>2</sub> and CH <sub>4</sub>	Yasunori Tohjima	NIES
Atoms. pCO <sub>2</sub> , Carbon properties	Akihiko Murata	RIGC/JAMSTEC
Microstructures in TC, UCTD, VMP, Deep Ninja, Surface buoy	Yusuke Sasaki	Univ. of Tokyo
DO, Carbon isotopes, Radio Cesium	Yuichiro Kumamoto	RIGC/JAMSTEC
Nutrients	Michio Aoyama	RIGC/JAMSTEC
CFCs, FDOM	Masahito Shigemitsu	RIGC/JAMSTEC
Chl-a, CDOM	Kosei Sasaoka	RIGC/JAMSTEC
DOC	Dennis A. Hansell	Univ. of Miami
Iodine isotopes	Yuanzhi Qi	Univ. of Tokyo
Prokaryotic Abundance	Taichi Yokokawa	XSTAR/JAMSTEC
Zoo plankton	Atsushi Yamaguchi	Hokkaido Univ.
XCTD	Katsuro Katsumata	RIGC/JAMSTEC
Meteorological properties	Masaki Katsumata	RIGC/JAMSTEC
Core/Deep Argo	Shigeki Hosoda	RIGC/JAMSTEC

### 3. Underway Measurements

#### 3.1 Navigation

##### (1) Personnel

Shinya Kouketsu	JAMSTEC: Principal investigator
Masanori Murakami	Nippon Marine Enterprises, Ltd (NME)
Wataru Tokunaga	NME
Fumine Okada	NME
Yoichi Inoue	MIRAI crew

##### (2) System description

Ship's position and velocity were provided by Navigation System on R/V MIRAI. This system integrates GNSS position, Doppler sonar log speed, Gyro compass heading and other basic data for navigation. This system also distributed ship's standard time synchronized to GPS time server via Network Time Protocol. These data were logged on the network server as "SOJ" data every 5 seconds. Sensors for navigation data are listed below;

a) GNSS system:  
R/V MIRAI has four GNSS systems, all GNSS positions were offset to radar-mast position, datum point. Anytime changeable manually switched as to GNSS receiving state.

- StarPack-D (version 11.01.02), Differential GNSS system.  
Antenna: Located on compass deck, starboard.
- StarPack-D (version 11.01.02), Differential GNSS system.  
Antenna: Located on compass deck, portside.
- Standalone GPS system.  
Receiver: Trimble SPS751  
Antenna: Located on navigation deck, starboard.
- Standalone GPS system.  
Receiver: Trimble SPS751  
Antenna: Located on navigation deck, portside.

b) Doppler sonar log:  
FURUNO DS-30, which use three acoustic beams for current measurement under the hull.

c) Gyro compass:  
TOKYO KEIKI TG-8000, sperry type mechanical gyro compass.

d) GPS time server:  
SEIKO TS-2550 Time Server, synchronizing to GPS satellites every 1 second.

##### (3) Data period (Times in UTC)

01:00, 13 Jul. 2021 to 23:40, 25 Aug. 2021

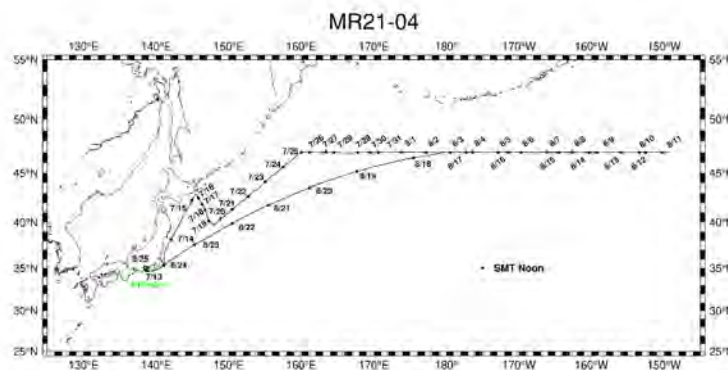


Fig.3.1 Cruise track of MR21-04

## 3.2 Swath Bathymetry

### (1) Personnel

Shinya Kouketsu	JAMSTEC: Principal investigator
Masanori Murakami	Nippon Marine Enterprises, Ltd (NME)
Wataru Tokunaga	NME
Fumine Okada	NME
Yoichi Inoue	MIRAI crew

### (2) Introduction

R/V MIRAI is equipped with a Multi narrow Beam Echo Sounding system (MBES), SEABEAM 3012 (L3 Communications, ELAC Nautik). The objective of MBES is collecting continuous bathymetric data along ship's track to make a contribution to geological and geophysical investigations and global datasets.

### (3) Data Acquisition

The "SEABEAM 3012" on R/V MIRAI was used for bathymetry mapping during this cruise.

To get accurate sound velocity of water column for ray-path correction of acoustic multibeam, we used Surface Sound Velocimeter (SSV) data to get the sea surface sound velocity (at 6.62m), and the deeper depth sound velocity profiles were calculated by temperature and salinity profiles from CTD, XCTD and Argo float data by the equation in Del Grosso (1974) during this cruise.

Table 3.2-1 shows system configuration and performance of SEABEAM 3012.

Table 3.2-1 SEABEAM 3012 system configuration and performance

---

Frequency:	12 kHz
Transmit beam width:	2.0 degree
Transmit power:	4 kW
Transmit pulse length:	2 to 20 msec.
Receive beam width:	1.6 degree
Depth range:	50 to 11,000 m
Number of beams:	301 beams
Beam spacing:	Equi-angle
Swath width:	60 to 150 degrees
Depth accuracy:	< 1 % of water depth (average across the swath)

### (4) Data processing

#### *i) Sound velocity correction*

Each bathymetry data were corrected with sound velocity profiles calculated from the nearest CTD and XCTD data in the distance. The equation of Del Grosso (1974) was used for calculating sound velocity. The data corrections were carried out using the HIPS software version 11.3 (Teledyne CARIS, Canada)

#### *ii) Editing and Gridding*

Editing for the bathymetry data were carried out using the HIPS. Firstly, the bathymetry data during ship's turning was basically deleted, and spike noise of each swath data was removed. Then the bathymetry data were checked by "Regular Grid Surface (resolution: 100 m averaged grid)".

Finally, all accepted data were exported as XYZ ASCII data (longitude [degree], latitude [degree], depth [m]), and converted to 150 m grid data using "nearneighbor" utility of GMT (Generic Mapping Tool) software.

Table 3.2-2 Parameters for gridding on “nearneighbor” in GMT

---

Gridding mesh size:	150 m
Search radius size:	150 m
Number of sectors around grid point:	16
Minimum number of sectors with data required for averaging:	2

---

**(5) Data archives**

These data obtained in this cruise will be submitted to the Data Management Group of JAMSTEC, and will be opened to the public via “Data Research System for Whole Cruise Information in JAMSTEC (DARWIN)” in JAMSTEC web site.

<http://www.godac.jamstec.go.jp/darwin/e>

**3.3 Surface Meteorological Observation**

**(1) Personnel**

Shinya Kouketsu	JAMSTEC: Principal investigator
Masanori Murakami	Nippon Marine Enterprises, Ltd (NME)
Wataru Tokunaga	NME
Fumine Okada	NME
Yoichi Inoue	MIRAI crew

**(2) Objectives**

Surface meteorological parameters are observed as a basic dataset of the meteorology. These parameters provide the temporal variation of the meteorological condition surrounding the ship.

**(3) Methods**

Surface meteorological parameters were observed during this cruise. In this cruise, the two systems for the observation were used.

*i) MIRAI Surface Meteorological observation (SMet) system*

Instruments of SMet system are listed in Table 3.3-1 and measured parameters are listed in Table 3.3-2. Data were collected and processed by KOAC-7800 weather data processor made by Koshin-Denki, Japan. The data set consists of 6 seconds averaged data.

*ii) Shipboard Oceanographic and Atmospheric Radiation (SOAR) measurement system*

SOAR system designed by BNL (Brookhaven National Laboratory, USA) consists of major five parts.

- a) Analog meteorological data sampling with CR1000 logger manufactured by Campbell Scientific Inc. Canada – wind, pressure, and rainfall (by a capacitive rain gauge) measurement.
- b) Digital meteorological data sampling from individual sensors - air temperature, relative humidity and precipitation (by optical rain gauge (ORG)) measurement.
- c) Radiation data sampling with CR1000X logger manufactured by Campbell Inc. and radiometers with ventilation unit manufactured by Hukseflux Thermal Sensors B.V. Netherlands – short and long wave downward radiation measurement.
- d) Photosynthetically Available Radiation (PAR) sensor manufactured by Biospherical Instruments Inc. (USA) - PAR measurement.
- e) Scientific Computer System (SCS) developed by NOAA (National Oceanic and Atmospheric Administration, USA) - centralized data acquisition and logging of all data sets.

SCS recorded radiation, air temperature, relative humidity, CR1000 and ORG data. SCS composed Event data (JamMet) from these data and ship’s navigation data every 6 seconds. Instruments and their locations are listed in Table 3.3-3 and measured parameters are listed in Table

### 3.3-4.

For the quality control as post processing, we checked the following sensors, before and after the cruise.

- a) Capacitive rain gauge (SMet and SOAR)
- b) Inspect of the linearity of output value from the rain gauge sensor to change input value by adding fixed quantity of test water.
- c) Barometer (SMet and SOAR)
- d) Comparison with the portable barometer value, PTB330, VAISALA
- e) Thermometer (air temperature and relative humidity) (SMet and SOAR)
- f) Comparison with the portable thermometer value, HMP75, VAISALA

#### (4) Preliminary results

Fig. 3.3-1 shows the time series of the following parameters.

- Wind (SMet)
- Air temperature (SMet)
- Relative humidity (SMet)
- Precipitation (SOAR ORG)
- Short/long wave radiation (SMet)
- Pressure (SMet)
- Sea surface temperature (SMet)
- Significant wave height (SMet)

#### (5) Data archives

These data obtained in this cruise will be submitted to the Data Management Group of JAMSTEC, and will be opened to the public via “Data Research System for Whole Cruise Information in JAMSTEC (DARWIN)” in JAMSTEC web site.

<http://www.godac.jamstec.go.jp/darwin/e>

#### (6) Remarks (Times in UTC)

- a) SST (Sea Surface Temperature) data were available in the following period.  
07:15UTC 13 Jul. 2021 - 06:00UTC 24 Aug. 2021
- b) Anemometer data were invalid due to system trouble in the following time or period.  
13:23:43UTC 28 Jul. 2021 - 13:23:49UTC 28 Jul. 2021  
13:58:55UTC 14 Aug. 2021 - 13:59:01UTC 14 Aug. 2021  
22:40:57UTC 16 Aug. 2021 - 22:41:29UTC 16 Aug. 2021
- c) Wave data were invalid due to system trouble in the following period.  
20:55UTC 05 Aug. 2021 - 00:55UTC 06 Aug. 2021
- d) Capacitive rain gauge data were invalid due to transmitting MF/HF radio in the following time.  
04:24UTC 13 Jul. 2021  
02:04UTC 25 Jul. 2021  
13:26UTC 15 Aug. 2021  
03:30UTC 22 Aug. 2021

Table 3.3-1 Instruments and installation locations of MIRAI Surface Meteorological observation system

Sensors	Type	Manufacturer	Location (Altitude from surface)
Anemometer	KS-5900	Koshin Denki, Japan	Foremast (25 m)
Tair/RH	HMP155	Vaisala, Finland	Compass deck (21 m)
with aspirated radiation shield	43408 Gill	R.M. Young, U.S.A.	starboard and port side

Thermometer: SST	RFN2-0	Koshin Denki, Japan	4th deck (-1m, inlet -5m)
Barometer	Model-370	Setra System, U.S.A.	Captain deck (13 m) Weather observation room
Capacitive rain gauge	50202	R. M. Young, U.S.A.	Compass deck (19 m)
Optical rain gauge	ORG-815DS	Osi, USA	Compass deck (19 m)
Radiometer (short wave)	MS-802	Eko Seiki, Japan	Radar mast (28 m)
Radiometer (long wave)	MS-202	Eko Seiki, Japan	Radar mast (28 m)
Wave height meter	WM-2	Tsurumi-seiki, Japan	Bow (10 m) Stern (8m)

Table 3.3-2 Parameters of MIRAI Surface Meteorological observation system

Parameter	Units	Remarks
1 Latitude	degree	
2 Longitude	degree	
3 Ship's speed	knot	MIRAI log
4 Ship's heading	degree	MIRAI gyro
5 Relative wind speed	m/s	6sec./10min. averaged
6 Relative wind direction	degree	6sec./10min. averaged
7 True wind speed	m/s	6sec./10min. averaged
8 True wind direction	degree	6sec./10min. averaged
9 Barometric pressure	hPa	adjusted to sea surface level 6sec. averaged
10 Air temperature (starboard)	degC	6sec. averaged
11 Air temperature (port)	degC	6sec. averaged
12 Dewpoint temperature (starboard)	degC	6sec. averaged
13 Dewpoint temperature (port)	degC	6sec. averaged
14 Relative humidity (starboard)	%	6sec. averaged
15 Relative humidity (port)	%	6sec. averaged
16 Sea surface temperature	degC	6sec. averaged
17 Rain rate (optical rain gauge)	mm/hr	hourly accumulation
18 Rain rate (capacitive rain gauge)	mm/hr	hourly accumulation
19 Downwelling shortwave radiation	W/m <sup>2</sup>	6sec. averaged
20 Downwelling infra-red radiation	W/m <sup>2</sup>	6sec. averaged
21 Significant wave height (bow)	m	hourly
22 Significant wave height (stern)	m	hourly
23 Significant wave period (bow)	second	hourly
24 Significant wave period (stern)	second	hourly

Table 3.3-3 Instruments and installation locations of SOAR system

Sensors (Meteorological)	Type	Manufacturer	Location (Altitude from surface)
Anemometer	05106	R.M. Young, USA	Foremast (25 m)
Barometer	PTB210	Vaisala, Finland	Foremast (23 m)
with pressure port	61002 Gill	R.M. Young, USA	Foremast (24 m)
Rain gauge	50202	R.M. Young, USA	Foremast (24 m)
Tair/RH	HMP155	Vaisala, Finland	Foremast (23 m)
with aspirated radiation shield	43408 Gill	R.M. Young, USA	Foremast (24 m)
Optical rain gauge	ORG-815DR	Osi, USA	Foremast (24 m)
Sensors (NPR)	Type	Manufacturer	Location (Altitude from surface)
Radiometer (short wave)	SR20	Hukseflux Thermal Sensors B.V., Netherlands	Foremast (25 m)
Radiometer (long wave)	IR20	Hukseflux Thermal Sensors	Foremast (25 m)

B.V., Netherlands

Sensor (PAR&UV)	Type	Manufacturer	Location (Altitude from surface)
PAR&UV sensor	PUV-510	Biospherical Instruments Inc., USA	Navigation deck (18m)

Table 3.3-4 Parameters of SOAR system (JamMet)

Parameter	Units	Remarks
1 Latitude	degree	
2 Longitude	degree	
3 SOG	knot	
4 COG	degree	
5 Relative wind speed	m/s	
6 Relative wind direction	degree	
7 Barometric pressure	hPa	
8 Air temperature	degC	
9 Relative humidity	%	
10 Rain rate (optical rain gauge)	mm/hr	
11 Precipitation (capacitive rain gauge)	mm/hr	reset at 50 mm
12 Down welling shortwave radiation	W/m <sup>2</sup>	
13 Down welling infra-red radiation	W/m <sup>2</sup>	
14 Diffuse irradiance	W/m <sup>2</sup>	
15 PAR	microE/cm <sup>2</sup> /sec	
16 UV 305 nm	microW/cm <sup>2</sup> /nm	
17 UV 320 nm	microW/cm <sup>2</sup> /nm	
18 UV 340 nm	microW/cm <sup>2</sup> /nm	
19 UV 380 nm	microW/cm <sup>2</sup> /nm	

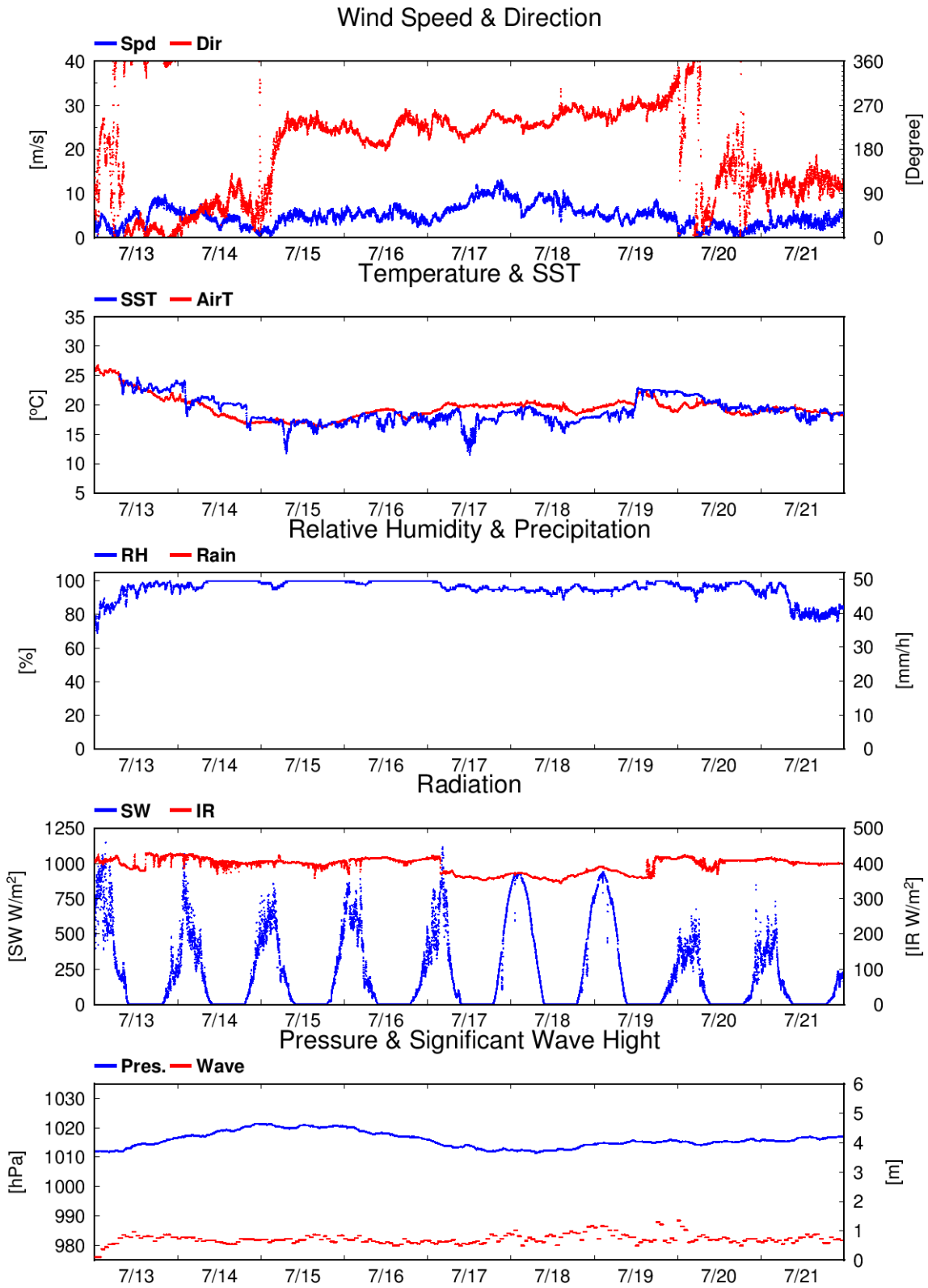


Fig. 3.3-1 Time series of surface meteorological parameters during this cruise

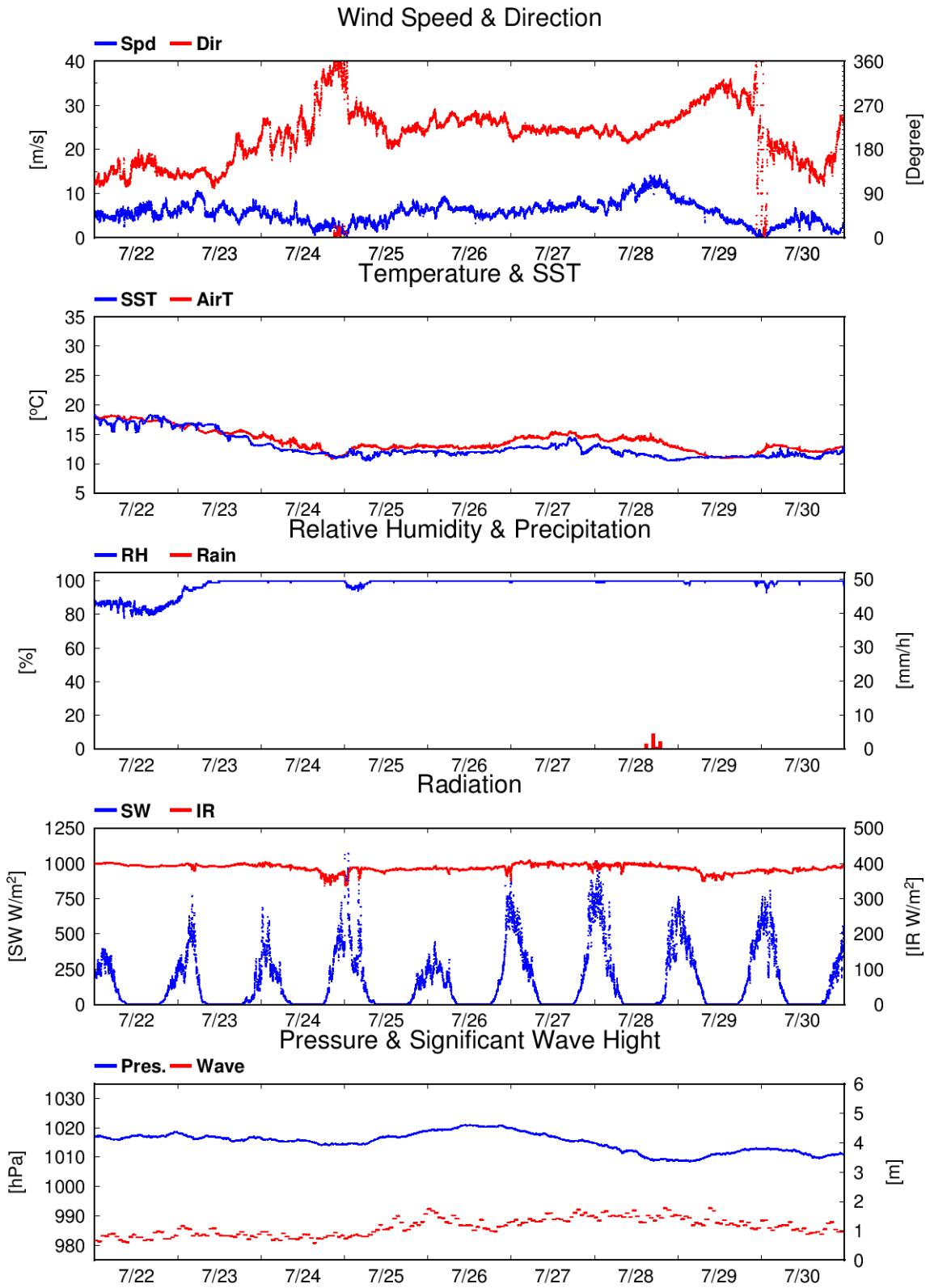


Fig. 3.3-1 (Continued)

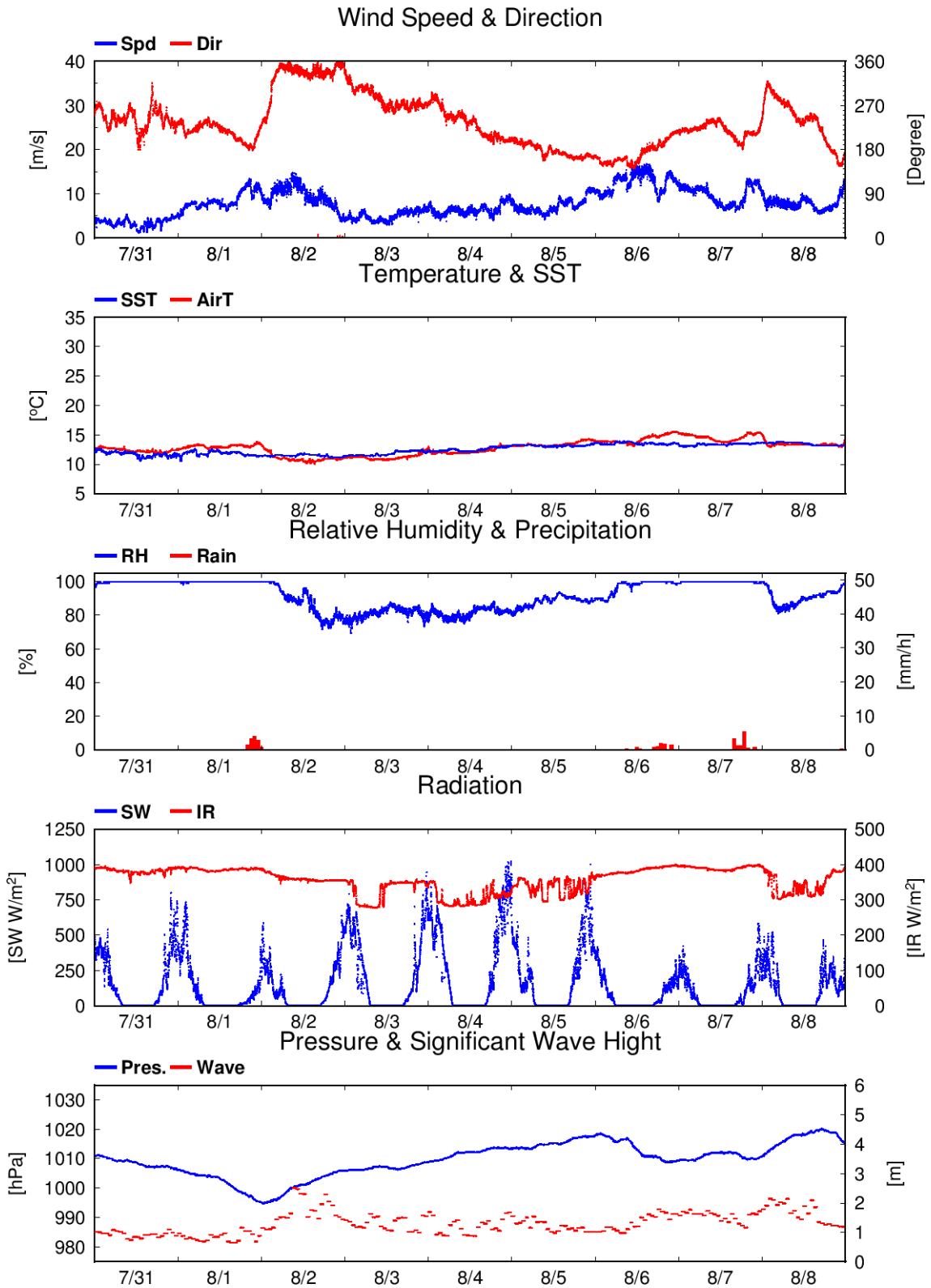


Fig. 3.3-1 (Continued)

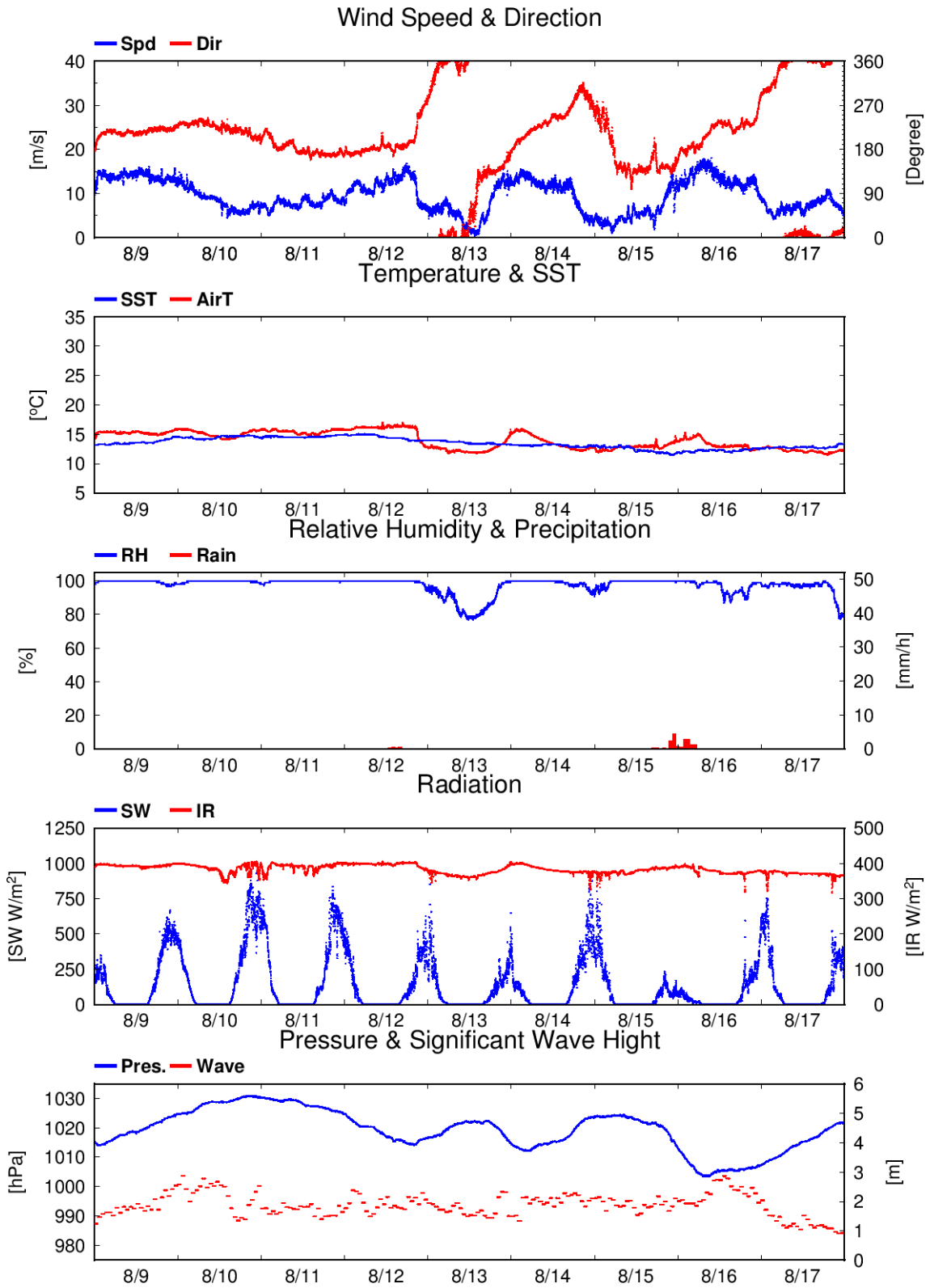


Fig. 3.3-1 (Continued)

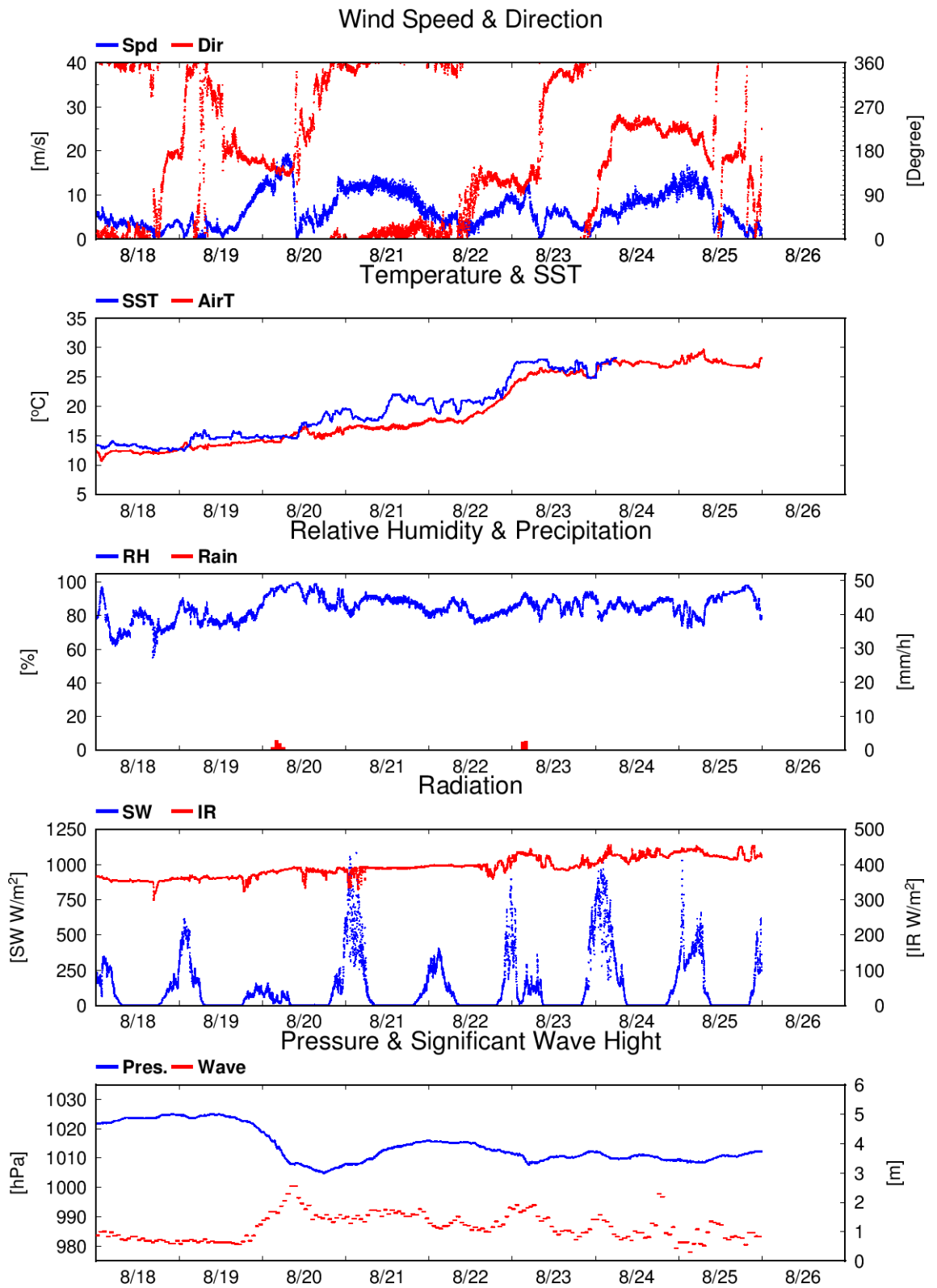


Fig. 3.3-1 (Continued)

### 3.4 Thermo-Salinograph and Related Properties

#### (1) Personnel

Uchida Hiroshi	JAMSTEC
Hiroaki Sako	MWJ
Misato Kuwahara	MWJ
Shiori Ariga	MWJ

#### (2) Objective

The objective of this measurements is to collect sea surface salinity, temperature, dissolved oxygen, fluorescence and total dissolved gas pressure data continuously along the cruise track.

#### (3) Note

Details of instruments and method including calibration and evaluation of data quality will be updated after the cruise.

### 3.5 Shipboard ADCP

#### (1) Personnel

Shinya Kouketsu	JAMSTEC: Principal investigator
Masanori Murakami	Nippon Marine Enterprises, Ltd (NME)
Wataru Tokunaga	NME
Fumine Okada	NME
Yoichi Inoue	MIRAI crew

#### (2) Objectives

To obtain continuous measurement data of the current profile along the ship's track.

#### (3) Instruments and methods

Upper ocean current measurements were made in this cruise, using the hull-mounted Acoustic Doppler Current Profiler (ADCP) system. For most of its operation, the instrument was configured for water-tracking mode. Bottom-tracking mode, interleaved bottom-ping with water-ping, was made to get the calibration data for evaluating transducer misalignment angle in the shallow water. The system consists of following components;

- a) R/V MIRAI has installed the Ocean Surveyor for vessel-mount ADCP (frequency 76.8 kHz; Teledyne RD Instruments, USA). It has a phased-array transducer with single ceramic assembly and creates 4 acoustic beams electronically. We mounted the transducer head rotated to a ship-relative angle of 45 degrees azimuth from the keel.
- b) For heading source, we use ship's gyro compass (Tokyo Keiki, Japan), continuously providing heading to the ADCP system directory. Additionally, we have Inertial Navigation System (Phins, IXBLUE SAS, France) which provide high-precision heading, attitude information, pitch and roll. They are stored in ".N2R" data files with a time stamp.
- c) Differential GNSS system (StarPack-D, Fugro, Netherlands) providing precise ship's position
- d) We used VmDas software version 1.50(TRDI) for data acquisition.
- e) To synchronize time stamp of ping with Computer time, the clock of the logging computer is adjusted to GPS time server continuously by the application software.
- f) Fresh water is charged in the sea chest to prevent bio fouling at transducer face.
- g) The sound speed at the transducer does affect the vertical bin mapping and vertical velocity measurement, and that is calculated from temperature, salinity (constant value; 35.0 PSU) and depth (6.5 m; transducer depth) by

equation in Medwin (1975).

h) Data was configured for “8 m” layer intervals starting about 19 m below sea surface, and recorded every ping as raw ensemble data (.ENR). Additionally, 30 seconds averaged data were recorded as short-term average (.STA). 300 seconds averaged data were long-term average (.LTA), respectively.

#### (4) Parameters

Major parameters for the measurement, Direct Command, are shown in Table 3.5-1.

Table 3.5-1. Major parameters

---

##### Environmental Sensor Commands

EA = 04500	Heading Alignment (1/100 deg)
ED = 00065	Transducer Depth (0 - 65535 dm)
EF = +001	Pitch/Roll Divisor/Multiplier (pos/neg) [1/99 - 99]
EH = 00000	Heading (1/100 deg)
ES = 35	Salinity (0-40 pp thousand)
EX = 00000	Coordinate Transform (Xform:Type; Tilts; 3Bm; Map)
EZ = 10200010	Sensor Source (C; D; H; P; R; S; T; U) C (1): Sound velocity calculates using ED, ES, ET (temp.) D (0): Manual ED H (2): External synchro P (0), R (0): Manual EP, ER (0 degree) S (0): Manual ES T (1): Internal transducer sensor U (0): Manual EU
EV = 0	Heading Bias(1/100 deg)
Water-Track Commands	
WA = 255	False Target Threshold (Max) (0-255 count)
WC = 120	Low Correlation Threshold (0-255)
WD = 111 100 000	Data Out (V; C; A; PG; St; Vsum; Vsum^2; #G; P0)
WE = 1000	Error Velocity Threshold (0-5000 mm/s)
WF = 0800	Blank After Transmit (cm)
WN = 100	Number of depth cells (1-128)
WP = 00001	Pings per Ensemble (0-16384)
WS = 800	Depth Cell Size (cm)
WV = 0390	Mode 1 Ambiguity Velocity (cm/s radial)

#### (5) Preliminary results

Horizontal velocity along the ship’s track is presented in [Fig.3.5-1](#).

#### (6) Data archives

These data obtained in this cruise will be submitted to the Data Management Group of JAMSTEC and will be opened to the public via “Data Research System for Whole Cruise Information in JAMSTEC (DARWIN)” in JAMSTEC web site.

<http://www.godac.jamstec.go.jp/darwin/e>

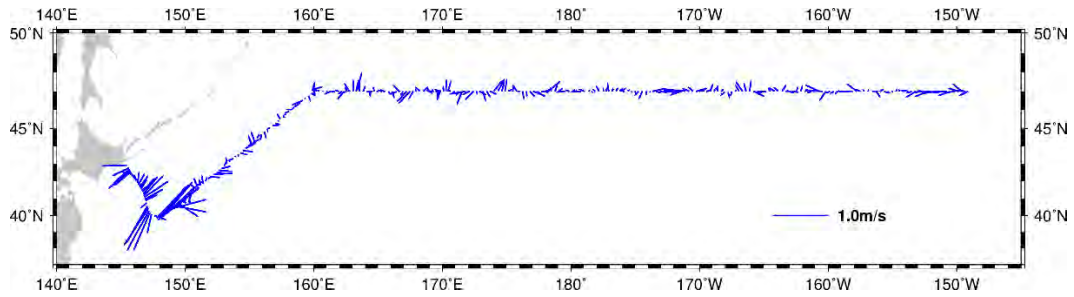


Fig.3.5-1. Horizontal Velocity along the ship's track.

(60 min. Average / Layer: 27-51m)

### 3.6 Ceilometer observation

#### (1) Personnel

Shinya Kouketsu	JAMSTEC: Principal investigator
Masanori Murakami	Nippon Marine Enterprises, Ltd (NME)
Wataru Tokunaga	NME
Fumine Okada	NME
Yoichi Inoue	MIRAI crew

#### (2) Objectives

The information of cloud base height and the liquid water amount around cloud base is important to understand a process on formation of the cloud. As one of the methods to measure them, the ceilometer observation was carried out.

#### (3) Parameters

- a) Cloud base height [m].
- b) Backscatter profile, sensitivity and range normalized at 10 m resolution.
- c) Estimated cloud amount [oktas] and height [m]; Sky Condition Algorithm.

#### (4) Methods

Cloud base height and backscatter profile were observed by ceilometer (CL51, VAISALA, Finland). The measurement configurations are shown in Table 3.6-1. On the archive dataset, cloud base height and backscatter profile are recorded with the resolution of 10 m.

Table 3.6-1 The measurement configurations

Property	Description
Laser source	Indium Gallium Arsenide (InGaAs) Diode
Transmitting center wavelength	910±10 nm at 25 degC
Transmitting average power	19.5 mW
Repetition rate	6.5 kHz
Detector	Silicon avalanche photodiode (APD)
Responsibility at 905 nm	65 A/W
Cloud detection range	0 ~ 13 km
Measurement range	0 ~ 15 km
Resolution	10 m in full range
Sampling rate	36 sec.
	Cloudiness in oktas (0 ~ 9)
	0 Sky Clear
	1 Few
Sky Condition	3 Scattered
	5-7 Broken
	8 Overcast
	9 Vertical Visibility

**(5) Preliminary results**

Fig.3.6-1 shows the time series of 1st, 2nd and 3rd cloud base height during the cruise.

**(6) Data archives**

These data obtained in this cruise will be submitted to the Data Management Group of JAMSTEC and will be opened to the public via “Data Research System for Whole Cruise Information in JAMSTEC (DARWIN)” in JAMSTEC web site.

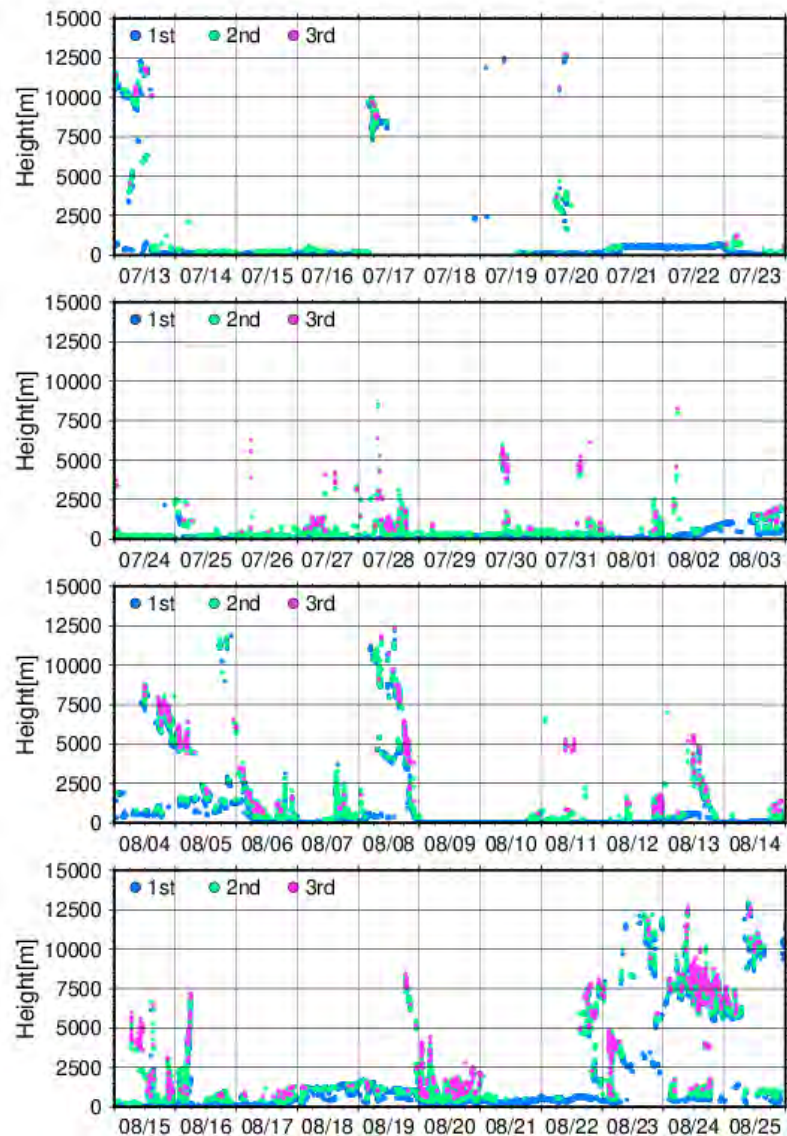
<http://www.godac.jamstec.go.jp/darwin/e>

**(7) Remarks (Times in UTC)**

The following time, the window was cleaned.

- 23:58, 12 Jul. 2021
- 09:02, 20 Jul. 2021
- 06:55, 27 Jul. 2021
- 06:00, 02 Aug. 2021
- 21:50, 17 Aug. 2021

Fig. 3.6-1 1st, 2nd and 3rd cloud base height during this cruise.



### 3.7 Optical Disdrometer

#### (1) Personnel

Masaki KATSUMATA	JAMSTEC (not on board)
Biao GENG	JAMSTEC (not on board)
Kyoko TANIGUCHI	JAMSTEC (not on board)

#### (2) Objectives

The disdrometer can continuously obtain size distribution of raindrops. The objective of this observation is (a) to reveal microphysical characteristics of the rainfall, depends on the type, temporal stage, etc. of the precipitating clouds, (b) to retrieve the coefficient to convert radar reflectivity (especially from C-band radar in Section 5.3) to the rainfall amount, and (c) to validate the algorithms and the products of the satellite-borne precipitation radars; TRMM/PR and GPM/DPR.

#### (3) Instrumentations and Methods

Two “Laser Precipitation Monitor (LPM)” (Adolf Thies GmbH & Co) are utilized. It is an optical disdrometer. The instrument consists of the transmitter unit which emit the infrared laser, and the receiver unit which detects the intensity of the laser come thru the certain path length in the air. When a precipitating particle fall thru the laser, the received intensity of the laser is reduced. The receiver unit detect the magnitude and the duration of the reduction and then convert them onto particle size and fall speed. The sampling volume, i.e. the size of the laser beam “sheet”, is 20 mm (W) x 228 mm (D) x 0.75 mm (H).

The particles are categorized by the detected size and fall speed and counted the number in each category every minutes. The categories are shown in [Table 3.7.1-1](#).

The LPMs are installed on the top (roof) of the anti-rolling system, as shown in [Fig. 3.7.1-1](#). Both are installed at the corner at the bow side and the starboard side. One (in aft) equipped the "wind protection element" to reduce the effect of the wind on the measurement, and to estimate the effectiveness of the "element" by comparing data from two sensors.

#### (4) Preliminary Results

The data have been obtained all through the cruise, except non-permitted territorial waters and EEZs. The further analyses for the rainfall amount, drop-size-distribution parameters, etc., will be carried out after the cruise.

#### (5) Data Archive

All data obtained during this cruise will be submitted to the JAMSTEC Data Management Group (DMG).

#### (6) Acknowledgment

The operations are supported by Japan Aerospace Exploration Agency (JAXA) Precipitation Measurement Mission (PMM).

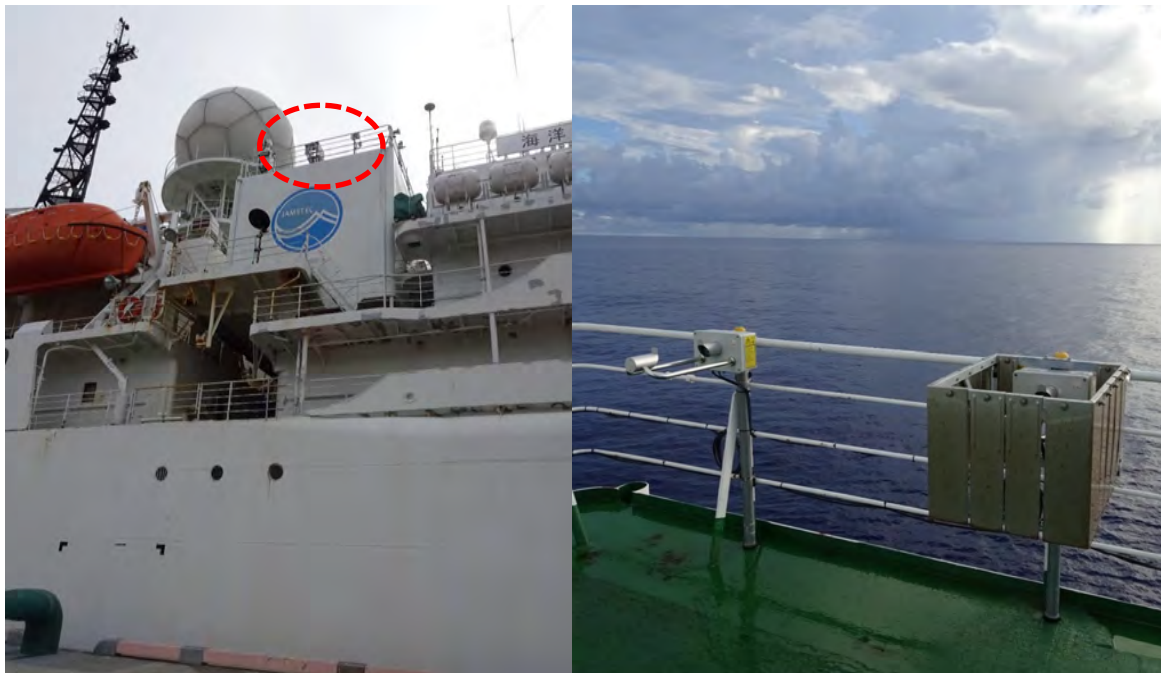


Fig. 3.7.1-1: Onboard LPM sensors. (Left) The location of the sensors, as designated by the red broken circle. (Right) The sensors. Right one (aft one) equipped wind protection element to reduce the effect of the wind, while left one (fore one) did not.

Table 3.7.1-1: Categories of the particle size and the fall speed.

Particle Size		
Class	Diameter [mm]	Class width [mm]
1	≥ 0.125	0.125
2	≥ 0.250	0.125
3	≥ 0.375	0.125
4	≥ 0.500	0.250
5	≥ 0.750	0.250
6	≥ 1.000	0.250
7	≥ 1.250	0.250
8	≥ 1.500	0.250
9	≥ 1.750	0.250
10	≥ 2.000	0.500
11	≥ 2.500	0.500
12	≥ 3.000	0.500
13	≥ 3.500	0.500
14	≥ 4.000	0.500
15	≥ 4.500	0.500
16	≥ 5.000	0.500
17	≥ 5.500	0.500
18	≥ 6.000	0.500
19	≥ 6.500	0.500
20	≥ 7.000	0.500
21	≥ 7.500	0.500
22	≥ 8.000	unlimited

Fall Speed		
Class	Speed [m/s]	Class width [m/s]
1	≥ 0.000	0.200
2	≥ 0.200	0.200
3	≥ 0.400	0.200
4	≥ 0.600	0.200
5	≥ 0.800	0.200
6	≥ 1.000	0.400
7	≥ 1.400	0.400
8	≥ 1.800	0.400
9	≥ 2.200	0.400
10	≥ 2.600	0.400
11	≥ 3.000	0.800
12	≥ 3.400	0.800
13	≥ 4.200	0.800
14	≥ 5.000	0.800
15	≥ 5.800	0.800
16	≥ 6.600	0.800
17	≥ 7.400	0.800
18	≥ 8.200	0.800
19	≥ 9.000	1.000
20	≥ 10.000	10.000

### 3.8 Micro Rain Radar

#### (1) Personnel

Masaki KATSUMATA	JAMSTEC (not on board)
Biao GENG	JAMSTEC (not on board)
Kyoko TANIGUCHI	JAMSTEC (not on board)

#### (2) Objectives

The micro rain radar (MRR) is a compact vertically-pointing Doppler radar, to detect vertical profiles of rain drop size distribution. The objective of this observation is to understand detailed vertical structure of the precipitating systems.

#### (3) Instruments and Methods

The MRR-2 (METEK GmbH) was utilized. The specifications are in Table 3.8.2-1. The antenna unit was installed at the starboard side of the anti-rolling systems (see Fig. 3.8.2-1), and wired to the junction box and laptop PC inside the vessel.

The data was averaged and stored every 1 minute. The vertical profile of each parameter was obtained every 100 meters in range distance (i.e. height) up to 3100 meters. The recorded parameters were; Drop size distribution, radar reflectivity, path-integrated attenuation, rain rate, liquid water content and fall velocity.



Fig. 3.8.2-1: Onboard MRR sensor. (Left) The location of the sensors, as designated by the red broken circle. (Right) The antenna unit.

Table 3.8.2-1: Specifications of the MRR-2.

Transmitter power	50 mW
Operating mode	FM-CW
Frequency	24.230 GHz (modulation 1.5 to 15 MHz)
3dB beam width	1.5 degrees
Spurious emission	< -80 dBm / MHz
Antenna Diameter	600 mm
Gain	40.1 dBi

#### (4) Preliminary Results

The data have been obtained all through the cruise, except non-permitted territorial waters and EEZs. The further analyses will be after the cruise.

#### (5) Data Archive

All data obtained during this cruise will be submitted to the JAMSTEC Data Management Group (DMG).

#### (6) Acknowledgment

The operations are supported by Japan Aerospace Exploration Agency (JAXA) Precipitation Measurement Mission (PMM).

### 3.9 C-band weather radar

#### (1) Personnel

Masaki KATSUMATA	JAMSTEC (not on board)
Biao GENG	JAMSTEC (not on board)
Masanori MURAKAMI	NME
Wataru TOKUNAGA	NME
Fumine OKADA	NME

#### (2) Objectives

The objective of weather radar observations is to investigate the structures and evolutions of precipitating systems over the high-latitude region including arctic ocean.

#### (3) Instrumentation and methods

##### *i) Radar specifications*

The C-band weather radar on board the R/V Mirai was used. Basic specifications of the radar are as follows:

Frequency:	5370 MHz (C-band)
Polarimetry:	Horizontal and vertical (simultaneously transmitted and received)
Transmitter:	Solid-state transmitter
Pulse Configuration:	Using pulse-compression
Output Power:	6 kW (H) + 6 kW (V)
Antenna Diameter:	4 meters
Beam Width:	1.0 degrees
Inertial Navigation Unit:	PHINS (IXBLUE S.A.S)

##### *ii) Available radar variables*

Radar variables, which were converted from the power and phase of the backscattered signal at vertically- and horizontally-polarized channels, were as follows:

Radar reflectivity:	$Z$
Doppler velocity:	$V_T$
Spectrum width of Doppler velocity:	$SW$
Differential reflectivity:	$Z_{DR}$
Differential propagation phase:	$\Phi_{DP}$
Specific differential phase:	$K_{DP}$
Co-polar correlation coefficients:	$\rho_{HV}$

##### *iii) Operation methodology*

The antenna was controlled to point the commanded ground-relative direction, by controlling the azimuth and elevation to cancel the ship attitude (roll, pitch and yaw) detected by the laser gyro. The

Doppler velocity was also corrected by subtracting the ship movement in beam direction.

For the maintenance, internal signals of the radar were checked and calibrated at the beginning and the end of the cruise. Meanwhile, the following parameters were checked daily; (1) frequency, (2) mean output power, (3) pulse width, and (4) PRF (pulse repetition frequency).

During the cruise, the radar was operated as in Table 3.9-1. A dual PRF mode was used for a volume scan. For RHI and surveillance PPI scans, a single PRF mode was used.

#### (4) Preliminary results

The C-band weather radar observations were conducted through the cruise, except in the area where the operations were prohibited by Japanese license. The observation started at 04UTC on 18 Jul. 2021, and continued until 12UTC on 23 Aug. 2021.

The obtained data will be analyzed after the cruise.

#### (5) Data archive

All data obtained during this cruise will be submitted to the JAMSTEC Data Management Group (DMG).

Table 3.9-1: Scan modes of C-band weather radar

	Surveillance PPI Scan	Volume Scan					RHI Scan
Repeated Cycle (min.)	30	6					6
Times in One Cycle	1	1					3
PRF(s) (Hz)	400	dual PRF (ray alternative)					1250
		667	833	938	1250	1333	
Azimuth (deg)	Full Circle					Option	
Bin Spacing (m)	150						
Max. Range (km)	300	150	100	60	100		
Elevation Angle(s) (deg.)	0.5	0.5	1.0, 1.8, 2.6, 3.4, 4.2, 5.1, 6.2, 7.6, 9.7, 12.2, 15.2	18.7, 23.0, 27.9, 33.5, 40.0	0.0 ~ 60.0		

### 3.10 GNSS precipitable water

#### (1) Personnel

Mikiko FUJITA JAMSTEC (not on board)  
Masaki KATSUMATA JAMSTEC

#### (2) Objectives

Getting the GNSS satellite data to estimate the total column integrated water vapor content of the atmosphere.

#### (3) Instruments and Methods

The GNSS satellite data was archived to the receiver (Trimble NetR9) with 5 sec interval. The GNSS antenna (Margrin) was set on the roof of aft wheel house. The observations were carried out all through the cruise.

#### **(4) Preliminary Results**

We will calculate the total column integrated water from observed GNSS satellite data after the cruise.

#### **(5) Data Archive**

Raw data is recorded as T02 format and stream data every 5 seconds. These raw datasets are available from Mikiko Fujita of JAMSTEC. Corrected data will be submitted to JAMSTEC Marine-Earth Data and Information Department and will be archived there.

### **3.11 Lidar**

#### **(1) Personnel**

Masaki KATSUMATA	JAMSTEC (not on board)
Kyoko TANIGUCHI	JAMSTEC (not on board)

#### **(3) Objectives**

The objective of this observation is to capture the vertical distribution of clouds, aerosols, and water vapor in high spatio-temporal resolution.

#### **(4) Instruments and Methods**

The Mirai Lidar system transmits a 10-Hz pulse laser in three wavelengths: 1064nm, 532nm, 355nm. For cloud and aerosol observation, the system detects Mie scattering at these wavelengths. The separate detections of polarization components at 532 nm and 355 nm obtain additional characteristics of the targets. The system also detects Raman water vapor signals at 660 nm and 408nm, Raman nitrogen signals at 607 nm and 387nm at nighttime. Based on the signal ratio of Raman water vapor to Raman nitrogen, the system offers water vapor mixing ratio profiles.

#### **(5) Preliminary Results**

The lidar system observed the lower atmosphere throughout the cruise, except on EEZs and territorial waters without permission. All data will be reviewed after the cruise to maintain data quality.

#### **(6) Data Archive**

All data obtained during this cruise will be submitted to the JAMSTEC Data Management Group (DMG).

#### **(7) Acknowledgment**

The operation on board was greatly helped by Nippon Marine Enterprises, Ltd.

### **3.12 Microwave Radiometer**

#### **(1) Personnel**

Masaki KATSUMATA	JAMSTEC
Akira KUWANO-YOSHIDA	Kyoto Univ. (not on board)
Masahiro MINOWA	Furuno Electric Co., Ltd. (not on board)

#### **(2) Objective**

To retrieve total column integrated water vapor content of the atmosphere.

#### **(3) Method**

The microwave radiometer (hereafter MWR; manufactured by Furuno Electric Co., Ltd.) is used. The MWR received natural microwave within the angle of 20 deg. from zenith, at the frequencies around 22 GHz. The received signal can be converted to the column integrated water vapor (or precipitable water). The observation was made every 20 seconds except when periodic auto-calibration was on-going (once in several minutes). The rain sensor is equipped to identify the period of rainfall.

In addition to the MWR, the whole sky camera was installed beside the MWR. This is to monitor cloud cover, which also affects the microwave signals. The camera obtained the whole-sky image every 2 minutes.

Both instruments were installed at the top of the roof of aft wheelhouse, as in Fig. 3.12-1. The data were continuously obtained all through the cruise period.

#### (4) Results

The all data are archived in the sensor unit. The obtained data will be retrieved and analyzed after the end of the cruise.

#### (5) Data archive

The data will be submitted to the JAMSTEC Data Management Group (DMG).

#### (6) Acknowledgment

The observation was supported by the JSPS KAKENHI Grant 20H04306.



Fig. 3.12-1: Outlook of the microwave radiometer (right) and the whole-sky camera (left) installed at the roof of the aft wheelhouse.

### 3.13 Satellite image acquisition

#### (1) Personnel

Shinya Kouketsu	JAMSTEC: Principal investigator
Masanori Murakami	Nippon Marine Enterprises, Ltd (NME)
Wataru Tokunaga	NME
Fumine Okada	NME
Yoichi Inoue	MIRAI crew

#### (2) Objectives

The objectives are to collect cloud data in a high spatial resolution mode from the Advance Very High Resolution Radiometer (AVHRR) on the NOAA and MetOp polar orbiting satellites.

#### (3) Methods

We received the down link High Resolution Picture Transmission (HRPT) signal from satellites, which passed over the area around the R/V MIRAI. We processed the HRPT signal with the in-flight calibration and computed the brightness temperature. A cloud image map around the R/V MIRAI was made from the data for each pass of satellites. We received and processed polar orbiting satellites data throughout this cruise.

#### (4) Data archives

These data obtained in this cruise will be submitted to the Data Management Group of JAMSTEC

and will be opened to the public via “Data Research System for Whole Cruise Information in JAMSTEC (DARWIN)” in JAMSTEC web site.

<http://www.godac.jamstec.go.jp/darwin/e>

### 3.14 Aerosol optical characteristics measured by Shipborne Sky radiometer

#### (1) Personnel

Kazuma Aoki	University of Toyama (not onboard)
Masanori Murakami	Nippon Marine Enterprises, Ltd (NME)
Wataru Tokunaga	NME
Fumine Okada	NME

#### (2) Objectives

Objective of this observation is to study distribution and optical characteristics of marine aerosols by using a ship-borne sky radiometer (POM-01 MK-III: PREDE Co. Ltd., Japan). Furthermore, collections of the data for calibration and validation to the remote sensing data were performed simultaneously.

#### (3) Instruments and methods

##### i) Sky radiometer measurement

The sky radiometer measures the direct solar irradiance and the solar aureole radiance distribution with seven interference filters (0.315, 0.4, 0.5, 0.675, 0.87, 0.94, and 1.02  $\mu\text{m}$ ). Analysis of these data was performed by SKYRAD.pack version 4.2 developed by Nakajima et al. 1996 and 2020.

##### ii) Parameters

- Aerosol optical thickness at five wavelengths (400, 500, 675, 870 and 1020 nm)
- Ångström exponent
- Single scattering albedo at five wavelengths
- Size distribution of volume (0.01  $\mu\text{m}$  – 20  $\mu\text{m}$ )

# GPS provides the position with longitude and latitude and heading direction of the vessel, and azimuth and elevation angle of the sun. Horizon sensor provides rolling and pitching angles.

#### (4) Data archive

Aerosol optical data are to be archived at University of Toyama (K.Aoki, SKYNET/SKY: <http://skyrad.sci.u-toyama.ac.jp/sobs/>) after the quality check and will be submitted to JAMSTEC.

#### (5) References

Nakajima, T., G.Tonna, R.Rao, P.Boi, Y.Kaufman and B.Holben (1996) Use of sky brightness measurements from ground for remote sensing of particulate polydispersions, *Appl. Opt.*, 35, 2672–2686, <https://doi.org/10.1364/AO.35.002672>.

Aoki, K., T.Takemura, K.Kawamoto, and T.Hayasaka (2013), Aerosol climatology over Japan site measured by ground-based sky radiometer, *AIP Conf. Proc.* 1531, 284-287 (2013); doi: 10.1063/1.4804762.

Nakajima, T., Campanelli, M., Che, H., Estellés, V., Irie, H., Kim, S.-W., Kim, J., Liu, D., Nishizawa, T., Pandithurai, G., Soni, V.K., Thana, B., Tugjurn, N.-U., Aoki, K., Hashimoto, M., Higurashi, A., Kazadzis, S., Khatri, P., Kouremeti, N., Kudo, R., Marengo, F., Momoi, M., Ningombam, S. S., Ryder, C.L., and Uchiyama, A. (2020) An overview and issues of the sky radiometer technology and SKYNET, *Atmos. Meas. Tech.*, 13, 4195–4218, 2020, <https://doi.org/10.5194/amt-13-4195-2020>.

### 3.15 Atmospheric CO<sub>2</sub> and CH<sub>4</sub>

#### (1) Personnel

Yasunori Tohjima	NIES: Principal investigator
Shigeyuki Ishidoya	AIST
Hideki Nara	NIES
Shinji Morimoto	Tohoku Univ.

#### (2) Objective

Carbon dioxide (CO<sub>2</sub>) and methane (CH<sub>4</sub>) are the first- and second-most-important anthropogenic greenhouse gases (GHGs) in the atmosphere. Recent systematic measurements of the atmospheric mixing ratios of these GHGs have clearly shown the steady increases, reflecting imbalances between the sources and sinks of the GHGs. The CO<sub>2</sub> emissions from fossil fuel combustion and land use change are major drivers of the atmospheric CO<sub>2</sub> increase while the ocean and land biosphere act as the sink of CO<sub>2</sub>, taking up about half of the anthropogenic CO<sub>2</sub> emissions. However, there are still large uncertainties of the present and future levels of these sink strengths, making it uncertain to predict the future atmospheric CO<sub>2</sub> growth. As for CH<sub>4</sub>, there are lots of anthropogenic sources including fugitive emissions from fossil fuel exploitation, paddy fields, landfill, and so on. Since these emissions and the distributions have large uncertainties, the prediction of the future CH<sub>4</sub> levels is also difficult. To reduce these uncertainties atmospheric inversion approach based on atmospheric transport models and the atmospheric observed data are useful. However, since the atmospheric observations are still limited, extending the observation network is highly required. Therefore, we measured the atmospheric CO<sub>2</sub> and CH<sub>4</sub> mole fractions aboard the R/V Mirai during the entire cruise period to clarify the distributions across the Pacific and fill the observation gap.

#### (3) Apparatus

Atmospheric CO<sub>2</sub>, CH<sub>4</sub>, and CO mixing ratios were measured by a wavelength-scanned cavity ring-down spectrometer (WS-CRDS, Picarro, G2401, see Photo 1). An air intake, capped with an inverted stainless-steel beaker covered with stainless steel mesh, was placed on the right-side of the upper deck. A diaphragm pump (GAST, MOA-P108) was used to draw in the outside air at a flow rate of ~8 L min<sup>-1</sup>. Water vapor in the sample air was reduced to a dew point of about -35°C by passing it consecutively through a thermoelectric dehumidifier (KELK, DH-109) and a Nafion drier (PERMA PURE, PD-50T-24), respectively. Then, the dried sample air was introduced into the WS-CRDS at a flow rate of 100 ml min<sup>-1</sup>. The WS-CRDS were automatically calibrated every 50 hours by introducing 3 standard airs with known CO<sub>2</sub>, CH<sub>4</sub> and CO mixing ratios. The analytical precisions for CO<sub>2</sub>, CH<sub>4</sub> and CO mixing ratios are about 0.02 ppm, 0.3 ppb and 3 ppb, respectively.

#### (4) Results

The atmospheric CO<sub>2</sub>, CH<sub>4</sub>, and CO mixing ratios were observed without any problems during the entire cruise period.

### 3.16 Atmospheric and surface seawater pCO<sub>2</sub>

#### (1) Personnel

Akihiko Murata	JAMSTEC: Principal investigator
Nagisa Fujiki	MWJ
Hiroshi Hoshino	MWJ
Minoru Kamikawa	MWJ

#### (2) Objective

Concentrations of CO<sub>2</sub> in the atmosphere are now increasing at a rate of about 2.0 ppmv y<sup>-1</sup> owing to human activities such as burning of fossil fuels, deforestation, and cement production. It is an urgent task to estimate as accurately as possible the absorption capacity of the oceans against the increased atmospheric CO<sub>2</sub>, and to clarify the mechanism of the CO<sub>2</sub> absorption, because the magnitude of the anticipated global warming depends on the levels of CO<sub>2</sub> in the atmosphere, and because the ocean currently absorbs 1/3 of the 6 Gt of carbon emitted into the atmosphere each year

by human activities.

In this cruise, we were aimed at quantifying how much anthropogenic CO<sub>2</sub> absorbed in the surface ocean in the western North Pacific. For the purpose, we measured pCO<sub>2</sub> (partial pressure of CO<sub>2</sub>) in the atmosphere and surface seawater along the WOCE P01 line along 47°N.

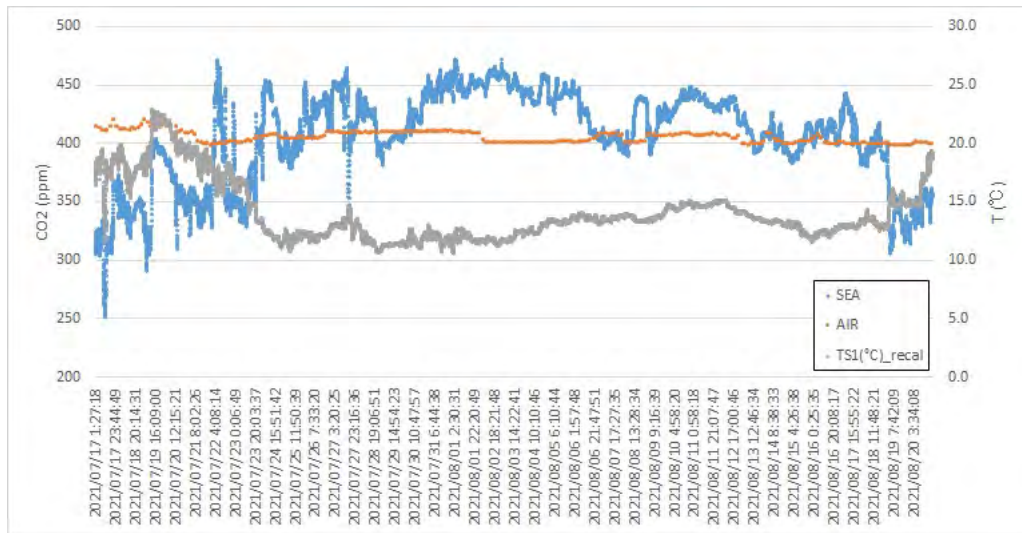
### (3) Apparatus

Continuous measurements of atmospheric and surface seawater pCO<sub>2</sub> were made with the CO<sub>2</sub> measuring system (Nihon ANS, Inc.) installed in the R/V *Mirai*. The system comprises of an off-axis integrated-cavity output spectroscopy gas analyzer (Off-Axis ICOS; 911-0011, Los Gatos Research), an air-circulation module and a shower-head type equilibrator. To measure concentrations (mole fraction) of CO<sub>2</sub> in dry air (xCO<sub>2a</sub>), air sampled from the bow of the ship (approx. 13 m above the sea level) was introduced into the NDIR and the Off-Axis ICOS through a dehydrating route. To measure surface seawater concentrations of CO<sub>2</sub> in dry air (xCO<sub>2s</sub>), the air equilibrated with seawater within the equilibrator was introduced into the NDIR and the Off-Axis ICOS through the same flow route for dehydration used for xCO<sub>2a</sub>. The flow rate of the equilibrated air was 600 – 800 ml min<sup>-1</sup>. The seawater was taken by a pump from the intake placed at the approx. 4.5 m below the sea surface. The flow rate of seawater in the equilibrator was 4000 – 5000 ml min<sup>-1</sup>. The CO<sub>2</sub> measuring system was set to repeat the measurement cycle such as 4 kinds of CO<sub>2</sub> standard gases of 260, 300, 391, and 461 ppmv, values of which are traceable to the WMO2007 scale, xCO<sub>2a</sub> (twice), and xCO<sub>2s</sub> (7 times). The xCO<sub>2</sub> were converted to pCO<sub>2</sub> at 100 % humidity with SST and SSS.

### (4) Results

The repeatability of xCO<sub>2</sub> measurement was estimated to be ~0.2 ppmv based on a standard gas measurement. Concentrations of CO<sub>2</sub> (xCO<sub>2</sub>) of marine air and surface seawater are shown in Fig. 3.16.1, together with SST.

Fig. 3.16.1 Preliminary results of concentrations of CO<sub>2</sub> (xCO<sub>2</sub>) in atmosphere and surface seawater observed during MR21-04.



### 3.17 Sea Surface Gravity

#### (1) Personnel

Shinya Kouketsu	JAMSTEC: Principal investigator
Masanori Murakami	Nippon Marine Enterprises, Ltd (NME)
Wataru Tokunaga	NME
Fumine Okada	NME
Yoichi Inoue	MIRAI crew

#### (2) Introduction

The local gravity is an important parameter in geophysics and geodesy. The gravity data were collected during this cruise.

#### (3) Parameters

Relative Gravity [CU: Counter Unit]

$$[\text{mGal}] = (\text{coef1: } 0.9946) * [\text{CU}]$$

#### (4) Data Acquisition

The relative gravity using LaCoste and Romberg air-sea gravity meter S-116 (Micro-g LaCoste, LLC) was measured during this cruise. To convert from the relative gravity to absolute one, we measured gravity, using portable gravity meter (Scintrex gravity meter CG-5), at Shimizu port as the reference points.

#### (5) Preliminary Results

Absolute gravity table is shown in Table 3.17-1.

Table 3.17-1. Absolute gravity table of the MR21-04 cruise

---

#### Absolute Sea Ship Gravity at S-116

No.	Date	UTC	Port	Gravity	Level	Draft	Sensor*	Gravity
	mm/dd			[mGal]	[cm]	[cm]	[mGal]	[mGal]
#1	07/13	00:08	Shimizu	979,728.87	149	670	979729.64	12005.42
#2	08/26	22:59	Shimizu	979,728.87	111	622	979729.42	12007.14

---

$$*: \text{Gravity at Sensor} = \text{Absolute Gravity} + \text{Sea Level} * 0.3086 / 100 + (\text{Draft} - 530) / 100 * 0.2222$$

#### (6) Data archives

These data obtained in this cruise will be submitted to the Data Management Group of JAMSTEC and will be opened to the public via “Data Research System for Whole Cruise Information in JAMSTEC (DARWIN)” in JAMSTEC web site.

<http://www.godac.jamstec.go.jp/darwin/e>

### 3.18 Sea Surface Magnetic Field

#### (1) Personnel

Shinya Kouketsu	JAMSTEC: Principal investigator
Masanori Murakami	Nippon Marine Enterprises, Ltd (NME)
Wataru Tokunaga	NME
Fumine Okada	NME
Yoichi Inoue	MIRAI crew

## (2) Introduction

Measurement of magnetic force on the sea is required for the geophysical investigations of marine magnetic anomaly caused by magnetization in upper crustal structure. We measured geomagnetic field using a three-component magnetometer during this cruise.

## (3) Principle of ship-board geomagnetic vector measurement

The relation between a magnetic-field vector observed on-board,  $H_{ob}$ , (in the ship's fixed coordinate system) and the geomagnetic field vector,  $F$ , (in the Earth's fixed coordinate system) is expressed as:

$$H_{ob} = \tilde{A} \tilde{R} \tilde{P} \tilde{Y} F + H_p \quad (a)$$

where  $\tilde{R}$ ,  $\tilde{P}$  and  $\tilde{Y}$  are the matrices of rotation due to roll, pitch and heading of the ship, respectively.  $\tilde{A}$  is a 3 x 3 matrix which represents magnetic susceptibility of the ship, and  $H_p$  is a magnetic field vector produced by a permanent magnetic moment of the ship's body. Rearrangement of Eq. (a) makes

$$\tilde{B} H_{ob} + H_{bp} = \tilde{R} \tilde{P} \tilde{Y} F \quad (b)$$

where  $\tilde{B} = \tilde{A}^{-1}$ , and  $H_{bp} = -\tilde{B} H_p$ . The magnetic field,  $F$ , can be obtained by measuring  $\tilde{R}$ ,  $\tilde{P}$ ,  $\tilde{Y}$  and  $H_{ob}$ , if  $\tilde{B}$  and  $H_{bp}$  are known. Twelve constants in  $\tilde{B}$  and  $H_{bp}$  can be determined by measuring variation of  $H_{ob}$  with  $\tilde{R}$ ,  $\tilde{P}$ , and  $\tilde{Y}$  at a place where the geomagnetic field,  $F$ , is known.

## (4) Instruments on R/V MIRAI

A shipboard three-component magnetometer system (Tierra Tecnica SFG2018) is equipped on-board R/V MIRAI. Three-axes flux-gate sensors with ring-cored coils are fixed on the fore mast. Outputs from the sensors are digitized by a 20-bit A/D converter (1 nT/LSB), and sampled at 8 times per second. Ship's heading, pitch, and roll are measured by the Inertial Navigation System (INS) for controlling attitude of a Doppler radar. Ship's position and speed data are taken from LAN every second.

## (5) Data archives

These data obtained in this cruise will be submitted to the Data Management Group of JAMSTEC and will be opened to the public via "Data Research System for Whole Cruise Information in JAMSTEC (DARWIN)" in JAMSTEC web site.

<http://www.godac.jamstec.go.jp/darwin/e>

## (6) Remarks (Times in UTC)

The following periods, we made a "figure-eight" turn (a pair of clockwise and anti-clockwise rotation) for calibration of the ship's magnetic effect.

07:57 - 08:18, 15 Jul. 2021 around 42-56N, 145-25E

15:04 - 15:30, 26 Jul. 2021 around 46-59N, 162-16E

12:29 - 12:55, 10 Aug. 2021 around 47-00N, 149-32W

## 4. Hydrographic Measurement

### 4.1 CTDO<sub>2</sub>

September 23, 2021

#### (1) Personnel

Hiroshi Uchida (JAMSTEC) (Principal investigator)  
Katsuro Katsumata (JAMSTEC)  
Shinya Kouketsu (JAMSTEC)  
Sayaka Yasunaka (JAMSTEC)  
Rei Ito (MWJ) (Operation leader)  
Takayuki Hashimukai (MWJ)  
Tomokazu Chiba (MWJ)  
Ko Morita (MWJ)  
Hiroyuki Nakajima (MWJ)

#### (2) Objective

The CTDO<sub>2</sub>/water sampling measurements were conducted to obtain vertical profiles of seawater properties by sensors and water sampling.

#### (3) Instruments and method

Instruments used in this cruise are as follows:

##### *Winch and cable*

Traction winch system (4.5 ton), Dynacon, Inc., Bryan, Texas, USA (Fukasawa et al., 2004)  
Armored cable ( $\phi = 9.53$  mm), Rochester Wire & Cable, LLC, Culpeper, Virginia, USA  
Compact underwater slip ring swivel, Hanayuu Co., Ltd., Shizuoka, Japan (Uchida et al., 2018) (except for stations 27, 28, 29, and 30)

##### *Deck unit*

SBE 11plus, Sea-Bird Scientific, Bellevue, Washington, USA  
Serial no. 11P54451-0872

##### *For 36-position sample bottles system*

##### *Frame and water sampler*

460 kg stainless steel frame for 36-position 12-L water sample bottles with an aluminum rectangular fin (54 × 90 cm) to resist frame's rotation  
(weight of the full CTD/water sampling package was about 930 kg)

36-position carousel water sampler, SBE 32, Sea-Bird Scientific  
Serial no. 3254451-0826

12-L sample bottle, model OTE 110, OceanTest Equipment, Inc., Fort Lauderdale, Florida, USA  
(No TEFLON coating)

##### *Underwater unit*

Pressure sensor, SBE 9plus, Sea-Bird Scientific  
Serial no. 09P54451-1027 (117457) (calibration date: July 8, 2020)

Deep standard reference thermometer, SBE 35, Sea-Bird Scientific  
Serial no. 0022 (calibration date: June 10, 2021) (for stations 1–53)  
Serial no. 0045 (calibration date: June 10, 2021) (for stations 54–90)

Temperature sensor, SBE 3F, Sea-Bird Scientific  
Primary serial no. 031525 (calibration date: June 1, 2019)

Secondary serial no. 031359 (calibration date: June 27, 2019) (for stations 1–38, 54–90)  
Secondary serial no. 03P2730 (calibration date: December 28, 2019) (for stations 39–40)

Secondary serial no. 031524 (calibration date: October 8, 2019) (for stations 41–53)

Conductivity sensor, SBE 4C, Sea-Bird Scientific  
Primary serial no. 042435 (calibration date: June 25, 2019)  
Secondary serial no. 041206 (calibration date: June 25, 2019)

Dissolved oxygen sensor  
primary, RINKO III, JFE Advantech Co., Ltd., Hyogo, Japan  
Serial no. 0287, Sensing foil no. 192326 (calibration date: June 10, 2021)  
Secondary, SBE 43, Sea-Bird Scientific  
Serial no. 432211 (calibration date: June 19, 2019)

Transmissometer, C-Star, WET Labs, Inc., Philomath, Oregon, USA  
Serial no. 1363DR

Chlorophyll fluorometer, Seapoint Sensors Inc., Exeter, New Hampshire, USA  
Serial no. 3618, Gain: 30X (0-5 ug/L) for stations 1, 27–90  
Gain: 10X (0-15 ug/L) for stations 2–26

Ultraviolet fluorometer, Seapoint Sensors Inc.  
Serial no. 6245, Gain 30X (0-50 QSU)

Turbidity meter, Seapoint Sensors Inc.  
Serial no. 14953, Gain 100X (0-25 FTU)

Photosynthetically Active Radiation (PAR) sensor, PAR-Log ICSW,  
Satlantic, LP, Halifax, Nova Scotia, Canada  
Serial no. 1025 (calibration date: July 6, 2015)

Altimeter, PSA-916T, Teledyne Benthos, Inc.  
Serial no. 1100

Pump, SBE 5T, Sea-Bird Scientific  
Primary serial no. 055816  
Secondary serial no. 054598

Other additional sensors  
Upward and downward looking lowered acoustic Doppler current profilers  
Micro Ridar (two micro temperature sensors)  
AFP07 (micro temperature and conductivity sensors or two micro temperature sensors)

For 12-position sample bottles system (only at station 10 cast 2)

Frame and water sampler

Aluminum frame for 12-position 12-L water sample bottles  
12-position carousel water sampler, SBE 32, Sea-Bird Scientific  
Serial no. 3227443-0389

12-L Niskin-X water sample bottle, model 1010X, General Oceanic, Inc., Miami,  
Florida, USA  
(No TEFLON coating)

Underwater unit

Pressure sensor, SBE 9plus, Sea-Bird Scientific  
Serial no. 09P27443-0677 (79511) (calibration date: July 8, 2020)

Deep standard reference thermometer, SBE 35, Sea-Bird Scientific  
Serial no. 0045 (calibration date: June 10, 2021)

Temperature sensor, SBE 3F, Sea-Bird Scientific  
Primary serial no. 031524 (calibration date: October 8, 2019)  
Secondary serial no. 03P2730 (calibration date: December 28, 2019)

Conductivity sensor, SBE 4C, Sea-Bird Scientific  
Primary serial no. 043036 (calibration date: June 25, 2019)  
Secondary serial no. 041203 (calibration date: October 4, 2019)

Dissolved oxygen sensor  
primary, RINKO III, JFE Advantech Co., Ltd., Osaka, Japan  
Serial no. 0278, Sensing foil no. 163010BA (calibration date: May 28, 2021)

Altimeter, PSA-916T, Teledyne Benthos, Inc.  
Serial no. 1157

Pump, SBE 5T, Sea-Bird Scientific  
Primary serial no. 053118  
Secondary serial no. 054595

#### Software

Data acquisition software, SEASAVE-Win32, version 7.26.7.121

Data processing software, SBEDataProcessing-Win32, version 7.26.7.129 and some original modules

### (4) Pre-cruise calibration

#### i) Pressure sensor

Pre-cruise sensor calibration for linearization was performed at Sea-Bird Scientific. The time drift of the pressure sensor was adjusted by periodic recertification corrections by using electric dead-weight testers (model E-DWT-H A70M and A200M, Fluke Co., Phoenix, Arizona, USA) and a barometer (model RPM4 BA100Ks, Fluke Co.):

Serial no. 181 (A70M) (for 10-70 MPa) (calibration date: December 7, 2020)

Serial no. 1305 (A200M) (for 90 to 100 MPa) (calibration date: December 7, 2020)

Serial no. 1453 (BA100Ks) (for 0 MPa) (calibration date: November 26, 2020)

These reference pressure sensors were calibrated by Ohte Giken, Inc. (Ibaraki, Japan) traceable to National Institute of Standards and Technology (NIST) pressure standards. The pre-cruise correction was performed at JAMSTEC (Kanagawa, Japan) by Marine Works Japan Ltd. (MWJ) (Kanagawa, Japan) (Fig. 4.1.1).

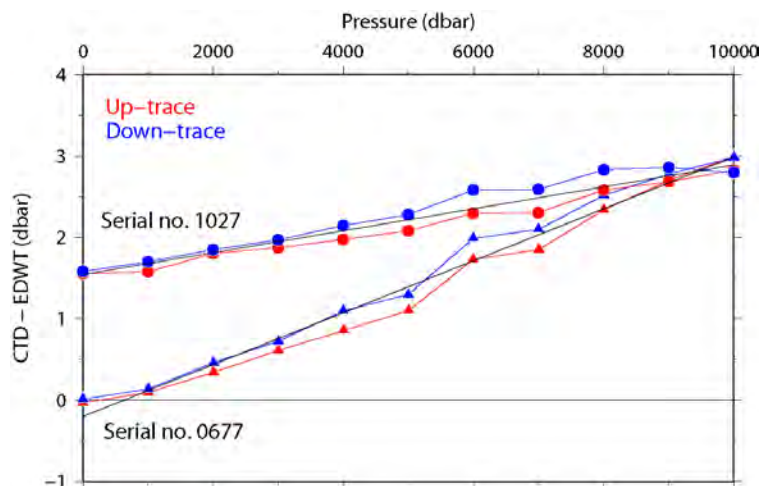


Fig. 4.1.1. Pre-cruise comparison of the CTD pressure and the reference pressure (E-DWT).

ii) Temperature sensors

Pre-cruise sensor calibrations of the SBE 3s were performed at Sea-Bird Scientific. Pre-cruise sensor calibration of the SBE 35 for linearization was also performed at Sea-Bird Scientific. The slow time drift of the SBE 35 was adjusted by periodic recertification corrections by measurements in thermodynamic fixed-point cells (water triple point [0.01 °C] and gallium melt point [29.7646b °C]) (Uchida et al., 2015). Since 2016, pre-cruise calibration was performed at JAMSTEC by using fixed-point cells traceable to National Metrology Institute of Japan (NMIJ) temperature standards (Fig. 4.1.2).

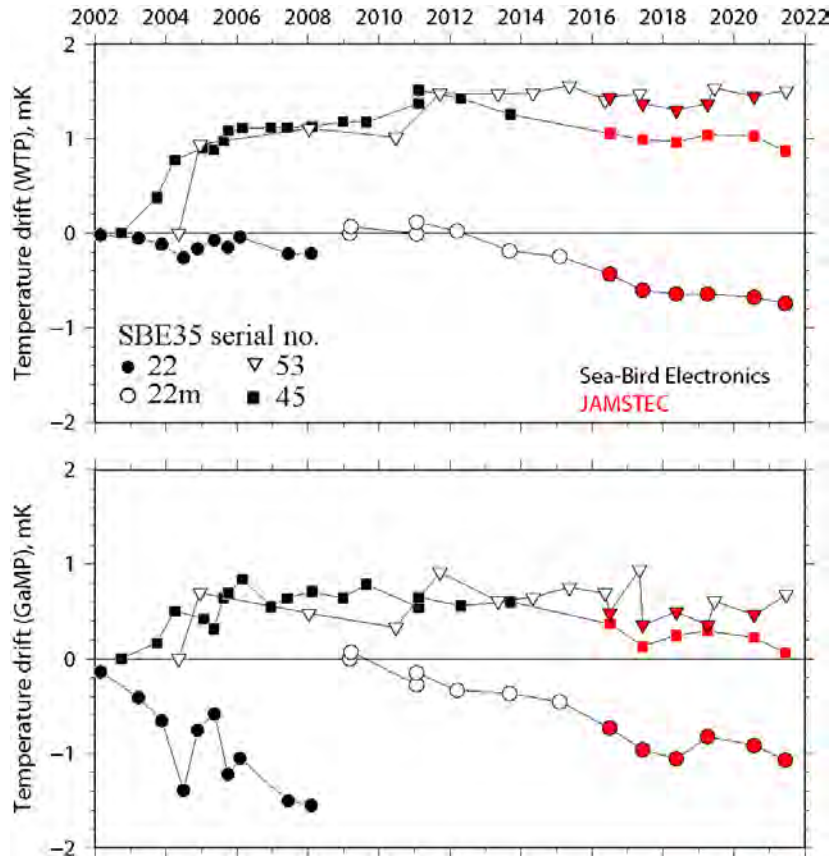


Fig. 4.1.2. Time drifts (temperature offsets relative to the first calibration) of four SBE 35s based on laboratory calibrations in fixed-point cells (water triple point: WTP, gallium melt point: GaMP).

iii) Conductivity sensors

Pre-cruise sensor calibrations were performed at Sea-Bird Scientific.

iv) Dissolved oxygen sensors

Pre-cruise sensor calibration of RINKO was performed at JAMSTEC by using O<sub>2</sub>/N<sub>2</sub> standard gases (JCSS Grande 1, Taiyo Nippon Sanso Co., Japan):

3.978% of O<sub>2</sub>, chamber no. 3MK-61964 (certification date: May 29, 2018)

9.979% of O<sub>2</sub>, chamber no. 1MK-52697 (certification date: May 29, 2018)

16.97% of O<sub>2</sub>, chamber no. 3MK-35986 (certification date: May 29, 2018)

24.96% of O<sub>2</sub>, chamber no. MK-84510 (certification date: May 24, 2018)

The standard gas-saturated pure water was measured by the RINKO at temperature of 1, 10, 20 and 29 °C. Oxygen saturation was calculated from oxygen concentration of the standard gases, water temperature, and the atmospheric pressure in the calibration vessel and used to calibrate the RINKO (serial no. 0252) by using the modified Stern-Volmer equation slightly modified from a

method by Uchida et al. (2010).

However, D/A converter circuit of the calibrated RINKO was broken just before the first cast of the cruise. Therefore, other RINKO (serial no. 0287) was used by replacing the sensing foil with the sensing foil for the pre-cruise calibrated RINKO (serial no. 0252).

The calibration coefficients for the pressure dependency were determined from the results from the previous cruises. Details of the calibration equations are described in the sub-section of the post-cruise calibration.

Pre-cruise sensor calibration of SBE 43 was performed at Sea-Bird Scientific.

v) *Transmissometer*

Light transmission ( $T_r$  in %) is calibrated as

$$T_r = (V - V_d) / (V_r - V_d) \times 100$$

where  $V$  is the measured signal (voltage),  $V_d$  is the dark offset for the instrument, and  $V_r$  is the signal for clear water.  $V_d$  can be obtained by blocking the light path. The calibration coefficients ( $V_d$  and  $V_r$ ) estimated from the previous cruise were used, because periodic recertification was not performed by the manufacturer for the transmissometer.

vi) *Turbidity meter, chlorophyll fluorometer, ultraviolet fluorometer, PAR, altimeter*

Periodic recertification was not performed by the manufacturer for these sensors.

## (5) Data collection and processing

i) *Data collection*

The CTD system was powered on at least 20 minutes in advance of the data acquisition to stabilize the pressure sensor. The data was acquired at least two minutes before and after the CTD cast to collect atmospheric pressure data on the ship's deck.

The CTD package was lowered into the water from the starboard side and held 10 m beneath the surface to activate the pump. After the pump was activated, the package was lifted to the surface and lowered at a rate of 1.0 m/s to 200 m (or 300 m when significant wave height was high) then the package was stopped to operate the heave compensator of the crane. The package was lowered again at a rate of 1.2 m/s to the bottom. For the up cast, the package was lifted at a rate of 1.1 m/s except for bottle firing stops. As a rule, the bottle was fired after waiting from the stop for more than 30 seconds and the package was stayed at least 5 seconds for measurement of the SBE 35 at each bottle firing stops. For depths where vertical gradient of water properties was expected to be large (from surface to thermocline), the bottle was fired after waiting from the stop for 60 seconds to enhance exchanging the water between inside and outside of the bottle. At 200 m (or 300 m) from the surface, the package was stopped to stop the heave compensator of the crane.

The water sample bottles and the stainless-steel frame of the CTD package were wiped with acetone before a cast taken water for CFCs.

ii) *Data collection problems*

There were many leaks and miss trip of the water sample bottles because the top or bottom cap of the bottle did not close correctly for the bottles model OTE 110 (OceanTest Equipment, Inc.).

At station 1, the chlorophyll fluorometer data were not obtained at the chlorophyll max layer (3-7 dbar in the down cast and 1-28 dbar in the up cast) due to low measurement range (0-5  $\mu\text{g/L}$ ) of the sensor. Therefore, the measurement range was changed to 0-15  $\mu\text{g/L}$  by replacing the sensor cable from station 2 to 26. Nonetheless, the data were not obtained at the chlorophyll max layer (9-10 dbar in the up cast) of station 9.

For the transmissometer, data quality of the sensor output was bad at station 43 (2612-4866 dbar in the down cast), 65 (4317-5737 dbar in the down cast), 68 (1208-5908 dbar in the down cast), 72 (2148-5491 dbar in the down cast), and 89 (602-5133 dbar in the down cast). Therefore, the bad data were replaced with the good data obtained at the same depth range of the up or down cast for

each station.

For the turbidity sensor, data quality of the sensor output was bad at station 24 (233-3371 dbar in the down cast), 38 (70-199 dbar in the down cast), 40 (5733-5576 dbar in the up cast), 45 (4377-5199 dbar in the down cast), 68 (1-3041 dbar in the up cast), 74 (738-834 dbar in the up cast), 79 (641-1858 dbar in the down cast), and 85 (613-3497 dbar in the down cast). Therefore, the bad data were replaced with the good data obtained at the same depth range of the up or down cast for each station.

At station 19, a fuse of the deck unit blew, and data logging stopped at 3750 dbar in the up cast. Data logging was restarted at the depth. Data during the stop of data logging were linearly interpolated in time at the data processing. The slip ring swivel was replaced after the cast.

At station 27, sensor error occurred at 2978 dbar in the down cast, and the cast was aborted. The second cast was conducted after removing the slip ring swivel. The slip ring swivel was attached to the system after station 30 with replacing the oil in the slip ring swivel.

At station 39, the secondary temperature sensor was changed from serial no. 1359 to 2730. At station 41, the secondary temperature sensor was changed from serial no. 2730 to 1524. At station 54, the secondary temperature sensor and the deep ocean standard thermometer (SBE 35) were changed from serial no. 1524 to 1359 and serial no. 22 to 45, respectively.

At station 66, the slip ring swivel was replaced.

The ultraviolet fluorometer data showed erroneous shift at all casts after station 16, probably due to crack of the LED light.

### *iii) Data processing*

The following are the data processing software (SBEDataProcessing-Win32) and original software data processing module sequence and specifications used in the reduction of CTD data in this cruise.

DATCNV converted the raw data to engineering unit data. DATCNV also extracted bottle information where scans were marked with the bottle confirm bit during acquisition. The duration was set to 4.4 seconds, and the offset was set to 0.0 second. The hysteresis correction for the SBE 43 data (voltage) was applied for both profile and bottle information data.

TCORP (original module, version 1.1) corrected the pressure sensitivity of the SBE 3 for both profile and bottle information data.

RINKOCOR (original module, version 1.0) corrected the time-dependent, pressure-induced effect (hysteresis) of the RINKO for both profile data.

RINKOCORROS (original module, version 1.0) corrected the time-dependent, pressure-induced effect (hysteresis) of the RINKO for bottle information data by using the hysteresis-corrected profile data.

BOTTLESUM created a summary of the bottle data. The data were averaged over 4.4 seconds.

ALIGNCTD converted the time-sequence of sensor outputs into the pressure sequence to ensure that all calculations were made using measurements from the same parcel of water. For a SBE 9plus CTD with the ducted temperature and conductivity sensors and a 3000-rpm pump, the typical net advance of the conductivity relative to the temperature is 0.073 seconds. So, the SBE 11plus deck unit was set to advance the primary and the secondary conductivity for 1.73 scans ( $1.75/24 = 0.073$  seconds). Oxygen data are also systematically delayed with respect to depth mainly because of the long time constant of the oxygen sensor and of an additional delay from the transit time of water in the pumped plumbing line. This delay was compensated by 5 seconds advancing the SBE 43 oxygen sensor output (voltage) relative to the temperature data. Delay of the RINKO data was also compensated by 1 second advancing sensor output (voltage) relative to the temperature data. Delay of the transmissometer data was also compensated by 2 seconds advancing sensor output (voltage) relative to the temperature data.

WILDEDIT marked extreme outliers in the data files. The first pass of WILDEDIT obtained an accurate estimate of the true standard deviation of the data. The data were read in blocks of 1000 scans. Data greater than 10 standard deviations were flagged. The second pass computed a standard deviation over the same 1000 scans excluding the flagged values. Values greater than 20 standard deviations were marked bad. This process was applied to pressure, temperature, conductivity, and SBE 43 output.

CELLTM used a recursive filter to remove conductivity cell thermal mass effects from the measured conductivity. Typical values used were thermal anomaly amplitude  $\alpha = 0.03$  and the time constant  $1/\beta = 7.0$ .

FILTER performed a low pass filter on pressure with a time constant of 0.15 seconds. To produce zero phase lag (no time shift) the filter runs forward first then backwards.

WFILTER performed as a median filter to remove spikes in fluorometer, turbidity meter, transmissometer, and ultraviolet fluorometer data. A median value was determined by 49 scans of the window. For the ultraviolet fluorometer data, an additional box-car filter with a window of 361 scans was applied to remove noise.

SECTIONU (original module, version 1.1) selected a time span of data based on scan number to reduce a file size. The minimum number was set to be the start time when the CTD package was beneath the sea-surface after activation of the pump. The maximum number was set to be the end time when the depth of the package was 1 dbar below the surface. The minimum and maximum numbers were automatically calculated in the module.

LOOPEDIT marked scans where the CTD was moving less than the minimum velocity of 0.0 m/s (traveling backwards due to ship roll).

DESPIKE (original module, version 1.0) removed spikes of the data. A median and mean absolute deviation was calculated in 1-dbar pressure bins for both down- and up-cast, excluding the flagged values. Values greater than 4 mean absolute deviations from the median were marked bad for each bin. This process was performed 2 times for temperature, conductivity, SBE 43, and RINKO output.

DERIVE was used to compute oxygen (SBE 43).

BINAVG averaged the data into 1-dbar pressure bins. The center value of the first bin was set equal to the bin size. The bin minimum and maximum values are the center value plus and minus half the bin size. Scans with pressures greater than the minimum and less than or equal to the maximum were averaged. Scans were interpolated so that a data record exist every dbar.

BOTTOMCUT (original module, version 0.1) deleted the deepest pressure bin when the averaged scan number of the deepest bin was smaller than the average scan number of the bin just above.

DERIVE was re-used to compute salinity, potential temperature, and density

SPLIT was used to split data into the down cast and the up cast.

Remaining spikes in the CTD data were manually eliminated from the 1-dbar-averaged data. The data gaps resulting from the elimination were linearly interpolated with a quality flag of 6.

## **(6) Post-cruise calibration**

### *i) Pressure sensor*

The CTD pressure sensor offset in the period of the cruise was estimated from the pressure readings on the ship's deck. For best results the Paroscientific sensor was powered on for at least 20 minutes before the operation. To get the calibration data for the pre- and post-cast pressure sensor drift, the CTD deck pressure was averaged over first and last one minute, respectively. Then the atmospheric pressure deviation from a standard atmospheric pressure (1013.25 hPa) was subtracted from the CTD deck pressure to check the pressure sensor time drift. The atmospheric pressure was measured at the captain deck (20 m high from the base line) and sub-sampled one-minute interval as

a meteorological data.

Time series of the CTD deck pressure is shown in Figs. 4.1.3 and 4.1.4. The CTD pressure sensor offset was estimated from the deck pressure. Mean of the pre- and the post-casts data over the whole period gave an estimation of the pressure sensor offset (0.34 and 0.11 dbar for the 36-position and 12-position sample bottle system, respectively) from the pre-cruise calibration. The post-cruise correction of the pressure data is not deemed necessary for the pressure sensors.

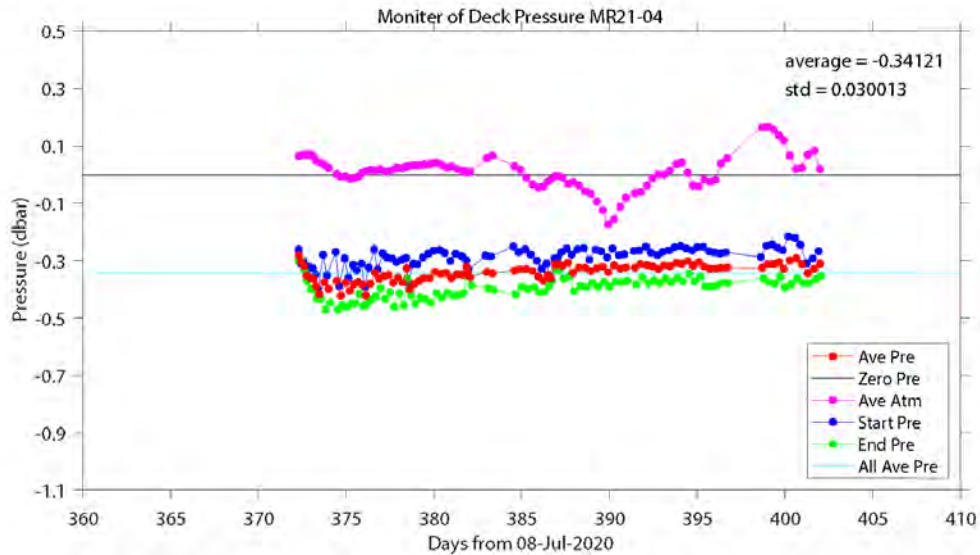


Fig. 4.1.3. Time series of the CTD deck pressure for the 36-position sample bottle system. Atmospheric pressure deviation (magenta dots) from a standard atmospheric pressure was subtracted from the CTD deck pressure. Blue and green dots indicate pre- and post-cast deck pressures, respectively. Red dots indicate averages of the pre- and the post-cast deck pressures.

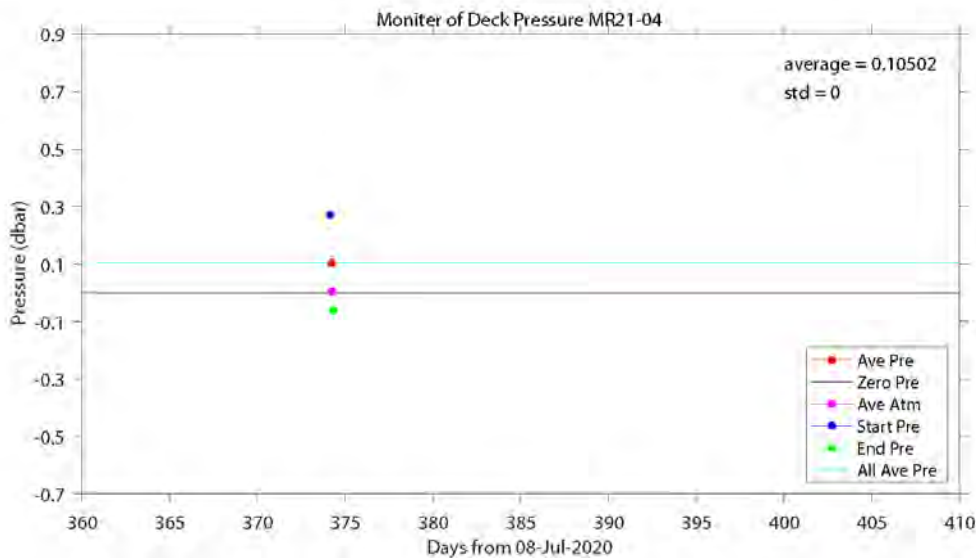


Fig. 4.1.4. Same as Fig. 4.1.3, but for the 12-position sample bottle system.

## (7) References

- Edwards, B., D. Murphy, C. Janzen and N. Larson (2010): Calibration, response, and hysteresis in deep-sea dissolved oxygen measurements, *J. Atmos. Oceanic Technol.*, 27, 920–931.
- Fukasawa, M., T. Kawano and H. Uchida (2004): Blue Earth Global Expedition collects CTD data aboard Mirai, BEAGLE 2003 conducted using a Dynacon CTD traction winch and

motion-compensated crane, *Sea Technology*, 45, 14–18.

García, H. E. and L. I. Gordon (1992): Oxygen solubility in seawater: Better fitting equations. *Limnol. Oceanogr.*, 37 (6), 1307–1312.

Uchida, H., G. C. Johnson, and K. E. McTaggart (2010): CTD oxygen sensor calibration procedures, The GO-SHIP Repeat Hydrography Manual: A collection of expert reports and guidelines, IOCCP Rep., No. 14, ICPO Pub. Ser. No. 134.

Uchida, H., Y. Maeda and S. Kawamata (2018): Compact underwater slip ring swivel: Minimizing effect of CTD package rotation on data quality, *Sea Technology*, 11, 30–32.

Uchida, H., T. Nakano, J. Tamba, J. V. Widiatmo, K. Yamazawa, S. Ozawa and T. Kawano (2015): Deep ocean temperature measurement with an uncertainty of 0.7 mK, *J. Atmos. Oceanic Technol.*, 32, 2199–2210.

#### **(8) Data archive**

These obtained data will be submitted to JAMSTEC Data Management Group (DMG).

## **4.2 Bottle Salinity**

August 22, 2021

#### **(1) Personnel**

Hiroshi Uchida	JAMSTEC
Tomokazu Chiba	MWJ
Rei Ito	MWJ

#### **(2) Objective**

Bottle salinities were measured to calibrate the CTD and TSG salinity data.

#### **(3) Instruments, materials, and method**

Salinity measurement was conducted basically based on the method by Kawano (2010). Instruments and materials used in this cruise were as follows:

- Standard Seawater: IAPSO Standard Seawater (Ocean Scientific International Ltd., Hampshire, UK)  
Batch P164
- Secondary Standard Seawater: MSSW (KANSO Co., Ltd., Japan)  
Lot PRE19
- Salinometer: Autosal model 8400B (Guildline Instruments, Ltd., Ontario, Canada)  
Serial no. 62556
- A peristaltic-type sample intake pump (Ocean Scientific International Ltd.)
- Thermometers: PRT model 1502A (Fluke Co., Everett, Washington, USA)  
Serial no. B81549 (for monitoring the bath temperature)  
Serial no. B78466 (for monitoring the room temperature)
- Stabilized power supply: model PCR1000LE (Kikusui Electronics Co., Japan)
- Sample bottles: 250 mL brown borosilicate glass bottles with screw caps (PTFE packing)
- Ultra-pure water: Milli-Q water (Millipore, Billerica, Massachusetts, USA)
- Sub-standard seawater: Surface seawater collected in the cruise MR19-04 by filtering with a 0.20  $\mu\text{m}$  pore capsule cartridge filter (ADVANTEC, Toyo Roshi Kaisha Ltd., Japan)
- Detergent: 2% neutral detergent, SCAT 20X-N (Dai-ichi Kogyo Seiyaku Co., Ltd., Japan)

The bath temperature of the salinometer was set to 24 °C. The salinometer was standardized only at the beginning of the cruise by using the IAPSO Standard Seawater (SSW). The standardization dial was set to 609 and never changed during the cruise. The mean and  $\pm$ standard deviation of the STANDBY and ZERO was  $5134 \pm 0.8$  and  $0.00000 \pm 0.000005$ , respectively. The mean and  $\pm$ standard deviation of the ambient room temperature was  $23.7 \pm 0.3$  °C, while that of the bath

temperature was  $23.995 \pm 0.0008$  °C.

The double conductivity ratios measured by the salinometer were used to calculate practical salinity using the algorithm for Practical Salinity Scale 1978 (IOC et al., 2010). A constant temperature of 24 °C was used in the calculation instead of using the measured bath temperature.

The measurement cell of the salinometer was rinsed with 2% neutral detergent and ultra-pure water after each day of measurement, and the electrode in the cell was soaked in ultra-pure water until next measurement. From July 27, the electrode was soaked in the neutral detergent for several hours or more after each day of measurement. This effectively reduced time drift of the salinometer as shown in Fig. 4.2.1.

Ultra-pure water and the IAPSO SSW were measured at the beginning and the end of each day of measurement (for samples of 1~3 stations). Sub-standard seawater was measured every about 10 samples to monitor stability of the salinometer during each day of measurement.

The results of the ultra-pure water and the IAPSO SSW measurement (Fig 4.2.1) suggest that the salinometer drifted in time by changing the span of the slope. However, the salinity range of the seawater sample was close to the salinity of SSW (about 35 g/kg) as described blow. Therefore, the offset time-drift correction is adequate for the seawater samples. The offset was estimated from average of the IAPSO SSW measurements for each day of measurement and the measured double conductivity ratios were corrected by using the estimated offset for each day of measurement (Fig. 4.2.1). The standard deviation of the IAPSO SSW measurements was 0.00001, which is equivalent to 0.0002 in salinity, after the time drift correction. Mean and  $\pm$ standard deviation of the ultra-pure water measurements was  $0.00016 \pm 0.000006$ .

The Multi-parametric Standard Seawater (MSSW) (lot PRE19) (Uchida et al. 2020) was also measured as a secondary standard at the same day of measurement for station 38 to check offset of the IAPSO Standard Seawater. Mean and  $\pm$ standard deviation was  $34.2740 \pm 0.0001$  for four bottles of PRE19.

The linearity error of the salinometer was estimated by using decade resistance substituters. For the salinometer (serial no. 62556) used in this cruise, the linearity error was estimated to be  $\pm 0.0005$  in salinity for salinity around 35 (Uchida et al. 2020).

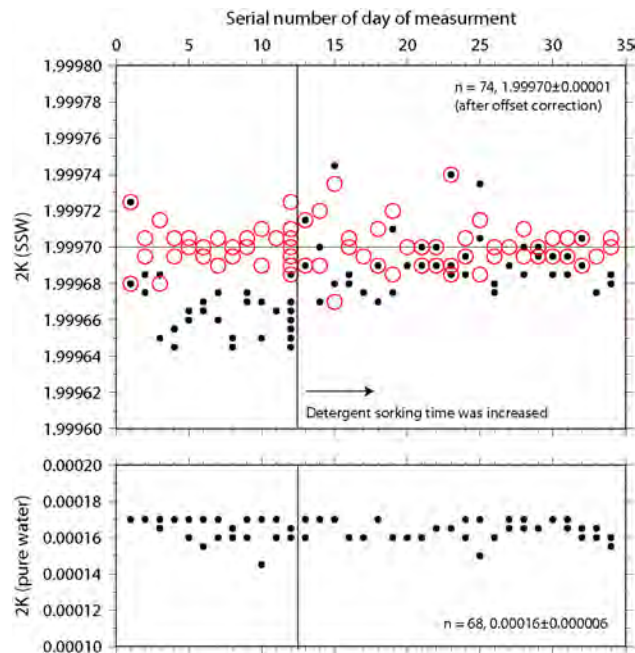


Figure 4.2.1. Time-series of the measured double conductivity ratios (closed circles) for the ultra-pure water (lower panel) and the IAPSO SSW (upper panel). The time-drift corrected double conductivity ratios for the IAPSO SSW were also shown in open red circles.

#### (4) Results

A total of 1,825 (41) samples were measured for the CTD/water sampling (thermo-salinograph) measurement. Minimum and maximum value of the measured salinity was 32.3 and 34.7, respectively

As for the data quality flag, ten samples (stations 8 #15, 10 #22, 12 #22, 14 #22, 19 #15, 32 #13, 44 #17, 79 #21, 83 #19, 83 #19 replicate) were set to flag 3 (questionable measurement) judging from relatively large deviation from the CTD sensor value.

A total of 218 pairs of replicate samples was collected and the standard deviation of the replicate samples was 0.00023 in salinity.

At station 31, duplicate samples were collected from all Niskin bottles at  $5000.1 \pm 0.4$  dbar. Mean with standard deviation for the duplicate samples was  $34.6882 \pm 0.00019$  in salinity.

At station 80, twelve samples were collected from Niskin bottles (#1, #3-#13) at  $2999.8 \pm 0.2$  dbar for testing of CFCs measurement. Samples were taken from Niskin bottles just after on deck (#1, #3), 2 hours after that (#4, #5), 4 hours after that (#6, #7), 8 hours after that (#8, #9), 16 hours after that (#10, #11), and 24 hours after that (#12, #13). There was no leak and miss trip of the bottle. However, salinity in the Niskin bottle might slightly increase with time from on deck due to unknown reason (Fig. 4.2.2).

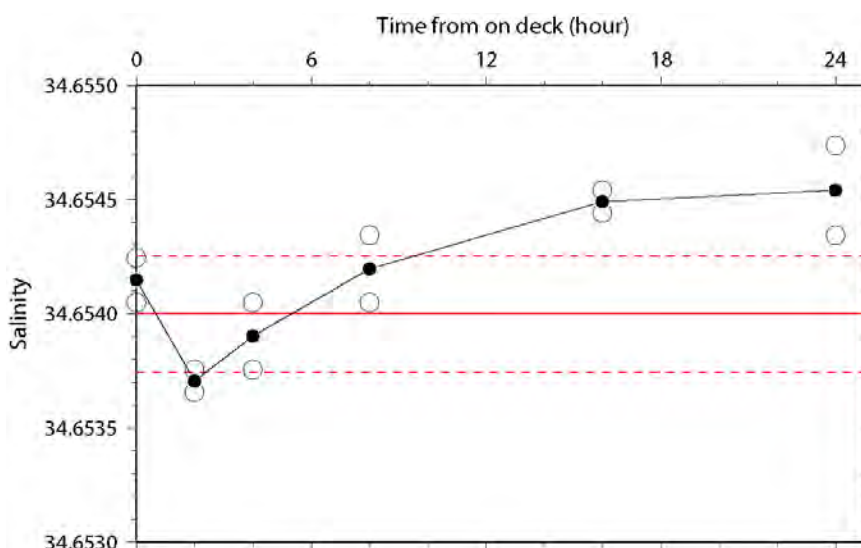


Figure 4.2.2. Stability in practical salinity with elapsed time from on deck of the Niskin bottles. Open circles indicate each measurement and closed circles indicate the average of the samples taken at the same time. The red solid and dashed lines indicate mean and  $\pm$ standard deviation of the salinity data for the first 8 samples.

#### (5) References

IOC, SCOR and IAPSO (2010): The international thermodynamic equation of seawater – 2010: Calculation and use of thermodynamic properties. Intergovernmental Oceanographic Commission, Manuals and Guides No. 56, UNESCO (English), 196 pp.

Kawano, T. (2010): Salinity. The GO-SHIP Repeat Hydrography Manual: A collection of Expert Reports and Guidelines, IOCCP Report No. 14, ICPO Publication Series No. 134, Version 1.

Uchida, H., T. Kawano, T. Nakano, M. Wakita, T. Tanaka and S. Tanihara (2020): An expanded batch-to-batch correction for IAPSO standard seawater. *J. Atmos. Oceanic Technol.*, doi:10.1175/JTECH-D-19-0184.1.

## (6) Data archive

These obtained data will be submitted to JAMSTEC Data Management Group (DMG).

## 4.3 Density and Refractive Index

August 20, 2021

### (1) Personnel

Hiroshi Uchida (JAMSTEC)

Yohei Kayukawa (NMIJ, AIST) (not onboard)

### (2) Objective

The objective of this study is to collect absolute salinity (also called “density salinity”) data and to evaluate the algorithm to estimate absolute salinity anomaly provided along with TEOS-10 (the International Thermodynamic Equation of Seawater 2010) (IOC et al., 2010).

### (3) Instruments and method

Seawater density for water samples were measured with a vibrating-tube density meter (DMA 5000M [serial no. 80570578], Anton-Paar GmbH, Graz, Austria) and a sample changer (Xsample 122 [serial no. 8548492], Anton-Paar GmbH). The sample changer is used to load samples automatically from up to ninety-six 12-mL glass vials.

Seawater refractive index was also simultaneously measured for the same water samples with a laboratory refractometer (Abbemat 650 [serial no. 99058548], Anton-Paar GmbH) by connected to the density meter. Light source of the refractometer is LED (wavelength of 589.3 nm).

The water samples collected in 250 mL brown borosilicate glass bottles with screw caps (PTFE packing) for practical salinity measurement were measured by taking the water sample into two 12-mL glass vials for each bottle just before practical salinity measurement. The glass vial was sealed with Parafilm M (Pechiney Plastic Packaging, Inc., Menasha, Wisconsin, USA) immediately after filling. Densities of the samples were measured at 20 °C by the density meter and refractometer two times (two vials) for each bottle and averaged to estimate the density and refractive index, respectively. It takes about 5 minutes and 15 seconds for one measurement of the density and refractive index, respectively. Resolution of the density meter is 0.001 kg/m<sup>3</sup>, and resolution of the refractometer is 0.000001 nD which is equivalent to 0.004 kg/m<sup>3</sup> in density.

The density meter was initially calibrated by measuring air and pure water according to the instrument manual. However, measured density for the IAPSO Standard Seawater deviates from density of TEOS-10 calculated from practical salinity and composition of seawater, probably due to non-linearity of the density meter (Uchida et al., 2011). The non-linearity can be corrected by measuring a reference sample simultaneously as:

$$\rho_{\text{corr}} = \rho - (\rho_{\text{ref}} - \rho_{\text{ref\_true}}) + c (\rho - \rho_{\text{ref\_true}}),$$

where  $\rho_{\text{corr}}$  is the corrected density of the sample,  $\rho$  is measured density of the sample,  $\rho_{\text{ref}}$  is measured density of the reference,  $\rho_{\text{ref\_true}}$  is true density of the reference, and  $c$  is non-linearity correction factor. The non-linearity correction factor is estimated to be 0.000341 for the density meter (serial no. 80570578). This factor was estimated from the density of the IAPSO Standard Seawater measured in this cruise and changed from the previous value (0.000411).

Time drift of the density meter and refractometer was corrected by periodically measuring the density of ultra-pure water (Milli-Q water, Millipore, Billerica, Massachusetts, USA) prepared from Yokosuka (Japan) tap water in October 2014 as the reference. The true density of the Milli-Q water at 20 °C was estimated to be 998.2041 kg m<sup>-3</sup> from the isotopic composition ( $\delta D = -8.86 \text{ ‰}$ ,  $\delta^{18}\text{O} = -59.9 \text{ ‰}$ ) and International Association for the Properties of Water and Steam (IAPWS)-95 standard. The ultra-pure water was measured at the beginning and the end of each day of measurement (for samples obtained at one to three stations).

For the refractometer, refractive index anomalies from the ultra-pure water measurement were

calculated for each day of measurement. Refractive index for pure water is about 1.332987 nD.

The IAPSO Standard Seawater (batch P164) and the Multi-parametric Standard Seawater (MSSW) (lot PRE19) (Uchida et al. 2020) were also measured to check the time drift correction. The IAPSO Standard Seawater was measured at the beginning and the end of each day of measurement (Fig. 4.3.1). The MSSW was measured at the same day of measurement for station 38. The measured densities are listed in Table 4.3.1. The measured refractive index anomalies are also listed in Table 4.3.2.

Table 4.3.1. Measured density at 20 °C of the IAPSO Standard Seawater and the Multi-parametric Standard Seawater (MSSW). True densities estimated from practical salinity and composition of seawater using TEOS-10 are also shown.

Standard Seawater	True density (kg/m <sup>3</sup> )	Measured density (kg/m <sup>3</sup> )	Number of measurements
P164	1024.7624	1024.7645±0.0013	73
PRE19	1024.2171	1024.2166±0.0009	5

Table 4.3.2. Measured refractive index anomaly from pure water measurement at 20 °C of the IAPSO Standard Seawater and the Multi-parametric Standard Seawater (MSSW).

Standard Seawater	Refractive index anomaly (10 <sup>5</sup> nD)	Number of measurements
P164	646.15±0.09	73
PRE19	633.13±0.04	5

#### (4) Results

Density and refractive index were measured for samples collected from all CTD/water sampling casts and from the continuous Sea Surface Water Monitoring System once in a day during the cruise. A total of 1770 samples were measured.

Density salinity (DNSSAL) can be back calculated from the measured density and temperature (20 °C) with TEOS-10. A total of 218 pairs of replicate samples was measured and the standard deviation of the replicate samples for density salinity and refractive index anomaly (RIANOMALY) was 0.0011 g/kg and 0.05 (in 10<sup>5</sup> nD), respectively.

The measured density salinity anomalies ( $\delta S_A$ ) are shown in Fig. 4.3.2. The measured  $\delta S_A$  was well agree with the  $\delta S_A$  estimated from Pawlowicz et al. (2011) which exploits the correlation between  $\delta S_A$  and nutrient concentrations (silicate and nitrate) and carbonate system parameters (total alkalinity and dissolved inorganic carbon) based on mathematical investigation.

The measured density salinity was well correlated with the measured refractive index anomaly (Fig. 4.3.3). The root-mean-square difference from the regression line (offset = -0.4084, slope = 0.0550571) was 0.0060 g/kg.

#### (5) References

IOC, SCOR and IAPSO (2010): The international thermodynamic equation of seawater – 2010: Calculation and use of thermodynamic properties. Intergovernmental Oceanographic Commission, Manuals and Guides No. 56, UNESCO (English), 196 pp.

Pawlowicz, R., D.G. Wright and F. J. Millero (2011): The effects of biogeochemical processes on ocean conductivity/salinity/density relationships and the characterization of real seawater. *Ocean Science*, 7, 363-387.

Uchida, H., T. Kawano, M. Aoyama and A. Murata (2011): Absolute salinity measurements of standard seawaters for conductivity and nutrients. *La mer*, 49, 237-244.

Uchida, H., T. Kawano, T. Nakano, M. Wakita, T. Tanaka and S. Tanihara (2020): An expanded batch-to-batch correction for IAPSO standard seawater. *J. Atmos. Oceanic Technol.*, doi:10.1175/JTECH-D-19-0184.1.

(6) Data archive

These obtained data will be submitted to JAMSTEC Data Management Group (DMG).

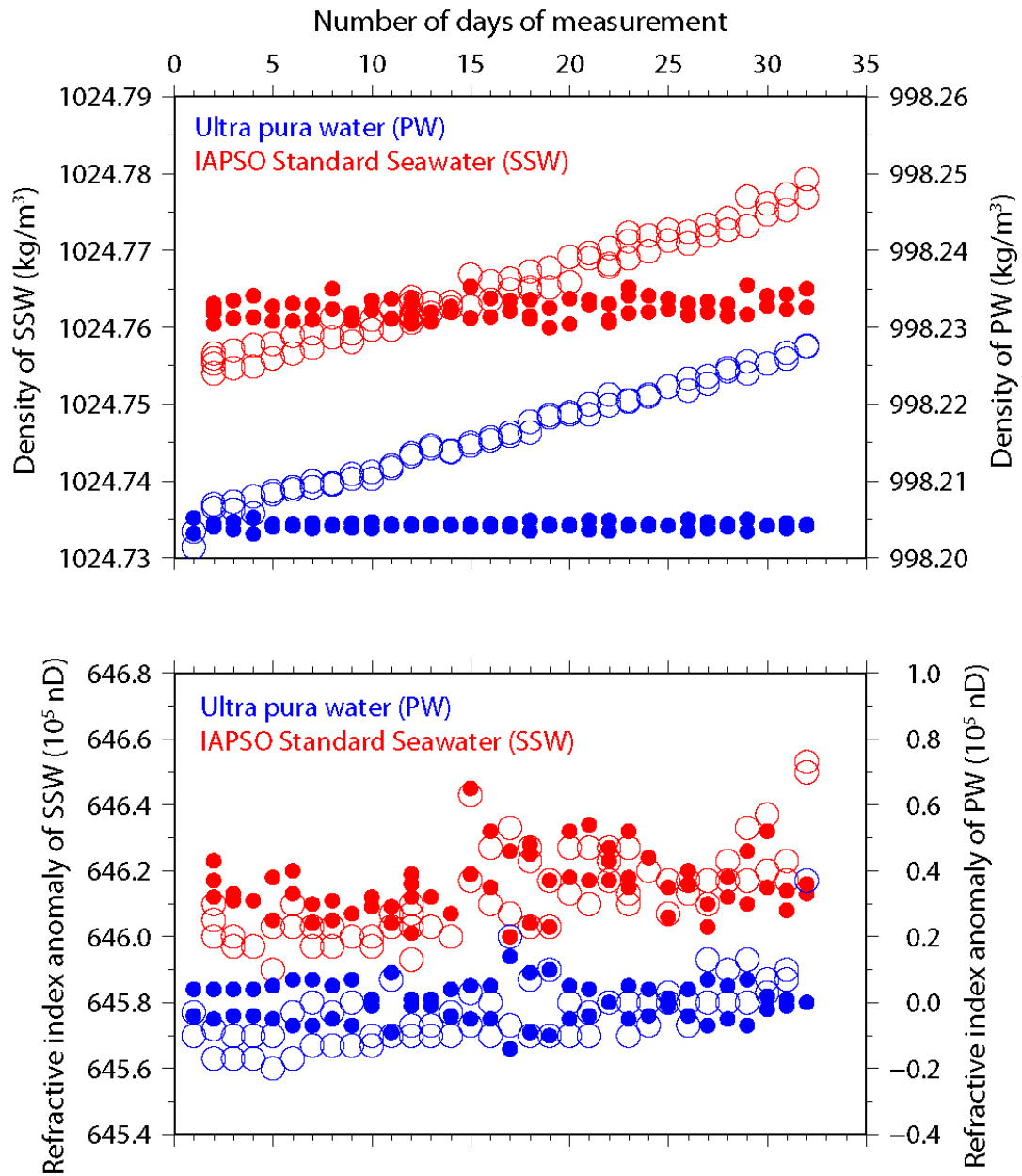


Figure 4.3.1. Time drift of the density meter and refractometer monitored with the ultra-pure water and the IAPSO Standard Seawater at each day of measurement. Open and closed circles indicate the data before and after the time drift correction, respectively.

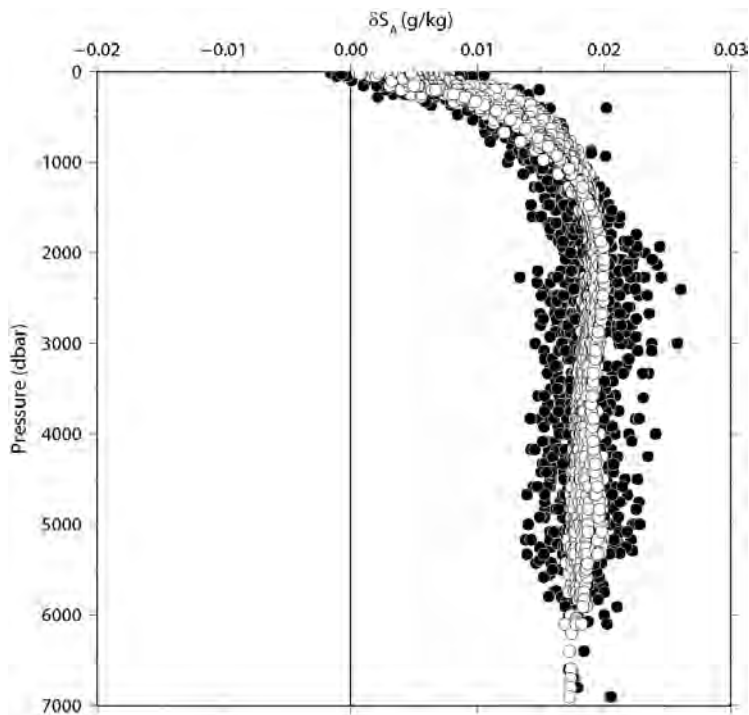


Figure 4.3.2. Vertical distribution of density salinity anomaly measured by the density meter (closed circles). Absolute salinity anomaly estimated from nutrients and carbonate system parameters (Pawlowicz et al., 2011) are also shown (open circles).

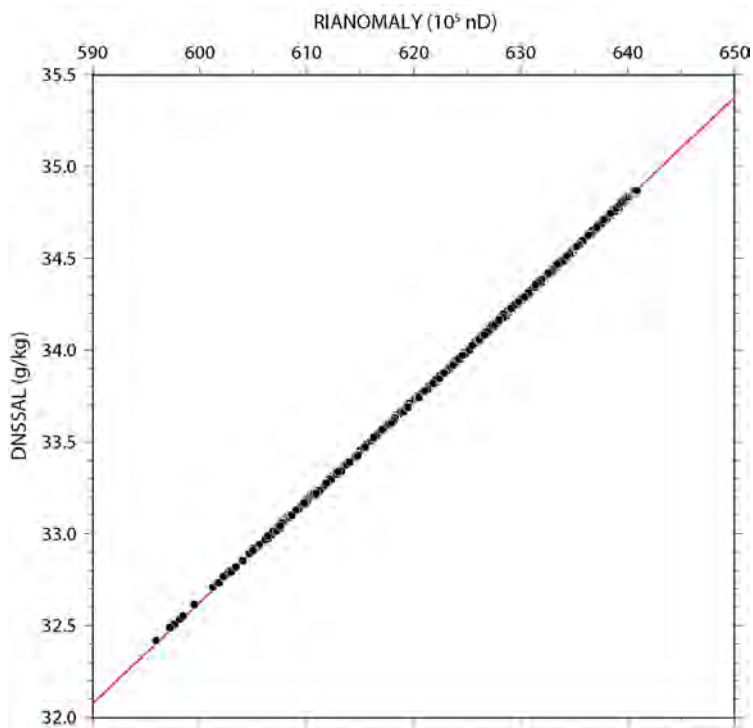


Figure 4.3.3. Comparison between density salinity (DNSSAL) measured by the density meter and refractive index anomaly (RIANOMALY) from pure water measurement. Red line shows the regression line.

## 4.4 Lowered Acoustic Doppler Current Profiler

### (1) Personnel

Shinya Kouketsu	JAMSTEC (principal investigator)
Katsuro Katsumata	JAMSTEC
Sayaka Yasunaka	JAMSTEC
Ichiro Yasuda	AORI
Yusuke Sasak	AORI

### (2) Overview of the equipment

Two acoustic Doppler current profilers (ADCP) were integrated with the CTD/RMS package. The lowered ADCP (LADCP)s, Workhorse Monitor WHM300 and WHM600 (Teledyne RD Instruments, San Diego, California, USA), which has 4 facing transducers with 20-degree beam angles, rated to 6000 m, make direct current measurements at the depth of the CTD, thus providing a full profile of velocity. The LADCPs were powered during the CTD casts by a 48 volts battery pack. The LADCP unit was set for recording internally prior to each cast. After each cast the internally stored observed data were downloaded to the computer in the onboard laboratory. After the cruise, by combining the measured velocity of the sea water and ocean bottom relative to the instrument, shipboard navigation data, and pressure time series from the CTD, the absolute velocity profiles will be obtained with the software implemented by A.Thunherr. The software is based on the method of Visbeck (2002) and available online at <ftp://ftp.ldeo.columbia.edu/pub/LADCP;>

The instruments used in this cruise were as follows.

St. 1-75: WHM600(S/N 8694; downward), WHM300(S/N 22595; upward)

St. 76-90: WHM300(S/N 91060; downward), WHM300(S/N 22595; upward)

### (3) Data collection

In this cruise, data were collected with the following configuration.

WHM600: Bin size: 4.0 m, Number of bins: 13

WHM300: Bin size: 8.0 m, Number of bins: 13

Some of the downloaded files were fragmented with occasional periods without data recordings (St. 2, 5-8, 11, 13, 19, 23, 31, 39, 40, 41, 42, 44, 45). We suspect this was caused by overloaded battery power with two sensors with the ping intervals set to 1s. With the longer ping intervals (1.5s in St. 46-48, 1.4s in St. 49-75) for WHM600 and WHM300, fragmentations did not occur. At St. 75, WHM600 stopped pinging during the downcast and the communication was lost. After recovery of the CTD package, the WHM600 was replaced with a WHM300. The ping intervals for the new WHM300 was set to 1.2s for St. 76-79, 89, 90. We set the ping interval to 1.3s for St. 80-88, because the file fragmentation was found again at St. 89 and 90.

Reference

Visbeck, M. (2002): Deep velocity profiling using Lowered Acoustic Doppler Current Profilers: Bottom track and inverse solutions. *J. Atmos. Oceanic Technol.*, **19**, 794-807.

## 4.5 Microstructure in Temperature and Conductivity

### (1) Personnel

Yusuke Sasaki	AORI (Principal investigator)
Ichiro Yasuda	AORI
Shinya Kouketsu	JAMSTEC
Katsuro Katsumata	JAMSTEC
Sayaka Yasunaka	JAMSTEC

## (2) Objective

The objective is to measure microstructure in temperature and conductivity to evaluate vertical mixing.

## (3) Instruments and method

Microstructure observations were carried out by micro-Rider 6000 (MR6000; Rockland Scientific International Inc.) and AFP07 (Rockland Scientific International Inc.), which were mounted on the CTD rosette and were powered from the CTD (SBE 9plus). We installed two fast response thermistors (FP07) on MR6000 to measure microstructure in temperature. On AFP07, which has also two sensor sockets, FP07 thermistor or micro-conductivity sensor (SBE-7) can be installed. For the first five stations (St.1-5), one FP07 thermistor and one micro-conductivity sensor were installed on AFP07. For the other stations (St.6-90), two FP07 thermistors were installed on both sockets of AFP07. We had to replace probes, as some of the probes failed during the cruise. MR6000 and AFP07 also measured high-frequency pressure and acceleration profiles. Low-frequency profiles of temperature and conductivity were recorded in the MR6000 (AFP07) with the input from the SBE-3 sensors on the CTD system. We downloaded the raw data from the instruments after each cast. We plan to examine methods for calibration and quality check of the data by comparing these micro temperature and conductivity with the CTD data and free fall micro shear structure data (VMP, see Section 4.7).

## (4) Measurements

### *i) Microstructure measurement*

For St.3-5, the downloaded files from MR6000 were sometimes fragmented into several parts. After the cast of St.5, MR6000 was removed from the CTD rosette, and the observation using MR6000 was not conducted for St.6-29. For these stations, microstructure data were recorded only by AFP07. The fragmentation was a result of excessive torque to the instrument lid applied after the internal battery replacement. Adjustment to the torque resulted in uninterrupted data recording. After resolving the problem, we mounted the MR6000 on the CTD rosette again and resumed the microstructure observation using MR6000 from St. 30.

For several stations (St. 31 for MR6000; St.13, 28, 42, 49 and 54 for AFP07), the data file did not exist. For these stations, the data file of AFP07 or MR6000 was either not created at all or recording stopped after a few minutes. We suspected that this was caused by the insufficient voltage of power supply from the CTD system when AFP07 (MR6000) was turned on. We tried to avoid the initial power peak by delaying the startup of MR6000 from that of AFP07, but the problem was not resolved. The cause of this problem was not known. In the latter stations, in order to prevent this startup failure, we maintained data connection to AFP07 after all other instruments were turned on. During this process, it was observed sometimes AFP07 did not start or stopped recording. When this happened, we turned off all powers including the CTD and re-started the startup process. After confirming a successful startup of AFP07 recording, we disconnected the data cable and proceeded to deploy the whole CTD package.

The probes installed on the instruments are described below:

#### MR6000

- Sensor socket 1: T2080 (St. 1-5), T2127 (St. 30-32), T2119 (St. 33-59) and T2121 (St. 60-90)
- Sensor socket 2: T2081 (St. 1-5), T2084 (St. 30-53) and T2120 (St. 54-90)

#### AFP07

- Sensor socket 1: T1967 (St. 1-14) and T2081 (St. 15-90)
- Sensor socket 2: C316 (St. 1-6), T2080 (St. 7-14) and T2082 (St. 15-90)

### *ii) Low-frequency Temperature and conductivity*

The low-frequency-temperature and conductivity profiles for several stations (St.36-40), which were obtained from AFP07, were corrupt, due to the problems in the cable connecting the SBE-3 sensor on the CTD system. The low frequency temperature and conductivity recorded in the AFP07

were not used for analysis for these stations.

**(5) Note for using data**

The file included in the data ‘mr6000.csv’ (‘AFP07.csv’) shows the correspondence between the station number and the data file name.

**4.6 Underway-CTD (UCTD)**

**(1) Personnel**

Yusuke Sasaki	AORI (Principal investigator)
Ichiro Yasuda	AORI
Taku Niinuma	AORI
Ryosuke Oyabu	AORI

**(2) Objective**

The purpose of this measurement is to explore the oceanic structure of temperature and salinity in the observation area. By using the Underway CTD (UCTD) system, the vertical profiles of temperature and salinity can be obtained successively without reducing the speed of the vessel.

**(3) Instruments and method**

The UCTD system consists of a probe unit and on-deck unit with a winch, rewinder and davit. The probe unit was released from the vessel with connection to the winch by a line, while the vessel was traveling with constant speed (The log speed at the first cast on each observation section is shown in [Table 4.6-1](#)). The probe unit measured temperature, conductivity, and other items (see below) during its descent with a speed of about 4 m/s in the water. After a predetermined time, we stopped feeding out the line and wound it up until the probe surfaced and approached the hull. The probe unit was on-deck only after all measurement casts on one observation section were finished. The data were internally recorded during the observation, which were retrieved after the probe was recovered.

[Table 4.6-1](#) shows the time and location of the first and last casts in each observation section. Most of the UCTD observation were carried out after a CTD station as the vessel headed to the next CTD station. In addition to these regular sections, we conducted UCTD observation along additional sections around the St. 38 ([Fig 4.6-1](#)).

The RINKO-profiler manufactured by JFE Advantech was used. We measured depth, temperature, conductivity, turbidity, chlorophyll and dissolved oxygen. The specification of the sensors is summarized in [Table 4.6-2](#). The data interval was set to 0.1 second in time.

Table 4.6-1: The UCTD observation information. Time is in UTC. Date is year/month/day

Section	First cast				Last cast				Log speed(knot)	filename
	Date	Time	Lat	Lon	Date	Time	Lat	Lon		
From St.4 to St.5	2021/07/15	19:19	42-46.87N	145-36.74E	2021/07/15	20:39	42-40.96N	145-40.58E	5	202107151917_ASTD152-ALC-R02_0710_191743.raw
From St.8 to St.9	2021/07/16	19:53	41-59.06N	146-15.27E	2021/07/16	20:58	41-56.18N	146-16.96E	6.9	202107161949_ASTD152-ALC-R02_0710_194942.raw
From St.12 to St.13	2021/07/17	19:10	41-38N	146-31.48E	2021/07/17	21:16	41-25.69N	146-39.94E	6.5	202107171905_ASTD152-ALC-R02_0710_190542.raw
From St.17 to St.18	2021/07/18	23:59	40-20.57N	147-6.97E	2021/07/19	00:40	40-13.58N	147-11.88E	12.5	202107182355_ASTD152-ALC-R02_0710_235515.raw
From St.21 to St.22	2021/07/19	23:51	40-3.58N	148-27.12E	2021/07/20	01:46	40-15.25N	148-45.5E	8.7	202107192315_ASTD152-ALC-R02_0710_231547.raw
From St.24 to St.25	2021/07/20	18:60	40-55.68N	149-52.74E	2021/07/20	20:32	41-11.33N	150-15.95E	11.4	202107201759_ASTD152-ALC-R02_0710_175914.raw
From St.28 to St.29	2021/07/21	22:35	42-20.69N	152-8.11E	2021/07/22	00:43	42-36.22N	152-33.59E	12.2	202107212240_ASTD152-ALC-R02_0710_224056.raw
From St.31 to St.32	2021/07/22	19:60	43-34.94N	154-12.59E	2021/07/22	22:57	44-0.05N	154-52.43E	11.8	202107221944_ASTD152-ALC-R02_0710_194415.raw
From St.34 to St.35	2021/07/23	18:49	45-5.05N	156-40.69E	2021/07/23	21:57	45-29.53N	157-20.9E	11.8	202107231847_ASTD152-ALC-R02_0710_184752.raw
K2_U1	2021/07/25	13:47	47-0.52N	160-1.3E	2021/07/25	15:51	47-7.37N	160-1.32E	4.7	202107251342_ASTD152-ALC-R02_0710_134258.raw
K2_U2	2021/07/25	16:43	47-0.61N	159-50.21E	2021/07/25	19:57	47-0.56N	160-11.02E	5	202107251622_ASTD152-ALC-R02_0710_162203.raw
From St.41 to St.42	2021/07/27	16:59	46-59.5N	163-24.56E	2021/07/27	19:23	46-59.84N	164-21.56E	11.2	202107271601_ASTD152-ALC-R02_0710_160154.raw
From St.44 to St.45	2021/07/28	17:59	46-58.21N	166-47.19E	2021/07/28	20:47	46-59.68N	167-41.74E	11.5	202107281710_ASTD152-ALC-R02_0710_171051.raw
From St.48 to St.49	2021/07/29	17:48	47-0.02N	169-5.32E	2021/07/29	19:46	46-59.81N	169-18.5E	4.7	202107291747_ASTD152-ALC-R02_0710_174734.raw
From St.52 to St.53	2021/07/30	17:34	46-59.15N	170-1.24E	2021/07/30	19:42	46-59.56N	170-22.51E	6.9	202107301741_ASTD152-ALC-R02_0710_174130.raw
From St.55 to St.56	2021/07/31	16:49	47-0.25N	172-44.39E	2021/07/31	20:08	47-0.35N	173-42.44E	11.9	202107311643_ASTD152-ALC-R02_0710_164330.raw
From St.58 to St.59	2021/08/01	17:05	46-59.65N	176-7.42E	2021/08/01	20:26	46-59.68N	177-3.75E	11.7	202108011704_ASTD152-ALC-R02_0710_170415.raw
From St.61 to St.62	2021/08/02	16:43	47-0.73N	179-27.78E	2021/08/02	19:56	46-59.31N	179-34.9W	11.2	202108021629_ASTD152-ALC-R02_0710_162931.raw
From St.64 to St.65	2021/08/03	21:16	46-59.97N	177-11.51W	2021/08/04	00:48	47-0.4N	176-11.39W	11.8	202108032114_ASTD152-ALC-R02_0710_211454.raw
From St.67 to St.68	2021/08/04	20:50	46-59.74N	173-46.11W	2021/08/05	00:33	46-59.4N	172-50.32W	11.7	202108042047_ASTD152-ALC-R02_0710_204710.raw
From St.70 to St.71	2021/08/05	21:52	46-59.79N	170-24.16W	2021/08/06	00:45	46-59.59N	169-30.33W	11.2	202108052130_ASTD152-ALC-R02_0710_213046.raw
From St.73 to St.74	2021/08/06	20:24	46-59.71N	167-3.75W	2021/08/06	23:50	47-0.54N	166-6.68W	11.5	202108062020_ASTD152-ALC-R02_0710_202050.raw
From St.76 to St.77	2021/08/07	19:21	47-0.62N	163-42.02W	2021/08/07	22:35	47-0.25N	162-47.11W	11.3	202108071920_ASTD152-ALC-R02_0710_192010.raw
From St.90 to St.89	2021/08/10	18:41	46-59.41N	149-10.7W	2021/08/10	22:37	46-59.43N	150-9.71W	11.4	202108101852_ASTD152-ALC-R02_0710_185215.raw
From St.87 to St.86	2021/08/11	17:52	46-59.73N	152-1.68W	2021/08/11	20:16	46-59.45N	152-26.5W	7.2	202108111750_ASTD152-ALC-R02_0710_175049.raw
From St.84 to St.83	2021/08/12	17:36	46-59.5N	154-46.88W	2021/08/12	20:32	46-59.33N	155-42.89W	11.6	202108121703_ASTD152-ALC-R02_0710_170334.raw
From St.81 to St.80	2021/08/13	17:46	47-0N	158-9.61W	2021/08/13	21:43	46-59.37N	159-9.34W	11.9	202108131757_ASTD152-ALC-R02_0710_175731.raw

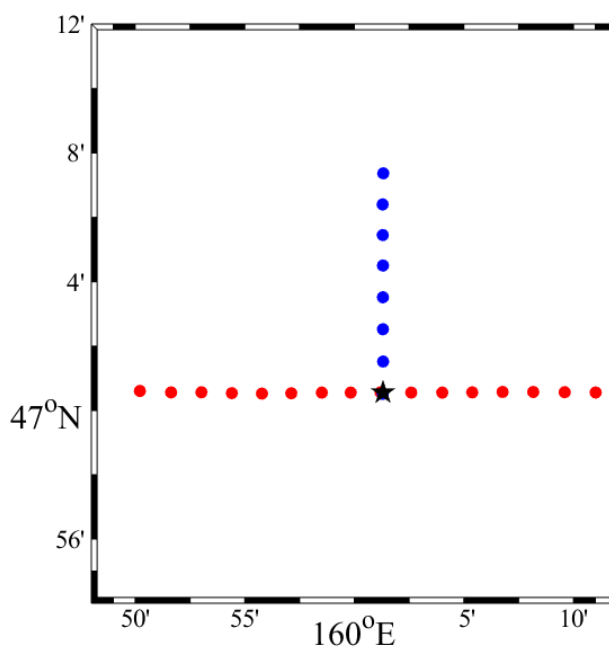


Fig 4.6-1: UCTD station locations around St. 38. Black star shows the location of St. 38. The blue circles show the UCTD station along the observation section 'K2\_U1'. The red circles are for 'K2\_U2'.

Table 4.6-2: The specification of the sensors in Rinko profiler

Parameter	Range	Resolution	Precision	Response
Depth	0 to 1000 m	0.01m	±0.3%FS	0.2 s

Temperature	-3 to 45 °C	0.001°C	±0.01°C	0.2 s
Conductivity	0.5 to 70mS/cm	0.001mS/cm	±0.01mS/cm	0.2 s
Turbidity	0 to 1000FTU	0.03FTU	±0.3FTU	0.2 s
Chlorophyll	0 to 400ppb	0.01ppb	±1%FS	0.2s
Dissolved Oxygen	0 to 20 mg/l	0.01mg/l	±2%FS	0.4s

## 4.7 Vertical Microstructure Profiler (VMP)

### (1) Personnel

Yusuke Sasaki	AORI (Principal investigator)
Taku Niinuma	AORI
Ryosuke Oyabu	AORI
Masanori Murakami	NME
Wataru Tokunaga	NME
Fumie Okada	NME

### (2) Objective

The objective is to measure microstructure in vertical shear of the horizontal velocity, temperature and conductivity to evaluate vertical mixing.

### (3) Instruments and method

Microstructure observations were carried out by VMP250-IR (“Internal Recording”) manufactured by Rockland Scientific International Inc. We used the two sets of instruments (VMP250\_SN354 and VMP250\_SN271), which have different sensor configurations. The probes on each VMP250 sensor set are as follows:

#### VMP250\_SN354

- Vertical shear of the horizontal velocity (two sensors, 512Hz)
- Fast thermistor temperature “FP07” (two sensors, 512Hz)
- Micro-Conductivity “SBE-7” (512Hz)
- Fine scale conductivity and temperature from JAC (JFE Advantech Co.) CT sensor (64Hz)
- Pressure (512Hz)
- Acceleration (512Hz)

#### VMP250\_SN271

- Vertical shear of the horizontal velocity (two sensors, 512Hz)
- Fast thermistor temperature “FP07” (two sensors, 512Hz)
- Fine scale conductivity and temperature from JAC (JFE Advantech Co.) CT sensor (64Hz)
- Pressure (512Hz)
- Acceleration (512Hz)
- Chlorophyll and turbidity from JAC FLTU sensor (512Hz)

The microscale parameters were measured while the sensor descended without artificial acceleration/deceleration (“free fall”). A cable (12 strand Vectran rope with a diameter = 5 mm) was attached to the probe for recovery of the instrument. The cable was always kept slack to maintain the free fall. After the predetermined time had passed, we stopped feeding out the cable and recovered the instrument to the surface. We downloaded the raw data from the instrument after each cast and replaced damaged probes when necessary.

### (4) Measurements

During the present cruise, 32 profiles were obtained. For the first three casts (St. V5, V10 and

V13), the observations were operated using the VMP250\_SN354. In the profiles of St. V13, the data of several sensors (S2, T1, C1 and JAC\_T) were noisy and we found the ingress of sea water in the instruments. From the 4th cast (St. V18), we used the VMP250\_SN271 instead. The serial number of sensor probes installed on the instruments are described below:

#### VMP250\_SN354

- Sensor socket S1: M1997 (St. V5-V13)
- Sensor socket S2: M2002 (St. V5-V13)
- Sensor socket T1: T1995 (St. V5-V13)
- Sensor socket T2: F-T1975 (St. V5-V13)
- Sensor socket C1: C293 (St. V5-V13)

#### VMP250\_SN271

- Sensor socket S1: M1815 (St. V18-V89)
- Sensor socket S2: M1816 (St. V18-V89)
- Sensor socket T1: T1608 (St. V18-V71), T1021 (St. V74-V89)
- Sensor socket T2: T1609 (St. V18-V89)

#### (5) Note for using data

The file included in the data 'TVMP.csv' shows the information of each profile (the station location, date, time and the file name).

### 4.8 Oxygen

August 25, 2021

Yuichiro Kumamoto

Japan Agency for Marine-Earth Science and Technology

#### (1) Personnel

Yuichiro Kumamoto	JAMSTEC
Shiori Ariga	MWJ
Misato Kuwahara	MWJ
Hiroaki Sako	MWJ

#### (2) Objectives

Dissolved oxygen is one of chemical tracers for the ocean circulation. Climate models predict a decline in dissolved oxygen concentration and a consequent expansion of oxygen minimum layer due to global warming, which results mainly from decreased interior advection and ongoing oxygen consumption by remineralization. In order to discuss the temporal change in oxygen concentration in the water column, we measured dissolved oxygen concentration from surface to bottom layer at all the water sampling stations in the North Pacific Ocean during this cruise.

#### (3) Reagents

Pickling Reagent I: Manganous chloride solution (3M) Lot: 1-21D, -21E

Pickling Reagent II: Sodium hydroxide (8M) / sodium iodide solution (4M) Lot: 2-21D, -21E

Sulfuric acid solution (5M) Lot: S-21D, -21E

Sodium thiosulfate (0.025M) Lot: T-21P, -21S, -21Q

Potassium iodate (0.001667M): Lot KCN5512, FUJIFILM Wako Pure Chemical Industries Ltd, Mass fraction:  $99.98 \pm 0.04$  % (expanded uncertainty) Lot of solution: K-21A

#### (4) Instruments

Detector: Automatic photometric titrator, DOT-15X manufactured by Kimoto Electronic Co. Ltd. Lot: DOT-09, -10

Burette: APB-620 and APB-510 manufactured by Kyoto Electronic Co. Ltd. / 10 cm<sup>3</sup> of titration piston Lot: DOT-09, MB-10/MY10-10; DOT-10, MB-02/MY10-02; KIO<sub>3</sub>, MB-06/MY10-06

Dispenser: FORTUNA Optifix 1 cm<sup>3</sup> Lot: Pickling Reagent I, MO-42; Pickling Reagent II, MO-43

#### (5) Seawater sampling

Seawater samples were collected using 12-liter sample bottles attached to the CTD-system. The seawater was transferred to a volume-calibrated glass flask (ca. 100 cm<sup>3</sup>) through a plastic tube. Three times volume of the flask of seawater was overflowed. Sample temperature was measured during the water sampling using a thermometer. Then two reagent solutions (Reagent I, II) of 1.0 cm<sup>3</sup> each were added immediately into the sample flask and the stopper was inserted carefully into the flask. The sample flask was then shaken to mix the contents and to disperse the precipitate finely throughout. After the precipitate has settled at least halfway down the flask, the flask was shaken again to disperse the precipitate. The sample flasks containing pickled samples were stored in an air-conditioned laboratory until they were measured.

#### (6) Sample measurement

At least two hours after the re-shaking, the pickled samples were measured on board. A magnetic stirrer bar and 1 cm<sup>3</sup> sulfuric acid solution were added into the sample flask and stirring began. Samples were titrated by sodium thiosulfate solution whose molarity was determined by potassium iodate solution. Temperature of sodium thiosulfate during titration was recorded by a thermometer. We measured dissolved oxygen concentration using two sets of the titration apparatus system, named DOT-09 and DOT-10. Molal concentration of dissolved oxygen (μmol kg<sup>-1</sup>) was calculated by the sample temperature during the water sampling, salinity, flask volume, and concentration and titrated volume of the sodium thiosulfate solution (titrant).

#### (7) Standardization

Concentration of the sodium thiosulfate titrant (0.025M) was determined by the potassium iodate standard solution. The potassium iodate was dried in an oven at 130°C. 1.78 g potassium iodate weighed out accurately was dissolved in deionized water and diluted to final volume of 5 dm<sup>3</sup> in a calibrated volumetric flask (0.001667M). Then the aliquot (about 400 ml) of the solution was stored in a brown glass bottle (500 ml). 10 cm<sup>3</sup> of the potassium iodate solution was added to a flask using a volume-calibrated dispenser. Then 90 cm<sup>3</sup> of deionized water, 1 cm<sup>3</sup> of sulfuric acid solution, and 1.0 cm<sup>3</sup> of pickling reagent solution II and I were added into the flask in order. Amount of titrated volume of sodium thiosulfate (usually 5 times measurements average) gave the molarity of the sodium thiosulfate titrant. Table 4.8.1 show results of the standardization during this cruise. The averaged coefficient of variation (C.V.) for the standardizations was 0.012 ± 0.006 % (standard deviation, n = 26). We changed the manufacturer and lot of potassium iodate from this year. Therefore, before this cruise, we compared concentrations of the potassium iodate solution prepared in this year and last year and found that there was no significant difference between them.

#### (8) Blank determination

The oxygen in the pickling reagents I (1.0 cm<sup>3</sup>) and II (1.0 cm<sup>3</sup>) was assumed to be 7.6 × 10<sup>-8</sup> mol (Murray *et al.*, 1968). The redox species apart from oxygen in the reagents (the pickling reagents I, II, and the sulfuric acid solution) also affect the titration, which is called the reagent blank. The reagent blank was determined as follows. 1 and 2 cm<sup>3</sup> of the standard potassium iodate solution were added to two flasks respectively. Then 100 cm<sup>3</sup> of deionized water, 1 cm<sup>3</sup> of sulfuric acid solution, and 1.0 cm<sup>3</sup> of pickling reagent II and I each were added into the two flasks in order. The reagent blank was determined by difference between the two times of the first (1 cm<sup>3</sup> of KIO<sub>3</sub>) titrated volume of the sodium thiosulfate and the second (2 cm<sup>3</sup> of KIO<sub>3</sub>) one. The three results of the blank determination were averaged (Table 4.8.1). The averaged coefficient of variation (C.V.) for the reagent blank determination against the titration volume of the potassium iodate standard (about 4 ml) or 250 μmol kg<sup>-1</sup> of dissolved oxygen concentration was 0.025 ± 0.012 % (standard deviation, n = 26). The redox species in seawater sample itself are measured as “dissolved oxygen”, which is called as the seawater blank, unless they are corrected. Because we did not measure the seawater

blank in this cruise, the dissolved oxygen concentration reported here includes the seawater blank concentration that is less than 1  $\mu\text{mol kg}^{-1}$  in the open ocean except those in suboxic and anoxic waters (Kumamoto *et al.*, 2015).

#### (9) Instrumental error

The difference in the concentrations of sodium thiosulfate solution determined by the standardization and blank determination using DOT-09 and DOT-10 were less than 0.1% (Table 4.8.1). The T-test at 95% confidence level suggests that there is no reason to believe that the two concentrations are different. Thus, we concluded that there was no instrumental error in measurements using DOT-09 and DOT-10.

Table 4.8.1 Results of standardization (End Point,  $\text{cm}^3$ ) and reagent blank determination ( $\text{cm}^3$ ).

No	Date (UTC)	Lot	KIO <sub>3</sub> Lot	Na <sub>2</sub> S <sub>2</sub> O <sub>3</sub> Lot	DOT-09		DOT-10		$\Delta$ (%)*	Remarks
					E.P.	blank	E.P.	blank		
1	2021/Jul/14	1	K-21A01	T-21P	3.951	-0.004	3.958	0.000	-0.08	Stn.001-005
2	2021/Jul/16	3	K-21A02	T-21P	3.951	-0.006	3.956	0.000	0.03	Stn.008-019
3	2021/Jul/19	4	K-21A03	T-21P	3.950	-0.006	3.958	0.002	0.00	Stn.021-032
4	2021/Jul/24	5	K-21A04	T-21P	3.950	-0.005	3.958	0.001	-0.05	Na <sub>2</sub> S <sub>2</sub> O <sub>3</sub> change
5	2021/Jul/24	6	K-21A04	T-21S	3.961	-0.007	3.967	-0.001	0.00	Stn.034-040
6	2021/Jul/27	7	K-21A05	T-21S	3.960	-0.006	3.966	-0.002	-0.05	Stn.042-054
7	2021/Aug/1	8	K-21A06	T-21S	3.961	-0.005	3.969	0.001	-0.05	Stn.056-066
8	2021/Aug/5	9	K-21A07	T-21S	3.962	-0.006	3.965	0.001	0.10	Na <sub>2</sub> S <sub>2</sub> O <sub>3</sub> change
9	2021/Aug/5	10	K-21A07	T-21Q	3.955	-0.006	3.960	-0.002	-0.03	Stn.068-077
10	2021/Aug/9	11	K-21A08	T-21Q	3.955	-0.008	3.960	-0.001	0.05	Stn.079,090-085
11	2021/Aug/13	12	K-21A09	T-21Q	3.956	-0.006	3.961	0.000	0.03	Stn.083, 081
12	2021/Aug/15	13	K-21A11	T-21Q	3.954	-0.003	3.960	-0.001	-0.10	Test
13	2021/Aug/16	14	K-21A10	T-21Q	3.954	-0.006	3.960	0.000	0.00	Final standardization

\*Difference between DOT-09 and DOT-10 (DOT-10 minus DOT-09) in sodium thiosulfate concentration determined by the standardization and blank determination.

#### (10) Replicate sample measurement

At all the water sampling stations, a pair of replicate samples was collected at one or two depths. The standard deviations from the difference of pairs of replicate measurements was estimated to be 0.11  $\mu\text{mol kg}^{-1}$  ( $n = 84$ ), which corresponds to 0.044% of the relative standard deviation against 250  $\mu\text{mol kg}^{-1}$ , using the standard operating procedure 23 in Dickson *et al.* (2007). The standard deviations of the difference between the pair of replicate measurement for the samples whose oxygen concentration is higher and lower than 100  $\mu\text{mol kg}^{-1}$  are 0.11 ( $n = 46$ ) and 0.12  $\mu\text{mol kg}^{-1}$  ( $n = 38$ ), respectively (Fig. 4.8.1). The difference between the two standard deviations is not significant (F-test at 95% confidence level) and there is no reason to believe contamination of atmospheric O<sub>2</sub> during the water sampling for the lower concentration samples.

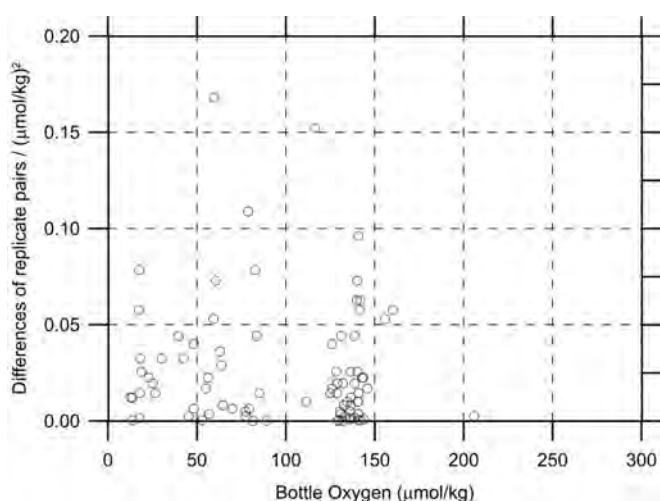


Figure 4.8.1 Oxygen difference between measurements of a replicate pair against oxygen concentration.

**(11) Duplicate sample measurement**

The duplicate samplings were conducted at Station 31 to confirm that the sampling bottles tripped correctly. All the 36 bottles were fired at 5000 dbar and dissolved oxygen concentration in each bottle was measured (Table 4.8.2). The standard deviation of the duplicate measurements was calculated to be  $0.16 \mu\text{mol kg}^{-1}$  ( $n = 36$ ). The F-test at 95% confidence level indicates that there is no reason to believe that the standard deviation of the duplicate measurements significantly is different from that of the replicate measurements ( $0.11 \mu\text{mol kg}^{-1}$ , Section 10). Therefore, we concluded that there is no difference among the results of the duplicate measurements, which suggested that all the bottles tripped correctly. We measured samples from the bottle #1~18 and #19~36 using DOT-10 and DOT-09, respectively. The means of the former and latter were  $157.09 \pm 0.11$  (standard deviation) and  $156.88 \pm 0.13 \mu\text{mol kg}^{-1}$ , respectively. The T-test at 95% confidence level denies that there is no reason to believe that the two means are different. Because there was not the instrumental error between DOT-09 and DOT-10 (Section 9), the significant difference ( $0.21 \mu\text{mol kg}^{-1}$ ) was derived from water sampling and/or unknown causes.

Table 4.8.2 Results of the duplicate sample measurements.

Bottle #	Bottle ID	Titration	Dissolved oxygen ( $\mu\text{mol/kg}$ )	Bottle #	Bottle ID	Titration	Dissolved oxygen ( $\mu\text{mol/kg}$ )
1	X12S01	DOT-10	157.04	19	X12S19	DOT-09	156.97
2	X12B34	DOT-10	157.14	20	X12S20	DOT-09	156.84
3	X12S03	DOT-10	157.19	21	X12S21	DOT-09	156.79
4	X12S04	DOT-10	157.10	22	X12S22	DOT-09	156.80
5	X12S05	DOT-10	157.24	23	X12S23	DOT-09	156.95
6	X12S06	DOT-10	157.13	24	X12S24	DOT-09	156.66
7	X12S07	DOT-10	157.10	25	X12S25	DOT-09	156.86
8	X12S08	DOT-10	156.89	26	X12S26	DOT-09	156.74
9	X12S09	DOT-10	156.88	27	X12S27	DOT-09	156.73
10	X12S10	DOT-10	156.93	28	X12S28	DOT-09	156.80
11	X12S11	DOT-10	157.03	29	X12S29	DOT-09	156.90
12	X12S12	DOT-10	157.14	30	X12S30	DOT-09	157.15
13	X12S13	DOT-10	157.06	31	X12S31	DOT-09	156.98
14	X12S14	DOT-10	157.01	32	X12S32	DOT-09	156.86
15	X12S15	DOT-10	157.28	33	X12S33	DOT-09	157.00
16	X12S16	DOT-10	157.13	34	X12S34	DOT-09	157.07
17	X12S17	DOT-10	157.11	35	X12S35	DOT-09	156.81

18	X12S18	DOT-10	157.18	36	X12S36	DOT-09	156.84
----	--------	--------	--------	----	--------	--------	--------

### (12) Quality control flag assignment

Quality flag values for oxygen data from sample bottles were assigned according to the code defined in Table 4.9 of WHP Office Report WHPO 90-1 Rev.2 section 4.5.2 (Joyce *et al.*, 1994). Measurement flags of 2 (good), 3 (questionable), 4 (bad), and 5 (missing) have been assigned (Table 4.8.3). For the choice between 2, 3, or 4, we basically followed a flagging procedure as listed below:

- If there was a glaring problem or error in the measurement, the datum was flagged 4.
- Bottle oxygen concentration at the sampling layer was plotted against sampling pressure and potential density. Any points not lying on a generally smooth trend were noted.
- Difference between bottle oxygen concentration and oxygen sensor output was then plotted against sampling pressure. If the noted datum deviated from a group of plots, it was flagged 3 or 4.
- If the bottle flag was 4 (did not trip correctly), a datum was flagged 4 (bad). In case of the bottle flag 3 (leaking) or 5 (unknown problem), a datum was flagged based on steps a, b, and c.

Table 4.8.3 Summary of assigned quality control flags.

Flag	Definition	Number*
2	Good	1550
3	Questionable	6
4	Bad	2
5	Not report (missing)	1
Total		1559

\*The replicate samples (n = 84) and duplicate samples (n = 36) were not included.

### (13) Uncertainty

We assume that the uncertainty of dissolved oxygen determination is derived from those of items listed in Table 4.8.4. Because we did not measure the seawater blank, the dissolved oxygen concentration reported here does include the seawater blank concentration (Section 8). Without the correction by the seawater blank, the combined uncertainty (k = 1) and the expanded combined uncertainty (k = 2) were calculated to be 0.06% and 0.12%, respectively. Note that this combined uncertainty does not include that derived from temporal change in temperature of sodium thiosulfate solution. However, that was negligible because the its variation was small (20.8-21.8°C). When we subtract the seawater blank from the oxygen concentration, the uncertainty due to the seawater blank should be added. If it is assumed that the seawater blank concentration is  $0.50 \pm 0.50 \mu\text{mol kg}^{-1}$  and the distribution of the possible values is uniform or rectangular, its standard uncertainty is calculated to be  $0.29 \mu\text{mol kg}^{-1}$  ( $= 0.50/\sqrt{3}$ ). This value corresponds to the standard uncertainty of 0.116% relative to  $250 \mu\text{mol kg}^{-1}$  of dissolved oxygen concentration. The combined standard uncertainty, which includes the uncertainty of the seawater blank concentration, is calculated to be 0.13% (the extended combined uncertainty is 0.26%). These combined uncertainties, however, are applicable only for the dissolved oxygen concentration corrected by the seawater blank concentration ( $0.50 \mu\text{mol kg}^{-1}$ ).

Table 4.8.4 Uncertainties of estimated items for the oxygen determination.

#	Estimated items	Relative uncertainty to $250 \mu\text{mol kg}^{-1}$ (%)	References
1	Sodium thiosulfate concentration	0.041	#2, 3, 4
2	Potassium iodate concentration	0.030	Kumamoto <i>et al.</i> (2015)
3	Titration of potassium iodate	0.012	Section 7
4	Reagent blank determination	0.025	Section 8
5	Titration of seawater sample	0.044	Section 10

6	Volume of sample flask	0.015	Kumamoto <i>et al.</i> (2015)
Combined uncertainty (k=1)		0.06	#1, 5, 6
Expanded combined uncertainty (k=2)		0.12	
7	Seawater blank	0.116	Kumamoto <i>et al.</i> (2015)
Combined uncertainty (k=1)		0.13	#1, 5, 6, 7
Expanded combined uncertainty (k=2)		0.26	

#### (14) Problem

- The titration was disturbed by air bubbles in the light path during the titration, which implies that the rotation speed of the stirrer (8 rpm) was too fast. The rotation speed was slowed down to 7 rpm and the disturbance by air bubble was reduced.
- During measurement of the sample from #12 (3250 dbar) at Station 12, the titration did not finish automatically because the final absorbance of light through the sample flask was higher than 0.15. We believe that this was derived from wrong positioning of the sample flask in the holder of the titrator.
- During measurements of 38 samples, most of which were measured using DOT-10, the titration did not finish automatically because the final absorbance of light through the sample flask decreased gradually. The causes of this decrease are unknown. We recalculated the end point from the raw data of the titrators using a geometric method.
- The end points of the titration in two sample measurements (#1 at Station 12 and #26 at Station 51) were evidently anomalous and flagged 4 (Section 12). The causes of these anomalies are unknown.

#### (15) Data archives

The data obtained in the cruises will be submitted to the Data Management Group of JAMSTEC and will be opened to the public via “Data Research System for Whole Cruise Information in JAMSTEC (DARWIN)” in the JAMSTEC web site.

#### References

Dickson, A. G., C.L. Sabine, and J.R. Christian (Eds.) (2007) Guide to best practices for ocean CO<sub>2</sub> measurements, PICES Special Publication 3, 191 pp.

Joyce, T., and C. Corry, eds., C. Corry, A. Dessier, A. Dickson, T. Joyce, M. Kenny, R. Key, D. Legler, R. Millard, R. Onken, P. Saunders, M. Stalcup (1994) Requirements for WOCE Hydrographic Programme Data Reporting, WHPO Pub. 90-1 Rev. 2, May 1994 Woods Hole, Mass., USA.

Kumamoto, Y., Y. Takatani, T. Miyao, H. Sato, and K. Matsumoto (2015) Dissolved oxygen, Guideline of Ocean Observations, vol. 3, chap. 1, G301JP:001–029 (in Japanese).

Murray, C.N., J.P. Riley, and T.R.S. Wilson (1968) The solubility of oxygen in Winkler reagents used for determination of dissolved oxygen, *Deep-Sea Res.*, 15, 237-238.

## 4.9 Nutrients

as of 24 August 2021 ver1.1

as of 17 November 2021 ver1.2

as of 19 November 2021 ver1.3

#### (1) Personnel

Michio AOYAMA (JAMSTEC/University of Tsukuba/University of Fukushima)

: Principal Investigator

Shinya Kouketsu (JAMSTEC)

Yuko MIYOSHI (MWJ): Operation Leader

Yasuhiro ARII (MWJ)

Yuta ODA (MWJ)

## (2) Objectives

The objective of this document is to show the present status of the nutrient concentrations during the R/V Mirai MR21-04 cruise (EXPCODE: 49NZ20210713) in the Pacific Ocean, and then evaluate the comparability of this obtained data set during this cruise using the certified reference materials of the nutrients in seawater.

## (3) Parameters

The parameters are nitrate, nitrite, silicate, phosphate and ammonia in seawater.

## (4) Instruments and methods

### *i) Analytical detail using QuAAtro 39 systems (BL TEC K.K.)*

The analytical systems were replaced from QuAAtro 2-HR to QuAAtro 39 in March 2021.

Nitrate + nitrite and nitrite were analyzed by the following methodology that was modified from the original method of Grasshoff (1976). The flow diagrams were shown in [Figure 4.9-1](#) for nitrate + nitrite and [Figure 4.9-2](#) for nitrite. For the nitrate + nitrite analysis, the sample were mixed with the alkaline buffer (Imidazole) and then the mixture was pushed through a cadmium coil which was coated with a metallic copper. This step was conducted due to reduce from nitrate to nitrite in the sample, which allowed us to determine nitrate + nitrite in the seawater sample. For the nitrite analysis, the sample was mixed with reagents without this reduction step. In the flow system, seawater sample with or without the reduction step was mixed with an acidic sulfanilamide reagent through a mixing coil to produce a diazonium ion. And then, the mixture was mixed with the N-1-naphthylethylenediamine dihydrochloride (NED) to produce a red azo dye. The azo dye compound was injected into the spectrophotometric detection to monitor the signal at 545 nm. Thus, for the nitrite analysis, sample was determined without passing through the Cd coil. Nitrate was computed by the difference between nitrate+nitrite concentration and nitrite concentration.

The silicate method is analogous to that described for phosphate (see below). The method is essentially that of Grasshoff et al. (1999). The flow diagrams were shown in [Figure 4.9-3](#). Silicomolybdic acid compound was first formed by mixing silicate in the sample with the molybdic acid. The silicomolybdic acid compound was then reduced to silicomolybdous acid, "molybdenum blue," using L-ascorbic acid as the reductant. And then the signal was monitored at 630 nm.

The methodology for the phosphate analysis is a modified procedure of Murphy and Riley (1962). The flow diagrams were shown in [Figure 4.9-4](#). Molybdic acid was added to the seawater sample to form the phosphomolybdic acid compound, and then it was reduced to phosphomolybdous acid compound using L-ascorbic acid as the reductant. And then the signal was monitored at 880 nm.

The ammonia in seawater was determined using the flow diagrams shown in [Figure 4.9-5](#). Sample was mixed with an alkaline solution containing EDTA, which ammonia as gas state was formed from seawater. The ammonia (gas) is absorbed in a sulfuric acid by way of 0.5 µm pore size membrane filter (ADVANTEC PTFE) at the dialyzer attached to the analytical system. And then the ammonia absorbed in sulfuric acid was determined by coupling with phenol and hypochlorite to form indophenols blue, and the signal was determined at 630 nm.

The details of a modification of analytical methods for four parameters, nitrate, nitrite, silicate and phosphate, are also compatible with the methods described in nutrients section in the new GO-SHIP repeat hydrography nutrients manual (Becker et al., 2019). This manual is a revised version of the GO-SHIP repeat hydrography nutrients manual (Hydes et al., 2010). The analytical method of ammonium is compatible with the determination of ammonia in seawater using a vaporization membrane permeability method (Kimura, 2000).

### *ii) Nitrate + Nitrite reagents*

50 % Triton solution

50 mL of Triton™ X-100 (CAS No. 9002-93-1) were mixed with 50 mL of ethanol (99.5 %).

Imidazole (buffer), 0.06 M (0.4 % w/v)

Dissolved 4 g of the imidazole (CAS No. 288-32-4) in 1000 mL ultra-pure water, and then added 2 mL of the hydrogen chloride (CAS No. 7647-01-0). After mixing, 1 mL of the 50 % triton solution was added.

Sulfanilamide, 0.06 M (1 % w/v) in 1.2 M HCl

Dissolved 10 g of 4-aminobenzenesulfonamide (CAS No. 63-74-1) in 900 mL of ultra-pure water, and then add 100 mL of the hydrogen chloride (CAS No. 7647-01-0). After mixing, 2 mL of the 50 % triton solution was added.

NED, 0.004 M (0.1 % w/v)

Dissolved 1 g of N-(1-naphthalenyl)-1,2-ethanediamine dihydrochloride (CAS No. 1465-25-4) in 1000 mL of ultra-pure water and then added 10 mL of hydrogen chloride (CAS No. 7647-01-0). After mixing, 1 mL 50 % of the Triton solution was added. This reagent was stored in a dark bottle.

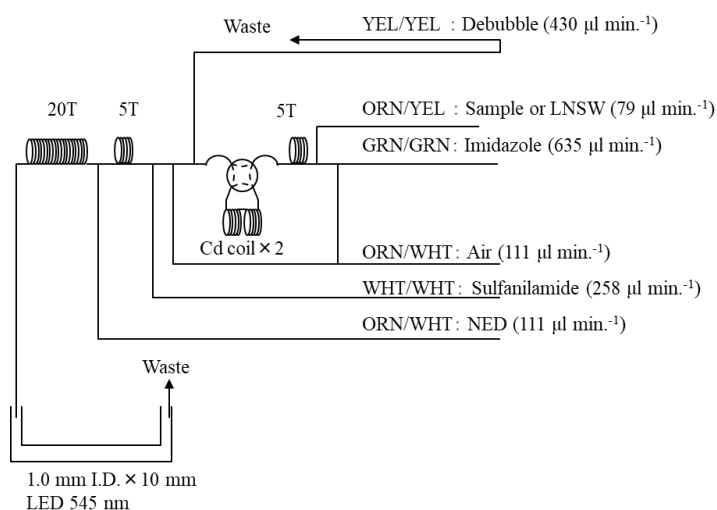


Figure 4.9-1 NO<sub>3</sub>+NO<sub>2</sub> (1ch.) flow diagram.

### iii) Nitrite reagents

50 % Triton solution

50 mL of the Triton™ X-100 (CAS No. 9002-93-1) were mixed with 50 mL ethanol (99.5 %).

Sulfanilamide, 0.06 M (1 % w/v) in 1.2 M HCl

Dissolved 10 g of 4-aminobenzenesulfonamide (CAS No. 63-74-1) in 900 mL of ultra-pure water, and then added 100 mL of hydrogen chloride (CAS No. 7647-01-0). After mixing, 2 mL of the 50 % triton solution were added.

NED, 0.004 M (0.1 % w/v)

Dissolved 1 g of N-(1-naphthalenyl)-1,2-ethanediamine dihydrochloride (CAS No. 1465-25-4) in 1000 mL of ultra-pure water and then added 10 mL of hydrogen chloride (CAS No. 7647-01-0). After mixing, 1 mL of the 50 % triton solution was added. This reagent was stored in a dark bottle.

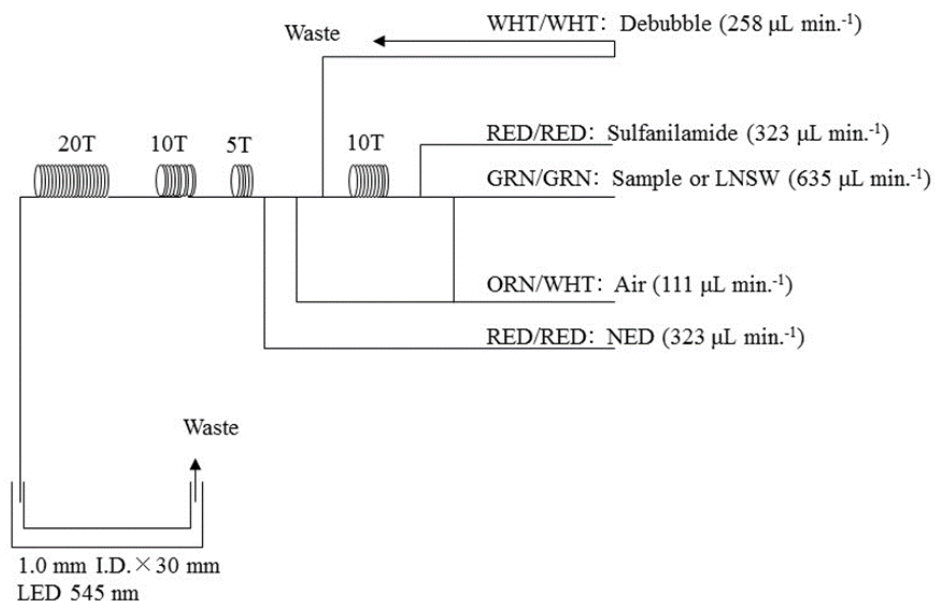


Figure 4.9-2 NO<sub>2</sub> (2ch.) flow diagram.

iv) *Silicate reagents*

15 % Sodium dodecyl sulfate solution

75 g of sodium dodecyl sulfate (CAS No. 151-21-3) was mixed with 425 mL ultra-pure water.

Molybdic acid, 0.03 M (1 % w/v)

Dissolved 7.5 g of sodium molybdate dihydrate (CAS No. 10102-40-6) in 980 mL ultra-pure water, and then added 12 mL of a 4.5M sulfuric acid. After mixing, 20 mL of the 15 % sodium dodecyl sulfate solution was added. Note that the amount of sulfuric acid was reduced from the previous report (MR19-03C) since we have modified the method of Grasshoff et al. (1999).

Oxalic acid, 0.6 M (5 % w/v)

Dissolved 50 g of oxalic acid (CAS No. 144-62-7) in 950 mL of ultra-pure water.

Ascorbic acid, 0.01 M (3 % w/v)

Dissolved 2.5 g of L-ascorbic acid (CAS No. 50-81-7) in 100 mL of ultra-pure water. This reagent was freshly prepared every day.

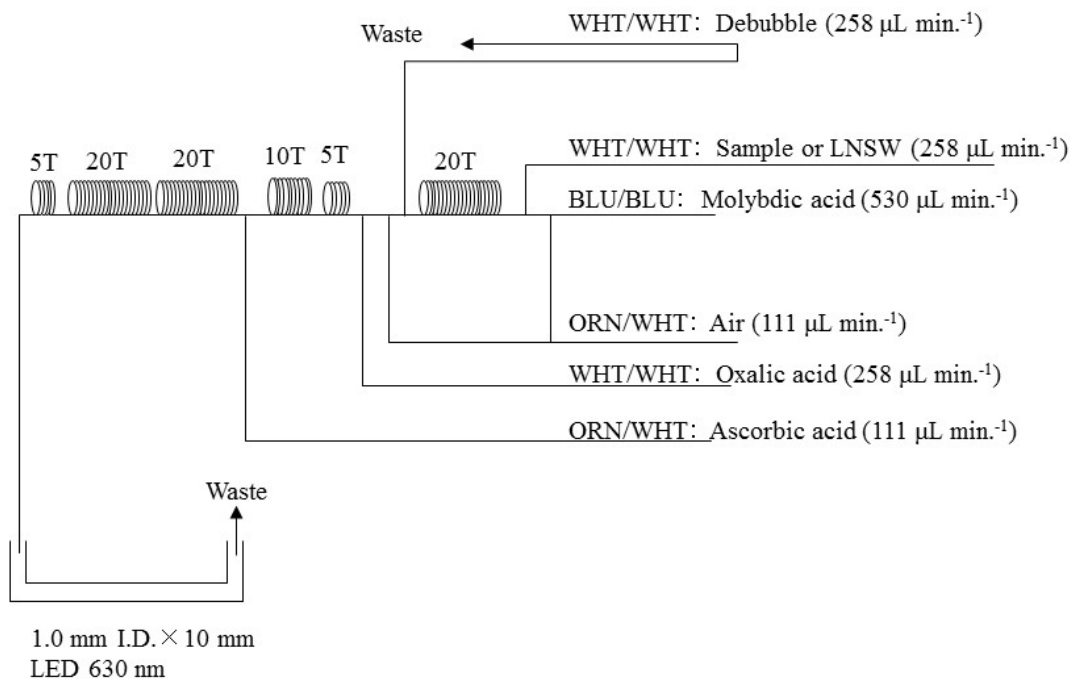


Figure 4.9-3 SiO<sub>2</sub> (3ch.) flow diagram.

v) *Phosphate reagents*

15 % Sodium dodecyl sulfate solution

75 g of sodium dodecyl sulfate (CAS No. 151-21-3) were mixed with 425 mL of ultra-pure water.

Stock molybdate solution, 0.03 M (0.8 % w/v)

Dissolved 8 g of sodium molybdate dihydrate (CAS No. 10102-40-6) and 0.17 g of antimony potassium tartrate trihydrate (CAS No. 28300-74-5) in 950 mL of ultra-pure water, and then added 50 mL of sulfuric acid (CAS No. 7664-93-9).

PO<sub>4</sub> color reagent

Dissolved 1.2 g of L-ascorbic acid (CAS No. 50-81-7) in 150 mL of the stock molybdate solution. After mixing, 3 mL of the 15 % sodium dodecyl sulfate solution was added. This reagent was freshly prepared before every measurement.

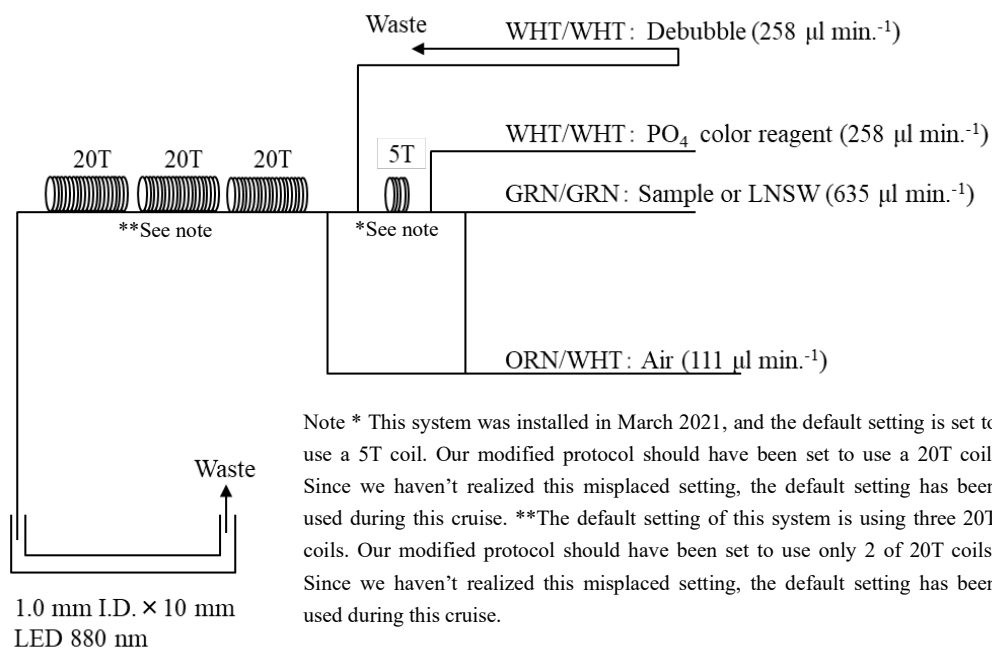


Figure 4.9-4 PO<sub>4</sub> (4ch.) flow diagram.

vi) Ammonia reagents

30 % Triton solution

30 mL of a Triton™ X-100 (CAS No. 9002-93-1) were mixed with 70 mL ultra-pure water.

EDTA

Dissolved 41 g of a tetrasodium; 2-[2-[bis(carboxylatomethyl)amino]ethyl-(carboxylatomethyl)amino]acetate;tetrahydrate (CAS No. 13235-36-4) and 2 g of a boric acid (CAS No. 10043-35-3) in 200 mL of ultra-pure water. After mixing, a 1 mL of the 30 % triton solution was added. This reagent is prepared every week.

NaOH liquid

Dissolved 1.5 g of a sodium hydroxide (CAS No. 1310-73-2) and 16 g of a tetrasodium; 2-[2-[bis(carboxylatomethyl)amino]ethyl-(carboxylatomethyl)amino]acetate; tetrahydrate (CAS No. 13235-36-4) in 100 mL of ultra-pure water. This reagent was prepared every week. Note that we reduced the amount of a sodium hydroxide from 5 g to 1.5 g because pH of C standard solutions has been lowered 1 pH unit due to the change of recipe of B standards solution (the detailed of those standard solution, see 6.2.4).

Stock nitroprusside

Dissolved 0.25 g of a sodium nitroferrocyanide dihydrate (CAS No. 13755-38-9) in 100 mL of ultra-pure water, and then added 0.2 mL of a 1M sulfuric acid. Stored in a dark bottle and prepared every month.

Nitroprusside solution

Added 4 mL of the stock nitroprusside and 4 mL of a 1M sulfuric acid in 500 mL of ultra-pure water. After mixing, 2 mL of the 30 % triton solution was added. This reagent was stored in a dark bottle and prepared every 2 or 3 days.

Alkaline phenol

Dissolved 10 g of a phenol (CAS No. 108-95-2), 5 g of a sodium hydroxide (CAS No.

1310-73-2) and 2 g of a sodium citrate dihydrate (CAS No. 6132-04-3) in 200 mL of ultra-pure water. Stored in a dark bottle and prepared every week.

#### NaClO solution

Mixed 3 mL of a sodium hypochlorite (CAS No. 7681-52-9) in 47 mL of ultra-pure water. Stored in a dark bottle and freshly prepared before every measurement. This reagent need be 0.3 % available chlorine.

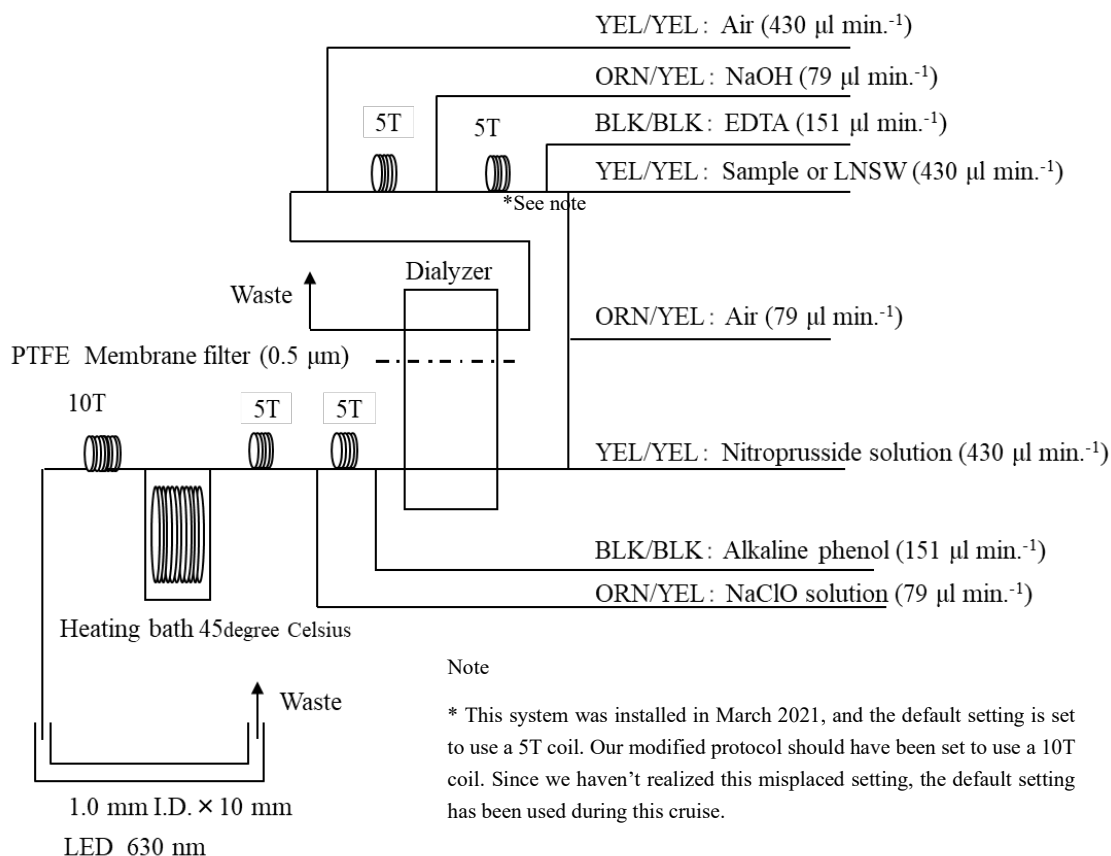


Figure 4.9-5 NH<sub>4</sub> (5ch.) flow diagram.

#### vii) Sampling procedures

Sampling for nutrient samples was conducted right after the sampling for other parameters (oxygen, trace gases and salinity). Samples were collected into two new 10 mL polyacrylates vials without any sample drawing tube that usually used for the oxygen samples. Each vial was rinsed three times before filling and then was sealed without any head-space immediately after the collection. The vials were put into a water bath that was adjusted to the ambient temperature at  $21.7 \pm 0.3$  degree Celsius, for more than 30 minutes to keep the constant temperature of samples.

No transfer from the vial to another container was made and the vials were set an autosampler tray directly. Samples were analyzed after collection within 24 hours.

#### viii) Data processing

Raw data from QuAAtro 39 were treated as follows:

- Checked if there were any baseline shift.
- Checked the shape of each peak and positions of peak values. If necessary, a change was made for the positions of peak values.

- Conducted carry-over correction and baseline drift correction to apply to the peak height of each sample followed by sensitivity correction.
- Conducted baseline correction and sensitivity correction using the linear regression.
- Using the pressure and the salinity from uncalibrated CTD data and the laboratory room temperature (20 degree Celsius), the density of each sample had been calculated tentatively. The obtained density was used to calculate the final nutrient concentration with the unit of  $\text{umol kg}^{-1}$ .
- Calibration curves to obtain the nutrients concentrations were assumed second order equations.

ix) *Summary of nutrients analysis*

During this cruise, 46 runs were conducted to obtain the values for the samples collected by 47 casts at 46 stations. The total number of the seawater samples were 3012. Each sample depth, we collected duplicate samples, and then determined all of the samples. The sampling locations for the nutrients was shown in Figure 4.9-6.

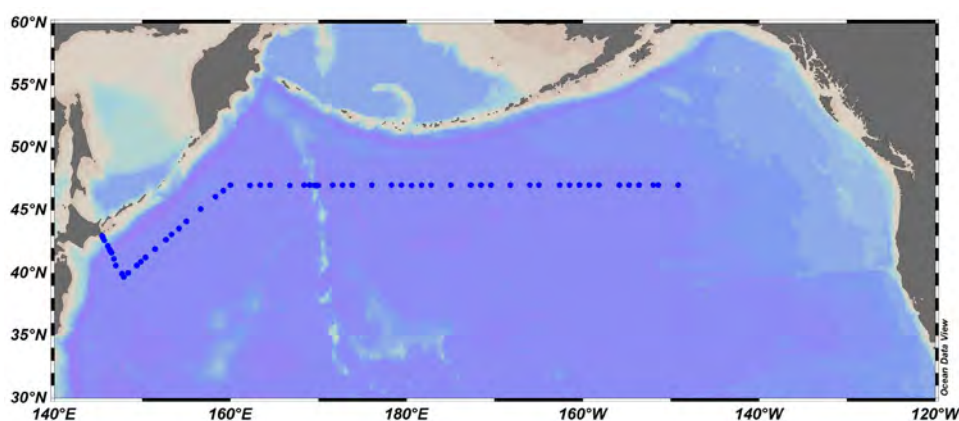


Figure 4.9-6 Sampling positions of nutrients sample.

**(5) Certified Reference Material of nutrients in seawater**

KANSO certified reference materials (CRMs, Lot: CE, CL, CO, CG, CB, CF) were used to ensure the comparability and traceability of nutrient measurements during this cruise. The details of CRMs are shown below.

**Production**

KANSO CRMs for inorganic nutrients in seawater were produced by KANSO Co.,Ltd. This CRM has been produced using autoclaved natural seawater based on the quality control system under ISO Guide 34 (JIS Q 0034).

KANSO Co.,Ltd. has been accredited under the Accreditation System of National Institute of Technology and Evaluation (ASNITE) as a CRM producer since 2011. (Accreditation No.: ASNITE 0052 R)

**Property value assignment**

The certified values were the arithmetic means of the results of 30 bottles from each batch (measured in duplicates) analyzed by both KANSO Co.,Ltd. and Japan Agency for Marine-Earth Science and Technology (JAMSTEC) using the colorimetric method (continuous flow analysis, CFA, method). The salinity of the calibration standards solution to obtain each calibration curve was adjusted to the salinity of the used CRMs within  $\pm 0.5$ .

## Metrological Traceability

Each certified value of nitrate, nitrite, and phosphate of KANSO CRMs were calibrated using one of Japan Calibration Service System (JCSS) standard solutions for each nitrate ions, nitrite ions, and phosphate ions. JCSS standard solutions were calibrated using the secondary solution of JCSS for each of these ions. The secondary solution of JCSS was calibrated using the specified primary solution produced by Chemicals Evaluation and Research Institute (CERI), Japan. CERI specified primary solutions were calibrated using the National Metrology Institute of Japan (NMIJ) primary standards solution of nitrate ions, nitrite ions and phosphate ions, respectively.

For the certified value of silicate of KANSO CRM was calibrated using a newly established silicon standards solution named “exp64” produced by JAMSTEC and KANSO. This silicon standard solution was produced by a dissolution technique with an alkaline solution. The mass fraction of Si in the produced solution was calibrated based on NMIJ CRM 3645-a Si standard solution by a technology consulting system of National Institute of Advanced Industrial Science and Technology (AIST), and this value is traceable to the International System of Units (SI).

The certified values of nitrate, nitrite, and phosphate of KANSO CRM are thus traceable to the SI through the unbroken chain of calibrations, JCSS, CERI and NMIJ solutions as stated above, each having stated uncertainties. The certified values of silicate of KANSO CRM are traceable to the SI through the unbroken chain of calibrations, NMIJ CRM 3645-a02 Si standard solution, having stated uncertainties.

As stated in the certificate of NMIJ CRMs, each certified value of dissolved silica, nitrate ions, and nitrite ions was determined by more than one method using one of NIST SRM of silicon standard solution and NMIJ primary standards solution of nitrate ions and nitrite ions. The concentration of phosphate ions as stated information value in the certificate was determined NMIJ primary standards solution of phosphate ions. Those values in the certificate of NMIJ CRMs are traceable to the SI.

One of the analytical methods used for certification of NMIJ CRM for nitrate ions, nitrite ions, phosphate ions and dissolved silica was a colorimetric method (continuous mode and batch mode). The colorimetric method is the same as the analytical method (continuous mode only) used for certification of KANSO CRM. For certification of dissolved silica, exclusion chromatography/isotope dilution-inductively coupled plasma mass spectrometry and ion exclusion chromatography with post-column detection was used. For certification of nitrate ions, ion chromatography by direct analysis and ion chromatography after halogen-ion separation was used. For certification of nitrite ions, ion chromatography by direct analysis was used.

NMIJ CRMs were analyzed at the time of certification process for CRM and the results were confirmed within expanded uncertainty stated in the certificate of NMIJ CRMs.

### *i) CRM for this cruise*

30 sets of CRM lots CE, CL, CO, CG, CB and CF were used, which almost cover a range of nutrients concentrations in the Pacific Ocean.

Each CRM's serial number was randomly selected. The CRM bottles were stored at a room named “BIOCHEMICAL LABORATORY” on the ship, where the temperature was maintained around 20.54 degree Celsius – 22.93 degree Celsius.

### *ii) CRM concentration*

Nutrients concentrations for the CRM lots CE, CL, CO, CG, CB and CF were shown in [Table 4.9-1](#).

Table 4.9-1 Certified concentration and the uncertainty (k=2) of CRMs.

unit:  $\mu\text{mol kg}^{-1}$

Lot	Nitrate	Nitrite**	Silicate	Phosphate	Ammonia***
CE*	0.01 ± 0.03	0.031 ± 0.03	0.06 ± 0.09	0.012 ± 0.006	0.69
CL	5.47 ± 0.15	0.017 ± 0.006	13.8 ± 0.3	0.425 ± 0.019	1.68
CO	15.86 ± 0.15	0.047 ± 0.04	34.72 ± 0.16	1.177 ± 0.014	0.54
CG	23.7 ± 0.2	0.073 ± 0.03	56.4 ± 0.5	1.70 ± 0.02	0.61
CB	35.79 ± 0.27	0.136 ± 0.0057	109.2 ± 0.62	2.520 ± 0.022	0.77
CF	43.4 ± 0.4	0.093 ± 0.02	159.7 ± 1.0	3.06 ± 0.03	0.46

\*Nitrate, silicate and phosphate values of CRM lot CE are below quantifiable detection limit and shown as only reference values.

\*\*Nitrite concentration values are measured on the ship before this cruise.

\*\*\*Ammonia values are not certified and shown as only reference values.

## (6) Nutrients standards

### i) Volumetric laboratory-ware of in-house standards

All volumetric glassware and polymethylpentene (PMP)-ware used were gravimetrically calibrated. Plastic volumetric flasks were gravimetrically calibrated at the temperature of use within 3K at around 20 degree Celsius.

#### Volumetric flasks

Volumetric flasks of Class quality (Class A) are used because their nominal tolerances are 0.05 % or less over the size ranges likely to be used in this work. Since Class A flasks are made of borosilicate glass, the standard solutions were transferred to plastic bottles as quickly as possible after the solutions were made up to volume and well mixed in order to prevent the excessive dissolution of silicate from the glass. PMP volumetric flasks were gravimetrically calibrated and used only within 3 K of the calibration temperature.

The computation of volume contained by the glass flasks at various temperatures other than the calibration temperatures were conducted by using the coefficient of linear expansion of borosilicate crown glass.

The coefficients of cubical expansion of each glass and PMP volumetric flask was determined by actual measurement in 2018 and 2019. The coefficients of cubical expansion of glass volumetric flask (SHIBATA HARIO) was 0.0000110 to 0.0000172  $\text{K}^{-1}$  and that of PMP volumetric flask (NALGEN PMP) was 0.00039 to 0.00045  $\text{K}^{-1}$ . The weights obtained in the

calibration weightings were corrected for the density of water and air buoyancy.

#### Pipettes

All glass pipettes have nominal calibration tolerances of 0.1 % or better. These were gravimetrically calibrated to verify and improve upon this nominal tolerance.

### (6.2) Reagents, general considerations

#### Specifications

For nitrate standard, “potassium nitrate 99.995 suprapur®” provided by Merck, Batch B1706365, CAS No. 7757-79-1, was used.

For nitrite standard solution, we used a nitrite ion standard solution ( $\text{NO}_2^-$  1000) provided by Wako, Lot ESG1055, Code. No. 146-06453. This standard solution was certified by Wako using the ion chromatography method. Calibration result is  $1004 \text{ mg L}^{-1}$  at 20 degree Celsius. Expanded uncertainty of calibration ( $k=2$ ) is 0.8 % for the calibration result.

For the silicate standard solution, we used our in-house Si standard solution “exp64” which was produced by alkali fusion technique from 5N  $\text{SiO}_2$  powder produced jointly by JAMSTEC and KANSO. The mass fraction of Si in the “exp64” solution was calibrated based on NMIJ CRM 3645-a02 Si standard solution.

For phosphate standard, we used a potassium dihydrogen phosphate anhydrous 99.995 suprapur®” provided by Merck, Batch B1781408, CAS No.: 7778-77-0, was used.

For ammonia standard, ammonium chloride (CRM 3011-a) provided by NMIJ, CAS No. 12125-02-9 was used. The purity of this standard was reported as >99.9 % by the manufacture. Expanded uncertainty of calibration ( $k=2$ ) was 0.022 %.

#### Ultra-pure water

Ultra-pure water (Milli-Q water) freshly drawn was used for the preparation of reagents, standard solutions and for measurements of the reagent and the system blanks.

#### Low nutrients seawater (LNSW)

Surface water having low nutrient concentration was taken and filtered using  $0.20 \mu\text{m}$  pore capsule cartridge filter around 17S and 100E during MR19-04 cruise in February 2020. This water was drained into 20 L cubitainers and stored in a cardboard box.

Nutrients concentrations in LNSW were measured on August 2020. The averaged nutrient concentrations in the LNSW were  $0.00 \mu\text{mol L}^{-1}$  for nitrate,  $0.00 \mu\text{mol L}^{-1}$  for nitrite,  $1.93 \mu\text{mol L}^{-1}$  for silicate,  $0.073 \mu\text{mol L}^{-1}$  for phosphate and  $0.00 \mu\text{mol L}^{-1}$  for ammonia. We observed phosphate concentration values were different in each cardboard box, so we measured the values for each box. The phosphate concentration value in the LNSW we used in this cruise was  $0.081 \mu\text{mol L}^{-1}$ . The concentrations of nitrate, nitrite and ammonia were lower than detection limit as stated in chapter (7.5).

#### Concentrations of nutrients for A, D, B and C standards

Concentrations of nutrients for A, D, B and C standards were adjusted as shown in [Table 4.9-2](#).

We used JAMSTEC-KANSO in-house Si standard solution for A standard of silicate, which doesn't need to neutralize by the hydrochloric acid. B standard was diluted from A standard with the following recipes shown in Table 4.9-3(a). In order to match the salinity and the density of the stock solution (B standard) to the LNSW, during this dilution step, B standard was added the solution that 15.30 g of a sodium chloride powder was dissolved in pure water, and then the final volume was adjusted to 500 mL.

The C standard solution was prepared in the LNSW following the recipes shown in Table 4.9-3(b). All volumetric laboratory tools were calibrated prior the cruise as stated in chapter (6.1). Then the actual concentrations of nutrients in each fresh standard solution were calculated based on the ambient and the solution temperature, together with the determined factors of volumetric laboratory wares.

The calibration curves for each run for nitrate, nitrite, silicate and phosphate were obtained using 6 levels, C-1, C-2, C-3, C-4, C-5 and C-6. For ammonia, that was obtained using 3 levels, C-6, C-7, C-8. C-1, C-2, C-3, C-4 and C-5 were the CRM of nutrients in seawater, C-6 and C-7 were diluting using the B standard solution, and C-8 was LNSW.

The D standard solutions were made to calculate the reduction rate of Cd coil. The D standard was diluted from the A standard solution into the pure water, final concentrations were shown in Table 4.9-2.

Table 4.9-2 Nominal concentrations of nutrients for A, D, B and C standards.

	A	B	D	C-1	C-2	C-3	C-4	C-5	C-6	C-7	C-8
NO <sub>3</sub>	45000	900	900	CE	CL	CO	CG	CB	53.8	-	-
NO <sub>2</sub>	21800	17	870	CE	CL	CO	CG	CB	1.04	-	-
SiO <sub>2</sub>	35600	2850		CE	CL	CO	CG	CB	173	-	-
PO <sub>4</sub>	6000	60		CE	CL	CO	CG	CB	3.7	-	-
NH <sub>4</sub>	2000	100		-	-	-	-	-	6.0	3.0	0.0

Unit:  $\mu\text{mol kg}^{-1}$

Table 4.9-3(a) B standard recipes. Final volume was 500 mL.

A Std.	
NO <sub>3</sub>	10 mL
NO <sub>2</sub>	10 mL
SiO <sub>2</sub>	40 mL
PO <sub>4</sub>	5 mL
NH <sub>4</sub>	25 mL

Table 4.9-3(b) Working calibration standard recipes. Final volume was 500 mL.

C Std.	B Std.
C-6	30 mL
C-7	15 mL

#### Renewal of in-house standard solutions

In-house standard solutions as stated in paragraph (6.2.4) were remade by each “renewal time” shown in Table 4.9-4(a) to (c).

Table 4.9-4(a) Timing of renewal of in-house standards.

NO <sub>3</sub> , NO <sub>2</sub> , SiO <sub>2</sub> , PO <sub>4</sub> , NH <sub>4</sub>	Renewal time
A-1 Std. (NO <sub>3</sub> )	maximum a month
A-2 Std. (NO <sub>2</sub> )	commercial prepared solution
A-3 Std. (SiO <sub>2</sub> )	JAMSTEC-KANSO Si standard solution
A-4 Std. (PO <sub>4</sub> )	maximum a month
A-5 Std. (NH <sub>4</sub> )	maximum a month
D-1 Std.	maximum 8 days
D-2 Std.	maximum 8 days
B Std. (mixture of A-1, D-2, A-3, A-4 and A-5 std.)	maximum 8 days

Table 4.9-4(b) Timing of renewal of working calibration standards.

Working standards	Renewal time
C Std. (diluted from B Std.)	every 24 hours

Table 4.9-4(c) Timing of renewal of in-house standards for reduction estimation.

Reduction estimation	Renewal time
36 µM NO <sub>3</sub> (diluted D-1 Std.)	when C Std. renewed
35 µM NO <sub>2</sub> (diluted D-2 Std.)	when C Std. renewed

#### (7) Quality control

##### *i) The precision of the nutrient analyses during the cruise*

The highest standard solution (C-6) was repeatedly determined every 7 to 13 samples to obtain the analytical precision of the nutrient analyses during this cruise. During each run, the total number of the C-6 determination was 9-15 times depending on the run. Each run, we obtained the analytical precision based on this C-6 results, shown in Figures 4.9-7 to 4.9-11. In this cruise, there was total 46 runs. Except for a few runs, the analytical precisions were less than 0.2% for nitrate (Figure 4.9-7), silicate (Figure 4.9-9), and phosphate (Figure 4.9-10).

The overall precisions throughout this cruise were calculated based on the analytical precisions obtained from all of the runs, and shown in Table 4.9-5. During this cruise, overall median precisions were 0.13 % for nitrate, 0.19 % for nitrite, 0.12 % for silicate, 0.12 % for phosphate and 0.31 % for ammonia, respectively. The overall median precision for each parameter during this cruise was comparable to the previously published the precisions during the R/V Mirai cruises conducted in 2009 - 2020.

Table 4.9-5 Summary of overall precision based on the replicate analyses ( $k=1$ )

	Nitrate CV %	Nitrite CV %	Silicate CV %	Phosphate CV %	Ammonia CV %
Median	0.13	0.19	0.12	0.12	0.31
Mean	0.13	0.22	0.11	0.12	0.32
Maximum	0.22	1.12	0.16	0.22	0.64

Minimum	0.04	0.08	0.05	0.05	0.13
N	44*	46	46	45**	46

\*The data of 2 runs was excepted because peak shape was bad due to not good Cd coil condition (see chapter 8).

\*\*The data of one run was excepted because there was a large baseline shift.

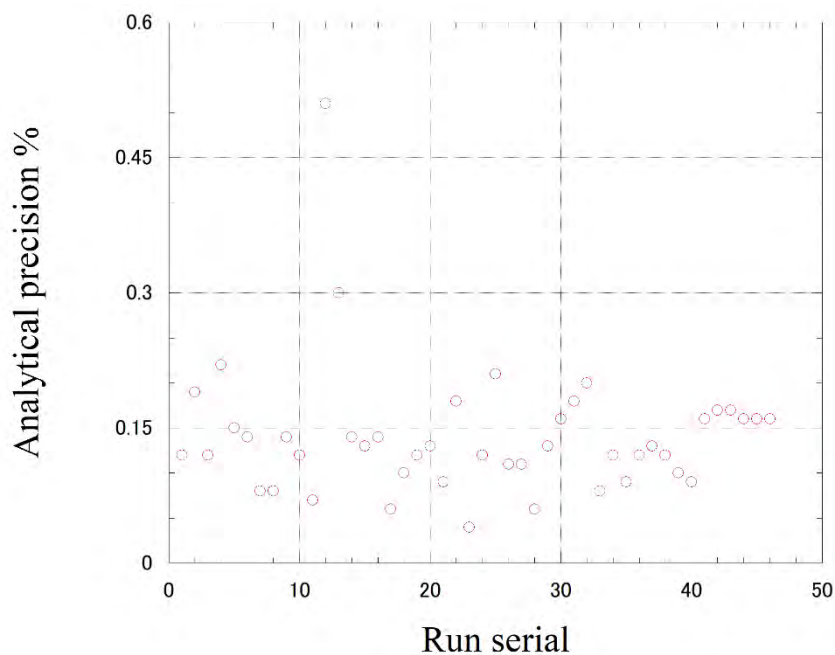


Figure 4.9-7 Time series of precision of nitrate in MR21-04. Analyses of run serial 12 and 13 had bad peaks because Cd coil was in bad condition (see chapter 8).

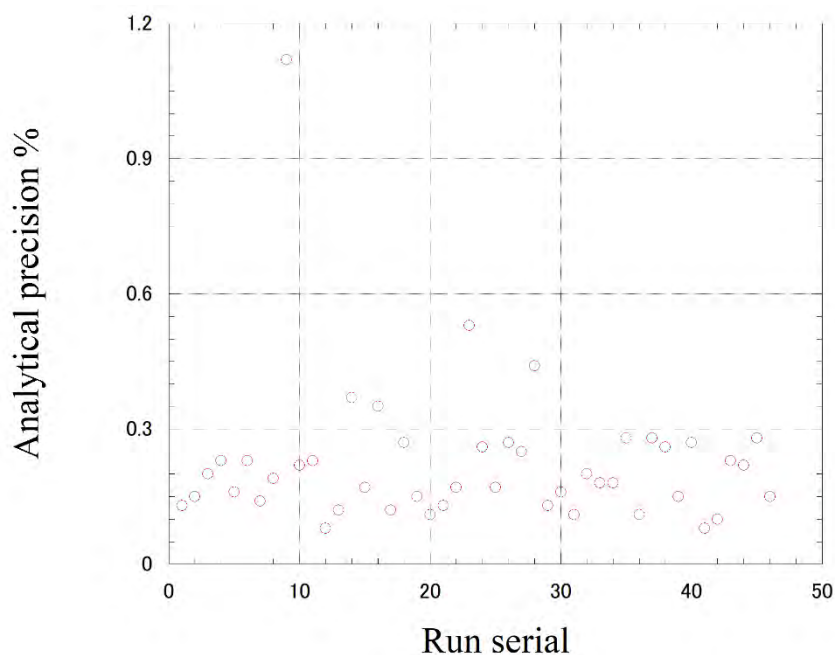


Figure 4.9-8 Time series of precision of nitrite in MR21-04.

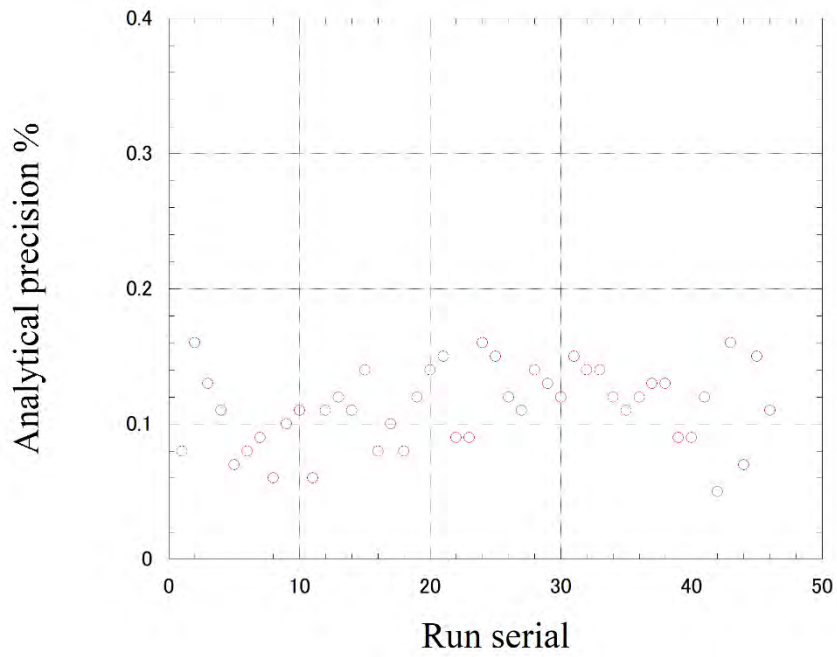


Figure 4.9-9 Time series of precision of silicate in MR21-04.

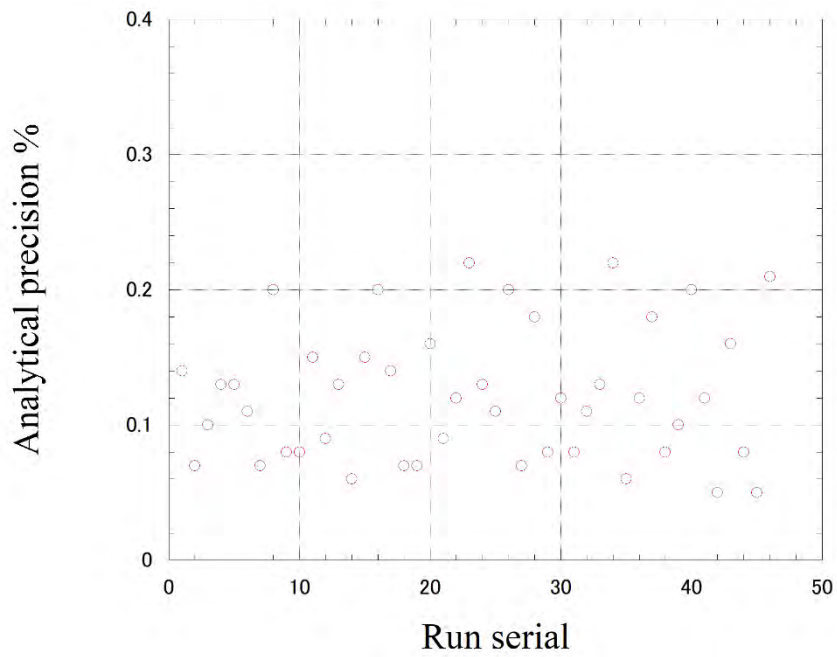


Figure 4.9-10 Time series of precision of phosphate in MR21-04. For run serial 23, there was a large baseline shift.

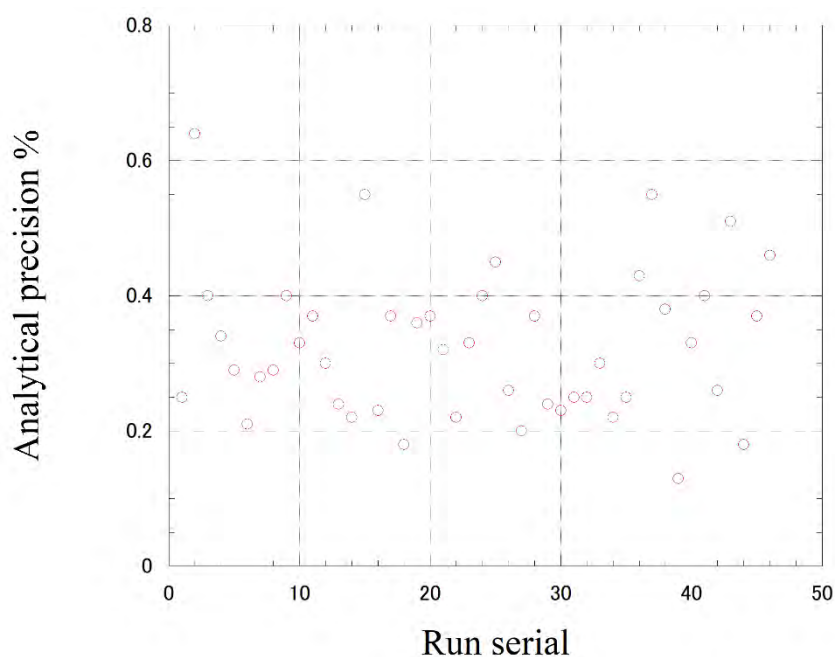


Figure 4.9-11 Time series of precision of ammonia in MR21-04.

*ii) CRM lot. CF measurement during this cruise*

CRM lot. CF was measured every run to evaluate the comparability throughout the cruise. The all of the results of lot. CF during this cruise were shown as Figures 4.9-12 to 4.9-16. All of the measured concentrations of CRM lot. CF was within the uncertainty of certified values for nitrate, nitrite, silicate and phosphate. The reported CRM values were shown in [Table 4.9-1](#). CRM lot. CF of run serial 7 & 8 had abnormal values especially for nitrite and ammonia.

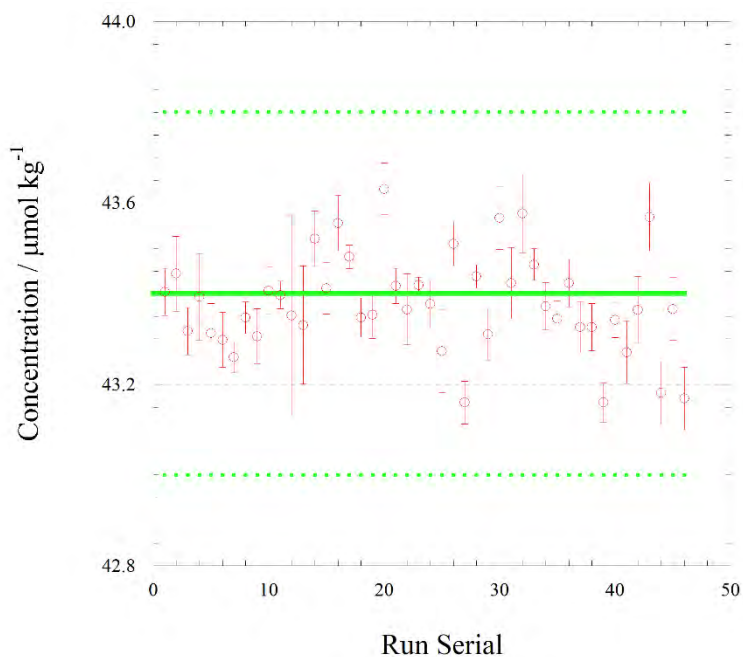


Figure 4.9-12 Time series of CRM-CF of nitrate in MR21-04. Solid green line is certified nitrate concentration of CRM and dotted green line show uncertainty of certified value at  $k=2$ .

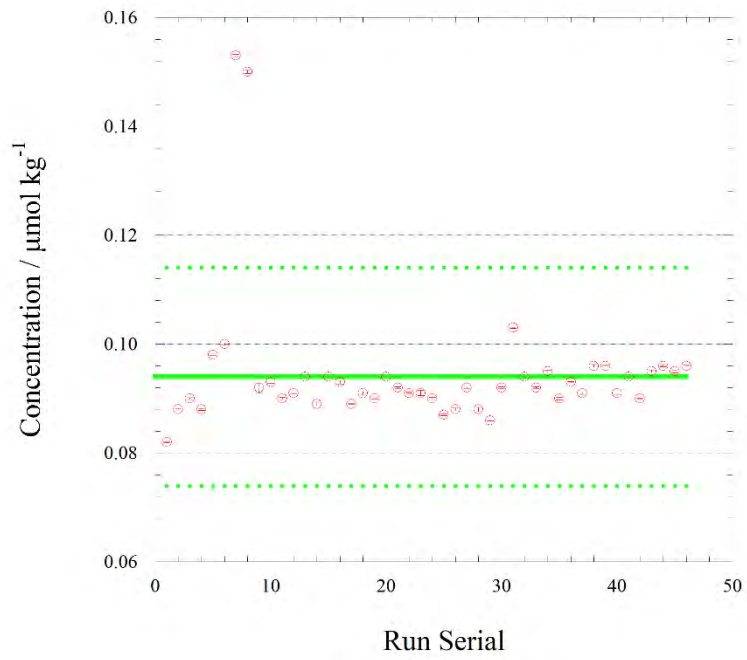


Figure 4.9-13 Same as Figure 4.9-12, but for nitrite.

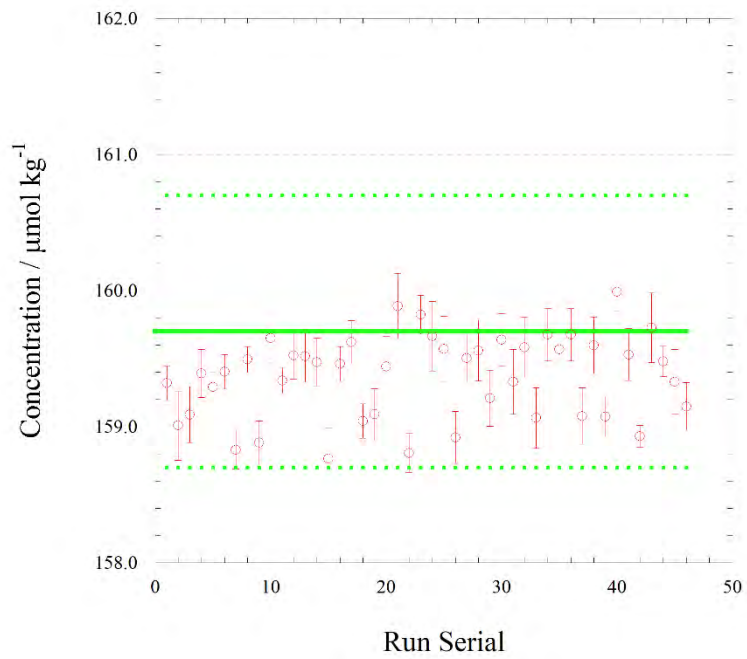


Figure 4.9-14 Same as Figure 4.9-12, but for silicate.

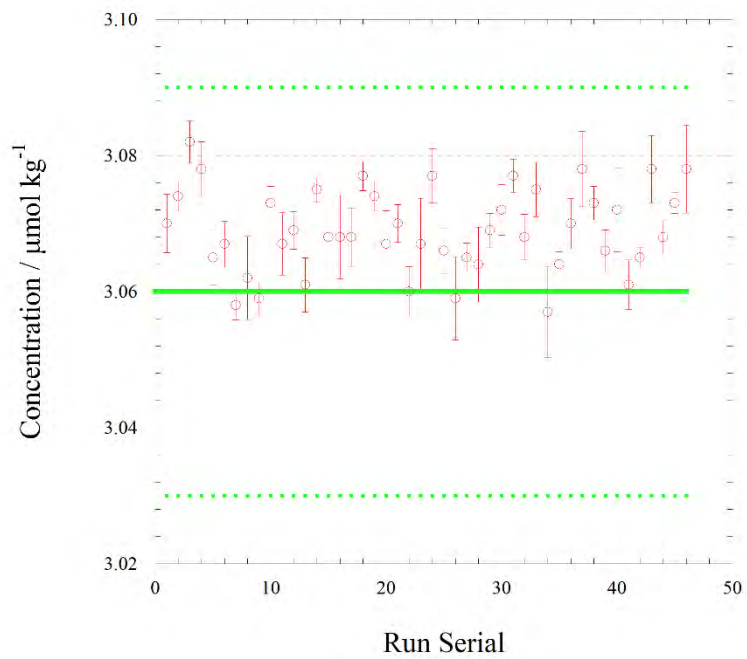


Figure 4.9-15 Same as Figure 4.9-12, but for phosphate.

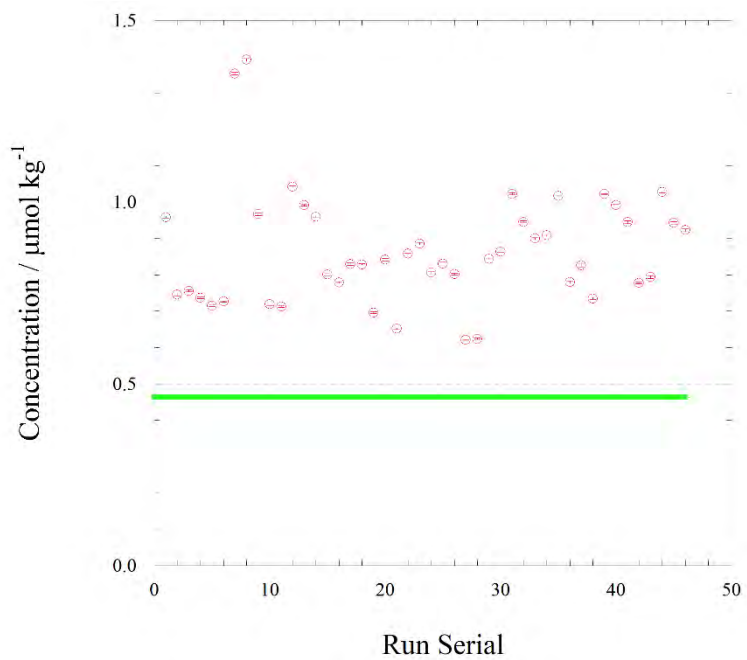


Figure 4.9-16 Time series of CRM-CF of ammonia in MR21-04. Green line is reference value for ammonia concentration of CRM-CF.

iii) Carryover

We also summarized the magnitudes of carry over throughout the cruise. In order to evaluate carryover in each run, we conducted determinations C-6 followed by determination of LNSW twice. The difference from LNSW-1 to LNSW-2 was obtained and used for this “carryover” evaluation. The Carryover (%) was obtained from the following equation.

$$\text{Carryover (\%)} = (\text{LNSW-1} - \text{LNSW-2}) / (\text{C-6} - \text{LNSW-2}) * 100 (\%)$$

The summary of the carryover (%) was shown in Table 4.9-6 and Figure 4.9-17 to 4.9-21. The results were low % (<0.1 % for silicate; <0.2% for nitrate, nitrite and phosphate; <1% for ammonia). The low % indicates that there is no significant issue during this cruise. In this Table 4.9-6 we took all 46 runs to summarize carryover statistics while for Table 4.9-5 of precision statistics we included precision data of which were runs for adapted data of the nutrient concentration.

Table 4.9-6 Summary of carryover throughout MR21-04.

	Nitrate %	Nitrite %	Silicate %	Phosphate %	Ammonia %
Median	0.14	0.13	0.07	0.19	0.56
Mean	0.15	0.11	0.07	0.22	0.59
Maximum	0.23	0.34	0.15	0.54	1.45
Minimum	0.06	0.00	0.03	0.04	0.00
N	46	46	46	46	46

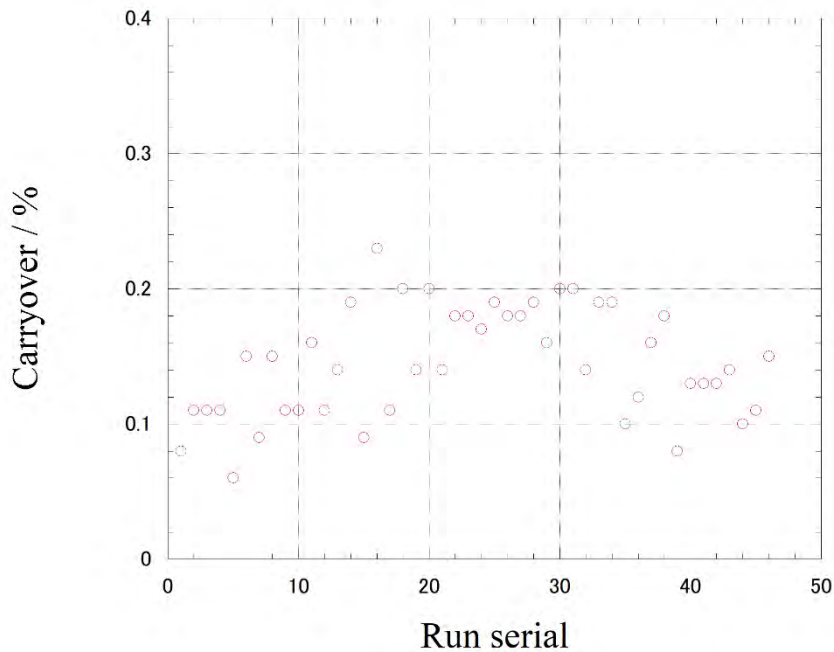


Figure 4.9-17 Time series of carry over of nitrate in MR21-04.

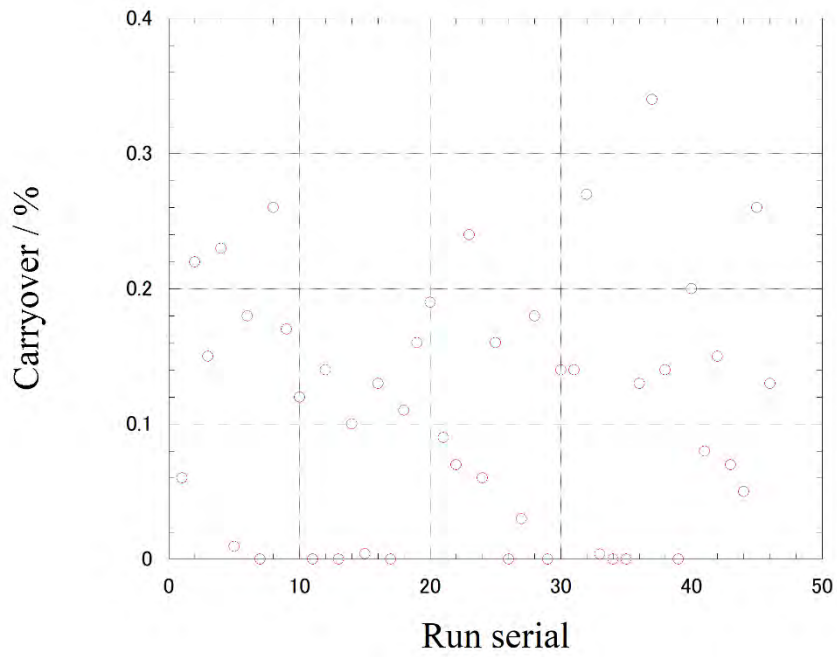


Figure 4.9-18 Same as 4.9-17 but for nitrite.

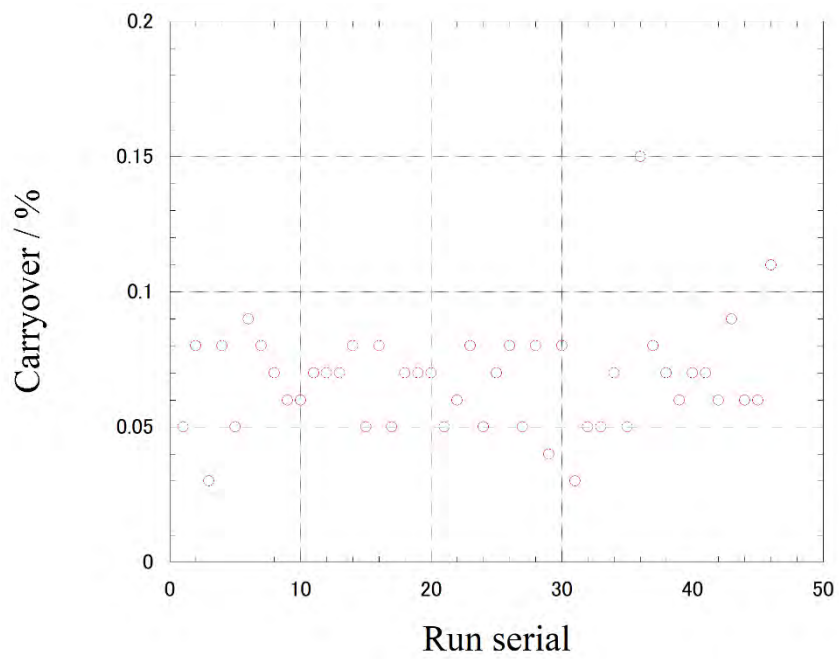


Figure 4.9-19 Same as 4.9-17 but for silicate

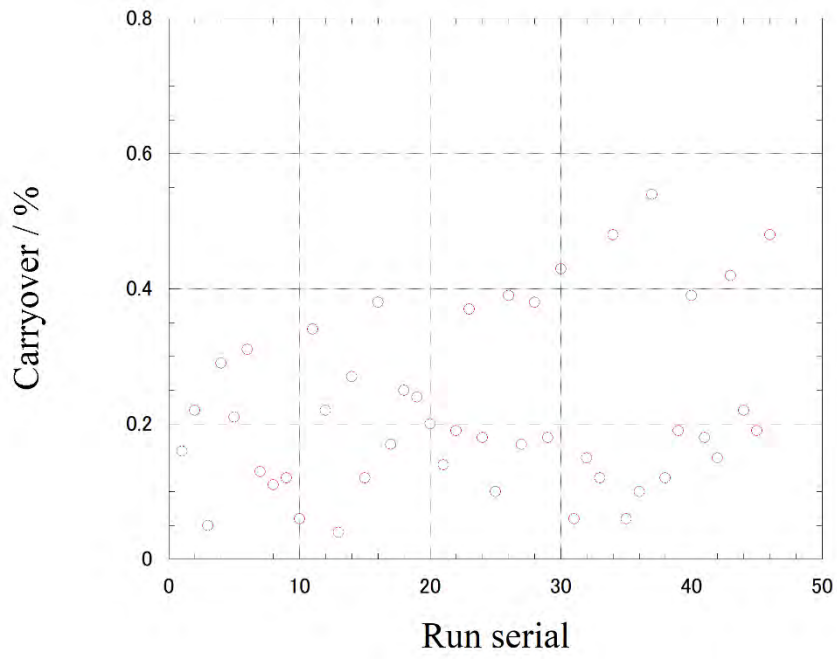


Figure 4.9-20 Same as 4.9-17 but for phosphate.

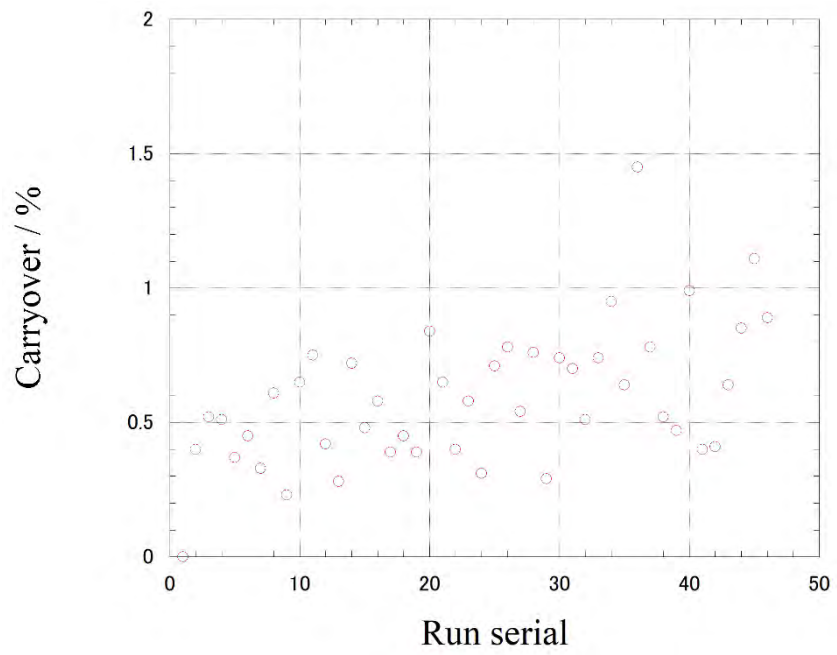


Figure 4.9-21 Same as 4.9-17 but for ammonia.

iv) *Estimation of uncertainty of nitrate, silicate, phosphate, nitrite and ammonia concentrations*

Empirical equations, eq. (1), (2) and (3) to estimate the uncertainty of measurement of nitrate, silicate and phosphate were obtained based on 46 measurements of 30 sets of CRMs (Table 4.9-1). These empirical equations are as follows, respectively. We didn't use values that were obviously abnormal or had bad peak.

Nitrate Concentration  $C_{NO_3}$  in  $\mu\text{mol kg}^{-1}$ :

$$\text{Uncertainty of measurement of nitrate (\%)} = 0.17905 + 1.2798 * (1 / C_{NO_3}) \quad \text{--- (1)}$$

where  $C_{NO_3}$  is nitrate concentration of sample.

Silicate Concentration  $C_{SiO_2}$  in  $\mu\text{mol kg}^{-1}$ :

$$\text{Uncertainty of measurement of silicate (\%)} = 0.13452 + 3.5493 * (1 / C_{SiO_2}) \quad \text{--- (2)}$$

where  $C_{SiO_2}$  is silicate concentration of sample.

Phosphate Concentration  $C_{PO_4}$  in  $\mu\text{mol kg}^{-1}$ :

$$\text{Uncertainty of measurement of phosphate (\%)} = 0.10891 + 0.30718 * (1 / C_{PO_4}) \quad \text{--- (3)}$$

where  $C_{PO_4}$  is phosphate concentration of sample.

Empirical equations, eq. (4) and (5) to estimate the uncertainty of measurement of nitrite and ammonia were obtained based on duplicate measurements of the samples.

Nitrite Concentration  $C_{NO_2}$  in  $\mu\text{mol kg}^{-1}$ :

$$\begin{aligned} \text{Uncertainty of measurement of nitrite (\%)} = \\ -0.085658 + 0.19735 * (1 / C_{NO_2}) - 0.000037425 * (1 / C_{NO_2}) * (1 / C_{NO_2}) \quad \text{--- (4)} \end{aligned}$$

where  $C_{NO_2}$  is nitrite concentration of sample.

Ammonia Concentration  $C_{NH_4}$  in  $\mu\text{mol kg}^{-1}$ :

$$\begin{aligned} \text{Uncertainty of measurement of ammonia (\%)} = \\ 1.5022 + 1.1854 * (1 / C_{NH_4}) - 0.0024978 * (1 / C_{NH_4}) * (1 / C_{NH_4}) \quad \text{--- (5)} \end{aligned}$$

where  $C_{NH_4}$  is ammonia concentration of sample.

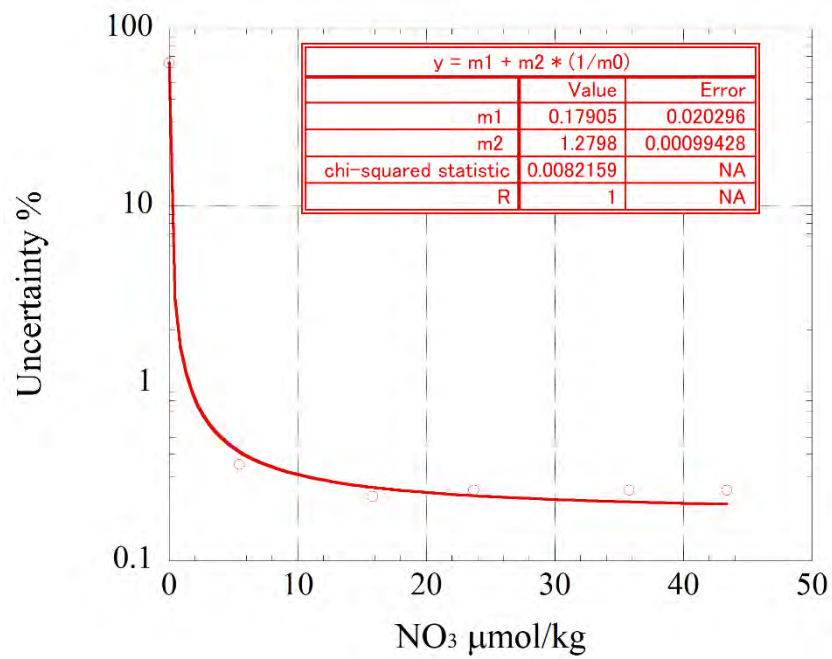


Figure 4.9-22 Estimation of uncertainty for nitrate.

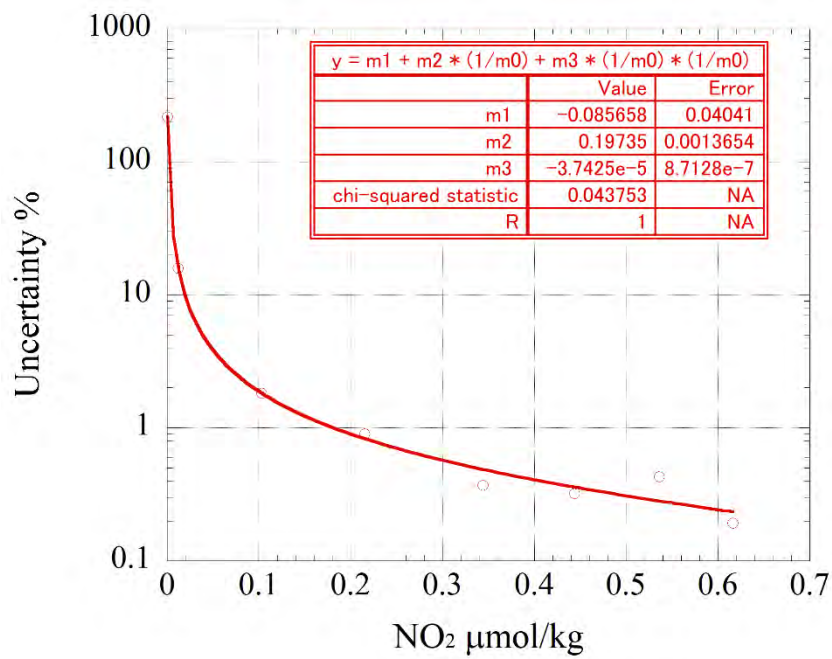


Figure 4.9-23 Estimation of uncertainty for nitrite.

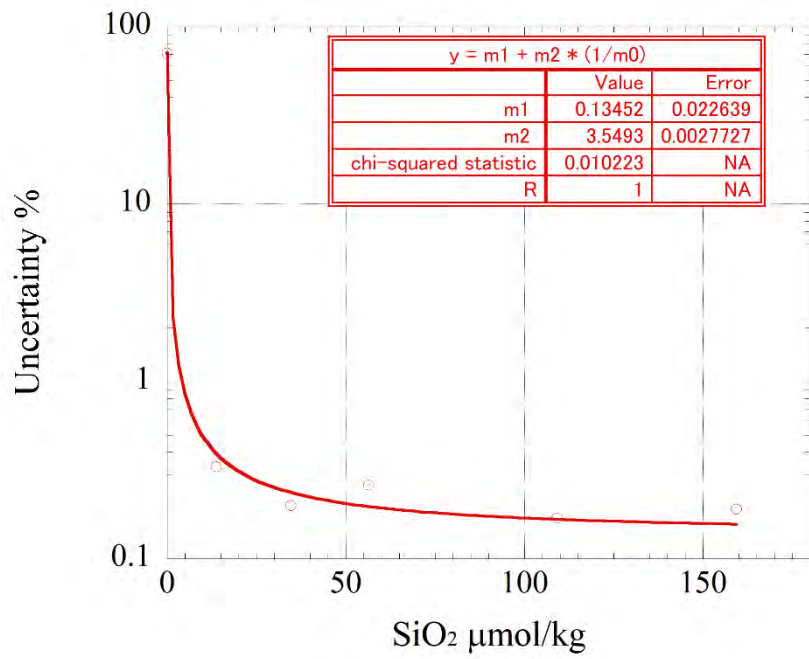


Figure 4.9-24 Estimation of uncertainty for silicate.

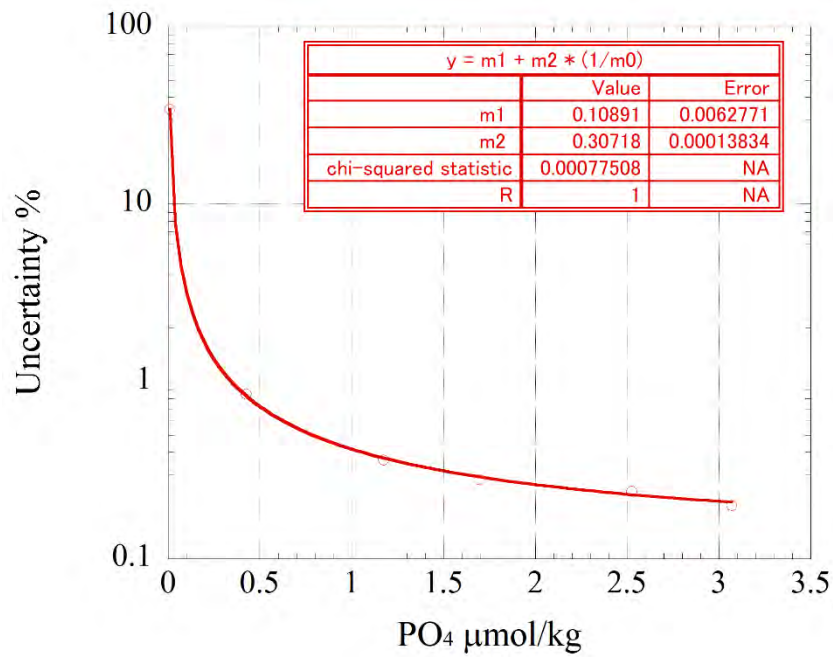


Figure 4.9-25 Estimation of uncertainty for phosphate.

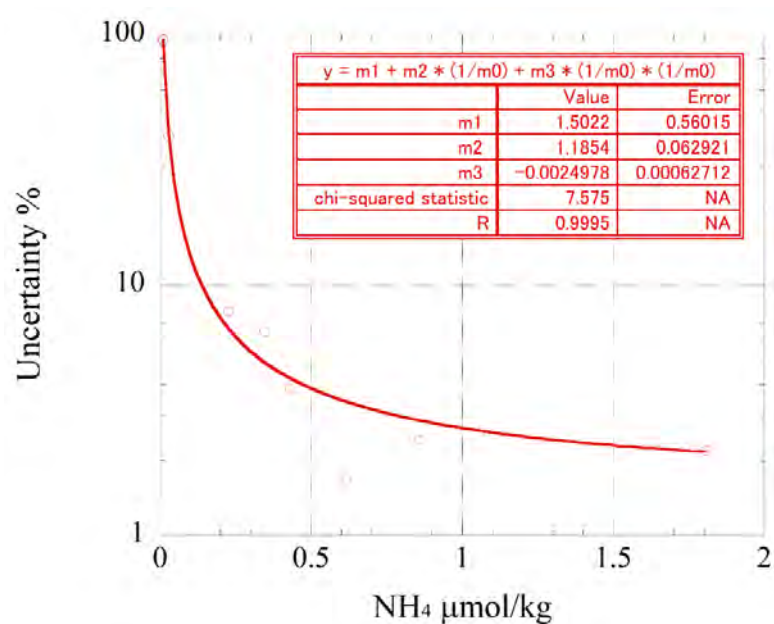


Figure 4.9-26 Estimation of uncertainty for ammonia.

v) *Detection limit and quantitative determination of nutrients analyses during the cruise*

The LNSW was determined every 7 to 13 samples to obtain detection limit of the nutrient analyses during this cruise. During each run, the total number of the LNSW determination was 8-14 times depending on the run. The detection limit was calculated based on the LNSW results obtained from all the runs by the following equation.

$$\text{Detection limit} = 3 * \text{standard deviation of repeated measurement of LNSW}$$

The summary of detection limit are shown in Table 4.9-7. During in this cruise, detection limit were 0.03  $\mu\text{mol kg}^{-1}$  for nitrate, 0.00  $\mu\text{mol kg}^{-1}$  for nitrite, 0.07  $\mu\text{mol kg}^{-1}$  for silicate, 0.005  $\mu\text{mol kg}^{-1}$  for phosphate and 0.02  $\mu\text{mol kg}^{-1}$  for ammonia, respectively.

The quantitative determination of nutrient analyses is the concentration of which uncertainty is 33 % in the empirical equations, eq. (1) to (5) in chapter (7.4). The summary of quantitative determination are shown in Table 4.9-7. During in this cruise, the quantitative determination were 0.04  $\mu\text{mol kg}^{-1}$  for nitrate, 0.01  $\mu\text{mol kg}^{-1}$  for nitrite, 0.11  $\mu\text{mol kg}^{-1}$  for silicate, 0.009  $\mu\text{mol kg}^{-1}$  for phosphate and 0.04  $\mu\text{mol kg}^{-1}$  for ammonia, respectively.

Table 4.9-7 Summary of detection limit and quantitative determination.

	Nitrate $\mu\text{mol kg}^{-1}$	Nitrite $\mu\text{mol kg}^{-1}$	Silicate $\mu\text{mol kg}^{-1}$	Phosphate $\mu\text{mol kg}^{-1}$	Ammonia $\mu\text{mol kg}^{-1}$
Detection limit	0.03	0.00	0.07	0.005	0.02
Quantitative determination	0.04	0.01	0.11	0.009	0.04

**(8) Problems and our actions/solutions**

During the sample analysis of Stations 29 and 30 (Run serial 12 & 13), the peaks of nitrate were significantly different from the previous runs. We have reanalyzed those samples, and then those nitrate peak shapes for those samples showed as usual. Those unusual peaks usually indicate the unstable functionality of those two Cd coils that should reduce nitrate to nitrite. Thus, we have done our usual protocol to reactivate those Cd coils. We washed Cd coils using acetone, hydrochloric acid, and then coated Cd coils with metallic copper again. After this treatment, the results during the re-runs improved and became acceptable for our protocol. This suggests that the issue of those abnormal peak shapes was caused by the issue of the Cd coil functionality.

**(9) List of reagents**

List of reagents is shown in Table 4.9-8.

Table 4.9-8 List of reagent in MR21-04.

IUPAC name	CAS Number	Formula	Compound Name	Manufacture	Grade
4-Aminobenzenesulfonamide	63-74-1	C <sub>6</sub> H <sub>8</sub> N <sub>2</sub> O <sub>2</sub> S	Sulfanilamide	FUJIFILM Wako Pure Chemical Corporation	JIS Special Grade
Ammonium chloride	12125-02-9	NH <sub>4</sub> Cl	Ammonium Chloride	National Metrology Institute of Japan	Certified Reference Material
Antimony potassium tartrate trihydrate	28300-74-5	K <sub>2</sub> (SbC <sub>4</sub> H <sub>2</sub> O <sub>6</sub> ) <sub>2</sub> ·3H <sub>2</sub> O	Bis[(+)-tartrato]diantimonate(III) Dipotassium Trihydrate	FUJIFILM Wako Pure Chemical Corporation	JIS Special Grade
Boric acid	10043-35-3	H <sub>3</sub> BO <sub>3</sub>	Boric Acid	FUJIFILM Wako Pure Chemical Corporation	JIS Special Grade
Hydrogen chloride	7647-01-0	HCl	Hydrochloric Acid	FUJIFILM Wako Pure Chemical Corporation	JIS Special Grade
Imidazole	288-32-4	C <sub>3</sub> H <sub>4</sub> N <sub>2</sub>	Imidazole	FUJIFILM Wako Pure Chemical Corporation	JIS Special Grade
L-Ascorbic acid	50-81-7	C <sub>6</sub> H <sub>8</sub> O <sub>6</sub>	L-Ascorbic Acid	FUJIFILM Wako Pure Chemical Corporation	JIS Special Grade
N-(1-Naphthalenyl)-1,2-ethanediamine, dihydrochloride	1465-25-4	C <sub>12</sub> H <sub>16</sub> Cl <sub>2</sub> N <sub>2</sub>	N-1-Naphthylethylenediamine Dihydrochloride	FUJIFILM Wako Pure Chemical Corporation	for Nitrogen Oxides Analysis
Oxalic acid	144-62-7	C <sub>2</sub> H <sub>2</sub> O <sub>4</sub>	Oxalic Acid	FUJIFILM Wako Pure Chemical Corporation	Wako Special Grade
Phenol	108-95-2	C <sub>6</sub> H <sub>6</sub> O	Phenol	FUJIFILM Wako Pure Chemical Corporation	JIS Special Grade
Potassium nitrate	7757-79-1	KNO <sub>3</sub>	Potassium Nitrate	Merck KGaA	Suprapur®
Potassium dihydrogen phosphate	7778-77-0	KH <sub>2</sub> PO <sub>4</sub>	Potassium dihydrogen phosphate anhydrous	Merck KGaA	Suprapur®
Sodium chloride	7647-14-5	NaCl	Sodium Chloride	FUJIFILM Wako Pure Chemical Corporation	TraceSure®
Sodium citrate dihydrate	6132-04-3	Na <sub>3</sub> C <sub>6</sub> H <sub>5</sub> O <sub>7</sub> ·2H <sub>2</sub> O	Trisodium Citrate Dihydrate	FUJIFILM Wako Pure Chemical Corporation	JIS Special Grade
Sodium dodecyl sulfate	151-21-3	C <sub>12</sub> H <sub>25</sub> NaO <sub>4</sub> S	Sodium Dodecyl Sulfate	FUJIFILM Wako Pure Chemical Corporation	for Biochemistry
Sodium hydroxide	1310-73-2	NaOH	Sodium Hydroxide for Nitrogen Compounds Analysis	FUJIFILM Wako Pure Chemical Corporation	for Nitrogen Analysis
Sodium hypochlorite	7681-52-9	NaClO	Sodium Hypochlorite Solution	Kanto Chemical co., Inc.	Extra pure
Sodium molybdate dihydrate	10102-40-6	Na <sub>2</sub> MoO <sub>4</sub> ·2H <sub>2</sub> O	Disodium Molybdate(VI) Dihydrate	FUJIFILM Wako Pure Chemical Corporation	JIS Special Grade
Sodium nitroferrocyanide dihydrate	13755-38-9	Na <sub>2</sub> [Fe(CN) <sub>5</sub> NO]·2H <sub>2</sub> O	Sodium Pentacyanonitrosylferrate(II) Dihydrate	FUJIFILM Wako Pure Chemical Corporation	JIS Special Grade

Sulfuric acid	7664-93-9	H <sub>2</sub> SO <sub>4</sub>	Sulfuric Acid	FUJIFILM Wako Pure Chemical Corporation	JIS Special Grade
tetrasodium;2-[2-(bis(carboxylatomethyl)amino)ethyl-(carboxylatomethyl)amino]acetate;tetrahydrate	13235-36-4	C <sub>10</sub> H <sub>12</sub> N <sub>2</sub> Na <sub>4</sub> O <sub>8</sub> ·4H <sub>2</sub> O	Ethylenediamine-N,N,N',N'-tetraacetic Acid Tetrasodium Salt Tetrahydrate (4NA)	Dojindo Molecular Technologies, Inc.	-
Synonyms: t-Octylphenoxy polyoxyethanol 4-(1,1,3,3-Tetramethylbutyl)phenyl-polyethylene glycol Polyethylene glycol tert-octylphenyl ether	9002-93-1	(C <sub>2</sub> H <sub>4</sub> O) <sub>n</sub> C <sub>14</sub> H <sub>22</sub> O	Triton™ X-100	Sigma-Aldrich Japan G.K.	-

#### (10) Data archives

These data obtained in this cruise will be submitted to the Data Management Group of JAMSTEC, and will be opened to the public via “Data Research System for Whole Cruise Information in JAMSTEC (DARWIN)” in JAMSTEC web site.

<<http://www.godac.jamstec.go.jp/darwin/e>>

#### (11) References

Susan Becker, Michio Aoyama E. Malcolm S. Woodward, Karel Bakker, Stephen Coverly, Claire Mahaffey, Toste Tanhua, (2019) The precise and accurate determination of dissolved inorganic nutrients in seawater, using Continuous Flow Analysis methods, n: The GO-SHIP Repeat Hydrography Manual: A Collection of Expert Reports and Guidelines. Available online at: <http://www.go-ship.org/HydroMan.html>. DOI: <http://dx.doi.org/10.25607/OBP-555>

Grasshoff, K. 1976. Automated chemical analysis (Chapter 13) in Methods of Seawater Analysis. With contribution by Almgreen T., Dawson R., Ehrhardt M., Fonselius S. H., Josefsson B., Koroleff F., Kremling K. Weinheim, New York: Verlag Chemie.

Grasshoff, K., Kremling K., Ehrhardt, M. et al. 1999. Methods of Seawater Analysis. Third, Completely Revised and Extended Edition. WILEY-VCH Verlag GmbH, D-69469 Weinheim (Federal Republic of Germany).

Hydes, D.J., Aoyama, M., Aminot, A., Bakker, K., Becker, S., Coverly, S., Daniel, A., Dickson, A.G., Grosso, O., Kerouel, R., Ooijen, J. van, Sato, K., Tanhua, T., Woodward, E.M.S., Zhang, J.Z., 2010. Determination of Dissolved Nutrients (N, P, Si) in Seawater with High Precision and Inter-Comparability Using Gas-Segmented Continuous Flow Analysers, In: GO-SHIP Repeat Hydrography Manual: A Collection of Expert Reports and Guidelines. IOCCP Report No. 14, ICPO Publication Series No 134.

Kimura, 2000. Determination of ammonia in seawater using a vaporization membrane permeability method. 7th auto analyzer Study Group, 39-41.

Murphy, J., and Riley, J.P. 1962. Analytica Chimica Acta 27, 31-36.

### 4.10 Chlorofluorocarbons and Sulfur hexafluoride

#### (1) Personnel

Masahito Shigemitsu	JAMSTEC
Yuichiro Kumamoto	JAMSTEC
Ken'ichi Sasaki	JAMSTEC
Aine Yoda	MWJ
Haruka Sato	MWJ

#### (2) Objectives

Chlorofluorocarbons (CFCs) and sulfur hexafluoride (SF<sub>6</sub>) are man-made stable gases. These atmospheric gases can slightly dissolve in sea surface water by air-sea gas exchange and then spread into the ocean interior. Thus, these dissolved gases could be used as chemical tracers for the ocean

circulation/ventilation. In this cruise, we try to gain insights into the ventilation rates and pathways in the North Pacific. To this end, we measured the concentrations of three chemical species of CFCs, CFC-11 ( $\text{CCl}_3\text{F}$ ), CFC-12 ( $\text{CCl}_2\text{F}_2$ ), and CFC-113 ( $\text{C}_2\text{Cl}_3\text{F}_3$ ), and  $\text{SF}_6$  in seawater on board.

### (3) Instruments and methods

#### *i) Bottle sampling*

Discrete water samples for each station were collected using 12 liter Niskin bottles mounted on a CTD system. Each sample was introduced to a glass bottle of 450 ml developed in JAMSTEC by connecting a spigot of Niskin bottle through Tygon tubing. Before water sampling, each glass bottle was filled with CFCs/ $\text{SF}_6$ -free  $\text{N}_2$ . We made seawater of twice the bottle volume overflow for each sample. The samples were stored in a thermostatic water bath kept at about  $7^\circ\text{C}$  immediately after water sampling, and then the samples were measured as soon as possible (usually within 18 hours after sampling).

#### *ii) Air sampling*

In order to confirm CFCs/ $\text{SF}_6$  concentrations of the standard gases and the stabilities of the concentrations as well as to check saturation levels in the sea surface water, the mixing ratios in background air were periodically analyzed. Air samples were continuously introduced into a laboratory by an air pump. The end of 10 mm OD Dekaron tubing was put on a head of the compass deck and the other end was connected onto the air pump in the laboratory. The tubing was relayed by a three-way stopcock. An air sample was collected from the flowing air into a 200 ml glass cylinder by attaching the cylinder to the cock.

#### *iii) CFCs/ $\text{SF}_6$ measurements*

The two  $\text{SF}_6$ /CFCs analyzing systems, which are based on purging and trapping gas chromatography, were used. The two systems are structurally same (hereafter, referred to as systems A and B). Constant volume of water sample (200 ml) is introduced into a sample loop. The sample is first drawn into a stripping chamber and the dissolved  $\text{SF}_6$  and CFCs are extracted by CFCs/ $\text{SF}_6$ -free  $\text{N}_2$  gas purging for 8 minutes at  $220 \text{ ml min}^{-1}$ . The extracted gases are dried by passing them through a magnesium perchlorate desiccant tube, and concentrated in a main trap column cooled down to  $-80^\circ\text{C}$ . The main trap column is a 30-cm length of 1/8-in stainless steel tubing packed with 80/100 mesh Porapak Q (5 cm in length) and 60/80 mesh Carboxen 1000 (5cm in length). Stripping efficiencies were confirmed by re-stripping of surface layer samples for every station and more than about 99 % of dissolved  $\text{SF}_6$  and CFCs were extracted on the first purge. The purging and trapping are followed by the isolation and heating to  $180^\circ\text{C}$  of the main trap column. After 1 minute heating, the desorbed gases are transferred to a focus trap (same as the main trap, except for 1/16-in tubing) cooled down to  $-80^\circ\text{C}$  for 30 seconds. Then, the sample gases held in the focus trap are desorbed by the same manner as in the main trap, and are transferred into a pre-column 1 (PC 1, ~6 m of Silica Plot capillary column with i.d. of 0.53 mm and film thickness of  $6 \mu\text{m}$ , held at  $95^\circ\text{C}$ ). The sample gases are roughly separated in the PC 1, and the  $\text{SF}_6$  and CFCs are eluted into a pre-column 2 (PC 2, ~5 m of Molsieve 5A Plot capillary column with i.d. of 0.53 mm and film thickness of  $15 \mu\text{m}$ , held at  $95^\circ\text{C}$ ). Then, the PC1 is connected to a cleaning line, and the remained gases with high boiling points are flushed by a counter flow of CFCs/ $\text{SF}_6$ -free  $\text{N}_2$ .  $\text{SF}_6$  and CFCs are quickly eluted from PC 2 onto a main-column 1 (MC 1, ~9 m of Pola Bond-Q capillary column with i.d. of 0.53 mm and film thickness of  $6 \mu\text{m}$  which is connected to ~18 m of Silica Plot capillary column, held at  $95^\circ\text{C}$ ) and  $\text{N}_2\text{O}$  is retained on PC 2. The PC 2 is then connected to a back-flush carrier gas line and  $\text{N}_2\text{O}$  is sent onto a main-column 2 (MC 2, ~3 m of Molsieve 5A Plot connected to ~9 m of Pola Bond-Q capillary column, held at  $95^\circ\text{C}$ ).  $\text{SF}_6$  and CFCs are further separated on the MC 1 and detected by the ECD #1.  $\text{N}_2\text{O}$  sent onto the MC 2 is detected by the ECD #2. However,  $\text{N}_2\text{O}$  was not targeted in this cruise. The PC1, PC2, MC1 and MC2 were in a Shimadzu GC-2014 gas chromatograph with the ECDs held at  $300^\circ\text{C}$ . Please note that the CFCs/ $\text{SF}_6$ -free  $\text{N}_2$  used in the water sampling and the measurements of  $\text{SF}_6$  and CFCs was filtered by a gas purifier column packed with Molecular Sieve 13X before the gas is introduced to the system. The mass flow rates of CFCs/ $\text{SF}_6$ -free  $\text{N}_2$  for the carrier and detector make-up gases are 10

ml min<sup>-1</sup> and 27 ml min<sup>-1</sup>, respectively.

iv) *Comparison between the standard gases used in this cruise (MR21-04) and the past cruise (MR19-04)*

In order to keep the comparability of measurements of CFCs/SF<sub>6</sub> in our laboratory, we compared the concentrations of standard gas used in this cruise (MR21-04) with those in the past cruise (MR19-04). We measured each standard gas three times and compared the determinations.

#### (4) Performance of CFCs/SF<sub>6</sub> measurements

The analytical precisions were estimated from replicate measurements. The estimated preliminary precisions were ± 0.028 pmol/kg, ± 0.020 pmol/kg, ± 0.024 pmol/kg, and ± 0.034 fmol/kg for CFC-11, CFC-12, CFC-113, and SF<sub>6</sub>, respectively.

#### (5) Extra experiments

i) *Estimation of blanks for Niskin bottle and Tygon tubing*

In order to estimate blanks of CFCs and SF<sub>6</sub> derived from Niskin bottle and Tygon tubing, we carried out the following extra experiment at Station 80. We closed twelve Niskin bottles at 3000 m depth where CFCs and SF<sub>6</sub> were thought to be at the lowest levels along the P01 transect. First, we sampled two of the bottles just after the Niskin bottles were returned to deck. The other pairs were taken 2, 4, 8, 16 and 24 hours after the first sampling. We measured CFCs and SF<sub>6</sub> for those samples (Fig. 4.10.1). SF<sub>6</sub> and CFC-113 were not detected in this experiment. However, CFC-11 and CFC-12 steadily increased with time. The sampling for CFCs and SF<sub>6</sub> was usually finished within about 1 hour after return to deck, and the blanks of CFC-11 and CFC-12 derived from Niskin bottle and Tygon tubing were estimated to be about 0.008-0.010 and 0.004-0.006 pmol kg<sup>-1</sup>, respectively.

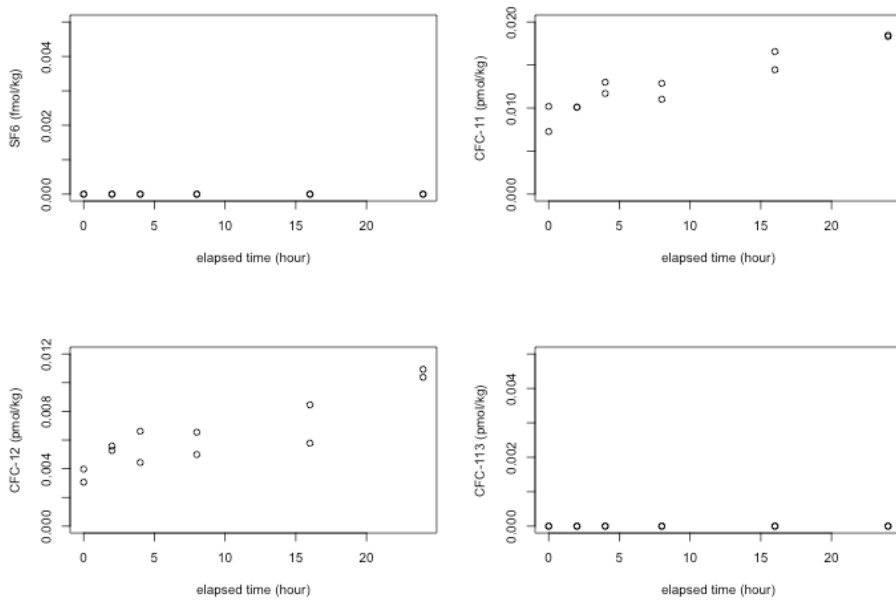


Fig. 4.10.1 CFCs/SF<sub>6</sub> concentrations as a function of time that waters are stored in the bottle

ii) *Confirmation of how headspace in Niskin bottle affects CFCs/SF<sub>6</sub> concentrations*

We conducted the other extra experiment to get an insight into how headspace in Niskin bottle

affects the measurements of CFCs and SF<sub>6</sub>. One bottle closed at about 3000 m depth in the above experiment (5-1) was sequentially sampled until all the water in the bottle was used up. The samples obtained in this way were measured (Fig. 4.10.2).

For CFC-11 and CFC-12, the effect of headspace was manifested from the 4<sup>th</sup> sample (about 6 liter headspace), while the effect for SF<sub>6</sub> and CFC-113 was confirmed from the 6<sup>th</sup> sample (about 9 liter headspace).

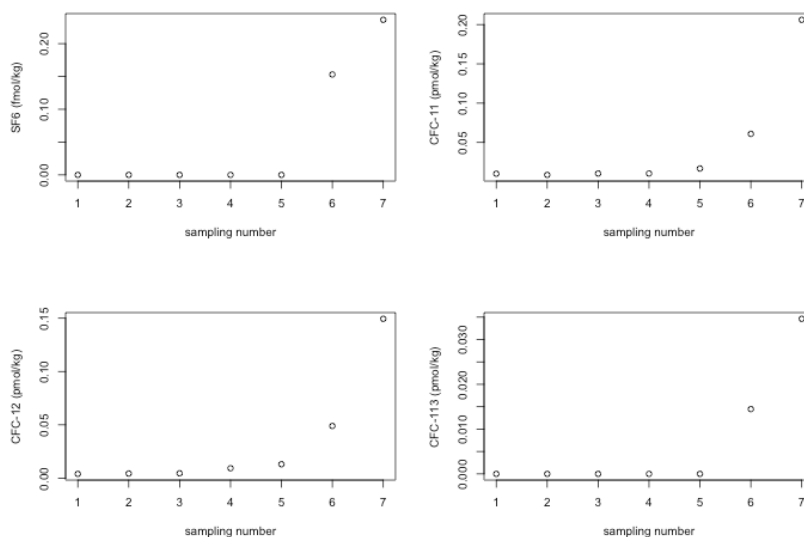


Figure 4.10.2 CFCs/SF<sub>6</sub> concentrations as function of sampling number

#### (6) Machine problems encountered in this cruise

May 20 During the measurements of the standard gas using the system A, the peaks on the chromatogram were smaller than usual peaks or not observed. We did not find any gas leaks and problems in the main and focus traps. We replaced all capillary columns with new ones and all the peaks were restored. Although the specific defects in the capillary columns were unknown, a capillary column that might have suspected defects should not be used.

July 15 The flow rate of the standard gas in the system B was reduced. Although we replaced the switching valve and the gas regulator for the standard gas cylinder, the problem was not solved. Thus, we replaced the narrow stainless steel tubing for the standard gas drain with the wide one and the enough flow rate was restored. Before replacements of valves or other parts, the narrow stainless steel tubing should be checked.

July 18 Valve #4 in the system A did not work correctly because of disconnection of its signal wire. The defect was fixed by the position readjustment of a bundle of signal wires behind the relay box. All soldered points of the signal wires in the systems A and B should be overhauled.

July 26 In the system B, the flow rate of the purge gas through the short desiccant tube B was reduced. We switched the flow path from the wetted tube B to the dried tube A, and the flow rate was restored. Then, the wetted desiccant tube B was replaced by a dried one, but the flow rate was not restored, which suggests that the clogged point was not in the wetted desiccant tube B. We washed the narrow stainless steel tubing connected to the tube B using pure water and acetone, and dried them. This treatment restored the flow rate through the tube B. It should be noted that narrow stainless steel tubing is easy to get clogged.

August 2 During the measurements of the standard gas using the system A, the heights of CFCs and SF<sub>6</sub> peaks on the chromatogram were reduced or disappeared. After the replacement of the

main and focus traps, the peaks were restored but the heights were still smaller than those in the normal condition. Finally, we found a pinhole on the narrow stainless steel tubing close to the focus trap, and replaced the tubing with a new one, which restored the standard gas peaks. The pinhole was probably derived from metallic fatigue during the back and forth movement of the trap. We should pay attention to the main and focus traps and the related stainless steel tubing because they are most frequently moving parts of the system.

August 6 When we switched the flow path from the wetted desiccant tube B to the dried tube A in the system B, slush of the wetted magnesium perchlorate in the desiccant tube B moved in the reverse direction to the purge gas because N<sub>2</sub> gas flow directions for purge gas and cleaning gas of desiccant are structurally designed to be opposite. This raises the possibility that wetted magnesium perchlorate gets into the narrow stainless steel tubing connected to the desiccant tube B. On the other hand, in the desiccant tube A, N<sub>2</sub> gas flow directions for the purge and cleaning gases are same. Thus, the desiccant tube A should be preferentially used instead of the desiccant tube B.

August 13 In the system B, the flow rate of the purge gas through the desiccant tube B was reduced again. We tried to check if the purge gas leaked around the connection of the volumetric glass tube and the glass tube was broken. Finally, we identified another cause for that, i.e., the stainless steel tubing connected to the desiccant tube B was clogged. A part clogged in the desiccant tube B should have been checked before purge gas leak and damage to glass tube are examined.

August 13 During the measurements of the standard gas using the system B, the gas peaks on the chromatogram disappeared. We did not find any gas leaks and problems in the main and focus traps. Finally, we found that the focus trap was frozen by the ice formation on it and did not move correctly. Again, we should pay attention to the main and focus traps because they are most frequently moving parts of the system.

August 13 The temperature in the capillary column oven dropped from 95°C to 38°C due to unknown reason, which resulted in the problematic peaks on the chromatogram. Thermometers in the chromatograph should be monitored carefully.

August 15 The reserve switch of valve #11 (standard gas loop M) in the system B did not work correctly. This should be repaired.

#### **(7) Data archives**

The data obtained in this cruise will be submitted to the Data Management Group of JAMSTEC, and will be open to the public via “Data Research System for Whole Cruise Information in JAMSTEC (DARWIN)” in the JAMSTEC web site.

### **4.11 Carbon properties**

#### **(1) Personnel**

Akihiko Murata	JAMSTEC: Principal investigator
Nagisa Fujiki	MWJ
Hiroshi Hoshino	MWJ
Minori Kamikawa	MWJ

#### **(2) Objective**

Concentrations of CO<sub>2</sub> in the atmosphere are now increasing at a rate of about 2.0 ppmv yr<sup>-1</sup> due to human activities such as burning of fossil fuels, deforestation, and cement production. It is an urgent task to estimate as accurately as possible the absorption capacity of the oceans against the increased atmospheric CO<sub>2</sub>, and to clarify the mechanism of the CO<sub>2</sub> absorption, because the magnitude of the anticipated global warming depends on the levels of CO<sub>2</sub> in the atmosphere, and because the ocean currently absorbs 1/3 of the 6 Gt of carbon emitted into the atmosphere each year by human activities.

In this cruise, we were aimed at quantifying how much anthropogenic CO<sub>2</sub> was absorbed in the Indian Ocean and Southern Ocean. For the purpose, we measured CO<sub>2</sub>-system parameters such as dissolved inorganic carbon (C<sub>T</sub>) and total alkalinity (A<sub>T</sub>) along the WHP P01 section along the latitude circle of ~47°N in the North Pacific.

### (3) Apparatus

#### i) C<sub>T</sub>

Measurement of C<sub>T</sub> was made with a total CO<sub>2</sub> measuring system (Nihon ANS, Inc.). The system comprised of a seawater dispensing system, a CO<sub>2</sub> extraction system and a coulometer. In this cruise, we used a coulometer Model 3000, which was constructed by Nippon ANS. The systems had a specification as follows:

The seawater dispensing system has an auto-sampler (6 ports), which dispenses seawater from a 300 ml borosilicate glass bottle into a pipette of about 15 ml volume by PC control. The pipette is kept at 20°C by a water jacket, in which water from a water bath set at 20°C is circulated. CO<sub>2</sub> dissolved in a seawater sample is extracted in a stripping chamber of the CO<sub>2</sub> extraction system by adding phosphoric acid (~9 % v/v) of about 2 ml. The stripping chamber is approx. 25 cm long and has a fine frit at the bottom. The acid is added to the stripping chamber from the bottom of the chamber by pressurizing an acid bottle for a given time to push out the right amount of acid. The pressurizing is made with nitrogen gas (99.9999 %). After the acid is transferred to the stripping chamber, a seawater sample kept in a pipette is introduced to the stripping chamber by the same method as in adding an acid. The seawater reacted with phosphoric acid is stripped of CO<sub>2</sub> by bubbling the nitrogen gas through a fine frit at the bottom of the stripping chamber. The CO<sub>2</sub> stripped in the chamber is carried by the nitrogen gas (flow rates is 140 ml min<sup>-1</sup>) to the coulometer through a dehydrating module. The module consists of two electric dehumidifiers (kept at ~2 °C) and a chemical desiccant (Mg(ClO<sub>4</sub>)<sub>2</sub>).

The measurement sequence such as system blank (phosphoric acid blank), ~1.5 % CO<sub>2</sub> gas in a nitrogen base, sea water samples (6) is programmed to repeat. The measurement of ~1.5 % CO<sub>2</sub> gas is made to monitor response of coulometer solutions purchased from UIC, Inc.

#### ii) A<sub>T</sub>

Measurement of A<sub>T</sub> was made based on spectrophotometry using a custom-made system (Nihon ANS, Inc.). The system comprises of a water dispensing unit, a HCl titration unit (Hamilton No.2), and a detection unit of a spectrophotometer (TM-UV/VIS C10082CAH, Hamamatsu Photonics, Japan) and an optical source (Ocean Photonics, Japan). The system was automatically controlled by a PC. The water dispensing unit had a water-jacketed pipette and a water-jacketed glass titration cell.

A seawater of approx. 42 ml was transferred from a sample bottle (borosilicate glass bottle; maximum = ~130 ml) into the water-jacketed (25°C) pipette by pressurizing the sample bottle (nitrogen gas), and was introduced into the water-jacketed (25°C) glass titration cell. The introduced seawater was used to rinse the titration cell. After dumping the seawater used for rinse, Milli-Q water was introduced into the titration cell to rinse it. The rinse by Milli-Q water is repeated twice. Then, a seawater of approx. 42 ml was weighted again by the pipette, and was transferred into the titration cell. Then, for seawater blank, absorbances were measured at three wavelengths (730, 616 and 444 nm). After the measurement, an acid titrant, which was a mixture of approx. 0.05 M HCl in 0.65 M NaCl and bromocresol green (BCG), was added into the titration cell. The volume of acid titrant solution was changed according to expected values of A<sub>T</sub> from 1.980 ml to 2.190 ml. The seawater and acid titrant were mixed for 5 minutes by a stirring tip and bubbling by nitrogen gas in the titration cell. Then, absorbances at the three wavelengths were measured again.

Calculation of A<sub>T</sub> was made by the following equation:

$$A_T = (-[H^+]_T V_{SA} + M_A V_A) / V_S,$$

where M<sub>A</sub> is the molarity of the acid titrant added to the seawater sample, [H<sup>+</sup>]<sub>T</sub> is the total excess

hydrogen ion concentration in the seawater, and  $V_S$ ,  $V_A$  and  $V_{SA}$  are the initial seawater volume, the added acid titrant volume, and the combined seawater plus acid titrant volume, respectively.  $[H^+]_T$  is calculated from the measured absorbances based on the following equation (Yao and Byrne, 1998):

$$pH_T = -\log[H^+]_T \\ = 4.2699 + 0.002578(35 - S) + \log((R - 0.00131)/(2.3148 - 0.1299R)) \\ - \log(1 - 0.001005S),$$

where  $S$  is the sample salinity, and  $R$  is the absorbance ratio calculated as:

$$R = (A_{616} - A_{750}) / (A_{444} - A_{750}),$$

where  $A_i$  is the absorbance at wavelength  $i$  nm. The absorbances used for the calculation are averages of 3 measurements both for seawater blank and acidified sample.

The HCl in the acid titrant was standardized on land ( $0.050001 \text{ mol L}^{-1}$  and  $0.050002 \text{ mol L}^{-1}$ ).

#### (4) Shipboard measurement

##### *i) C<sub>T</sub>*

All seawater samples were collected from depth with 12 liter Niskin bottles basically at every other stations. The seawater samples for  $C_T$  were taken with a plastic drawing tube (PFA tubing connected to silicone rubber tubing) into a 250 ml DURAN<sup>®</sup> glass bottle. The glass bottle was filled with seawater smoothly from the bottom following a rinse with a seawater of 2 full, bottle volumes. The glass bottle was closed by an inner cap loosely, which was fitted tightly to the bottle mouth after mercuric chloride was added.

At a chemical laboratory on ship, a volume of about 3mL seawater was removed with a plastic pipette from sampling bottles to have a headspace of approx. 1% of the bottle volume. A saturated mercuric chloride of 100  $\mu\text{l}$  was added to poison seawater samples. The seawater samples were kept at 5°C in a refrigerator until analysis. A few hours just before analysis, the seawater samples were kept at 20°C in a water bath.

##### *ii) A<sub>T</sub>*

All seawater samples were collected from depth using 12 liter Niskin bottles at the same stations as for  $C_T$ . The seawater samples for  $A_T$  were taken with a plastic drawing tube (PFA tubing connected to silicone rubber tubing) into a 100 ml DURAN<sup>®</sup> glass bottle. The glass bottle was filled with seawater smoothly from the bottom after rinsing it with a seawater of 2 full, bottle volume.

The samples were stored at about 5°C in a refrigerator A few hours before analysis, the seawater samples were kept at 25 °C in a water bath.

#### (5) Results

The means and standard deviations of differences of replicate samples were estimated to be  $1.2 \pm 1.1 \mu\text{mol kg}^{-1}$  and  $1.6 \pm 1.4 \mu\text{mol kg}^{-1}$  for  $C_T$  and  $A_T$ , respectively. Cross sections of  $C_T$  and  $A_T$  along WHP P01 line are illustrated in Figs. 4.11.1 and 4.11.2, respectively.

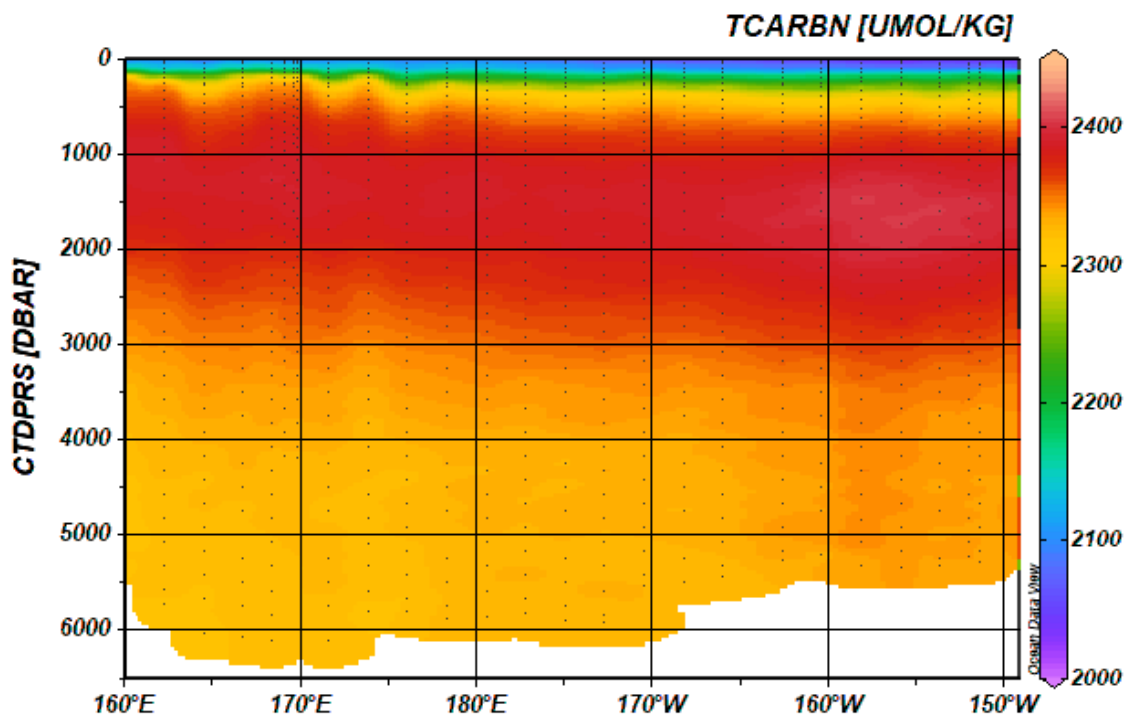


Fig. 4.11.1 Distributions of  $C_T$  along the P01 line.

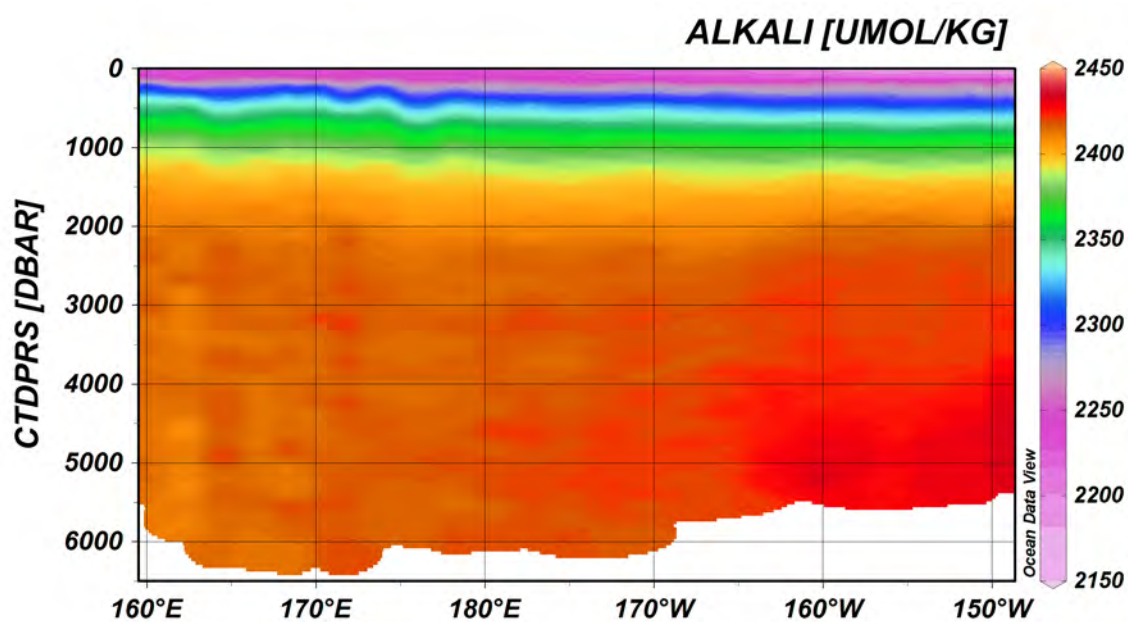


Fig. 4.11.2. Distributions of  $A_T$  along the P10 line.

## References

Yao W. and R. H. Byrne (1998) Simplified seawater alkalinity analysis: Use of linear array spectrometers. *Deep-Sea Research I* 45, 1383-1392.

## 4.12 Chlorophyll *a*

### (1) Personnel

Kosei Sasaoka	JAMSTEC
Hiroaki Sako	MWJ
Misato Kuwahara	MWJ
Shiori Ariga	MWJ

### (2) Objectives

Chlorophyll *a* is one of the most convenient indicators of phytoplankton stock, and has been used extensively for the estimation of phytoplankton abundance in various aquatic environments. In this study, we investigated horizontal and vertical distribution of phytoplankton biomass along the P01 section in the North Pacific. The chlorophyll *a* data is also utilized for calibration of fluorometers, which were installed in the surface water monitoring and CTD profiler system.

### (3) Instrument and Method

Seawater samples were collected in 250 mL brown Nalgene bottles without head-space. All samples were gently filtrated by low vacuum pressure (<0.02 MPa) through Whatman GF/F filter (diameter 25 mm) in the dark room. Whole volume of each sampling bottle was precisely measured in advance. After filtration, phytoplankton pigments were immediately extracted in 7 ml of N,N-dimethylformamide (DMF), and samples were stored at  $-20^{\circ}\text{C}$  under the dark condition to extract chlorophyll *a* more than 24 hours. Chlorophyll *a* concentrations were measured by the Turner fluorometer (10-AU-005, TURNER DESIGNS), which was previously calibrated against a pure chlorophyll *a* (Sigma-Aldrich Co., LLC) (Figure 4.12.1). To estimate the chlorophyll *a* concentrations, we applied to the fluorometric “Non-acidification method” (Welschmeyer, 1994).

### (4) Results

Vertical distributions of chlorophyll *a* concentration at each station along the P01 line during the cruise are shown in Figure 4.12.2. Cross section of chlorophyll *a* concentration along the P01 line is shown in Figure 4.12.3. Particularly, high chlorophyll *a* concentrations (over  $1.0\text{ mgm}^{-3}$ ) were clearly seen in the surface layer at westward stations from 150E. The chlorophyll *a* concentration was highest ( $6.58\text{ mgm}^{-3}$ ) at the chlorophyll *a* maximum depth (7m) of Stn.1. To examine the measurement precision, 80-pairs of replicate samples were obtained from hydrographic casts at the chlorophyll *a* maximum and 10m depth. The absolute values of the difference between replicate samples were 0-0.12  $\text{mgm}^{-3}$ , and those standard deviation were approximately 0.03.

### (5) Reference

Welschmeyer, N. A. (1994): Fluorometric analysis of chlorophyll *a* in the presence of chlorophyll *b* and pheopigments. *Limnol. Oceanogr.*, 39, 1985-1992.

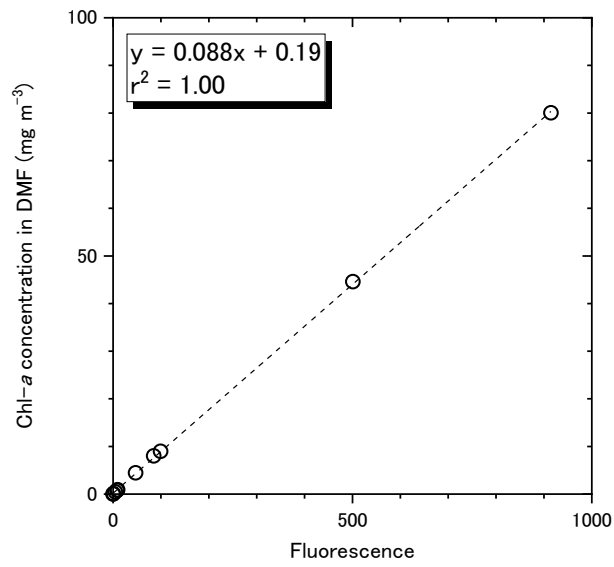
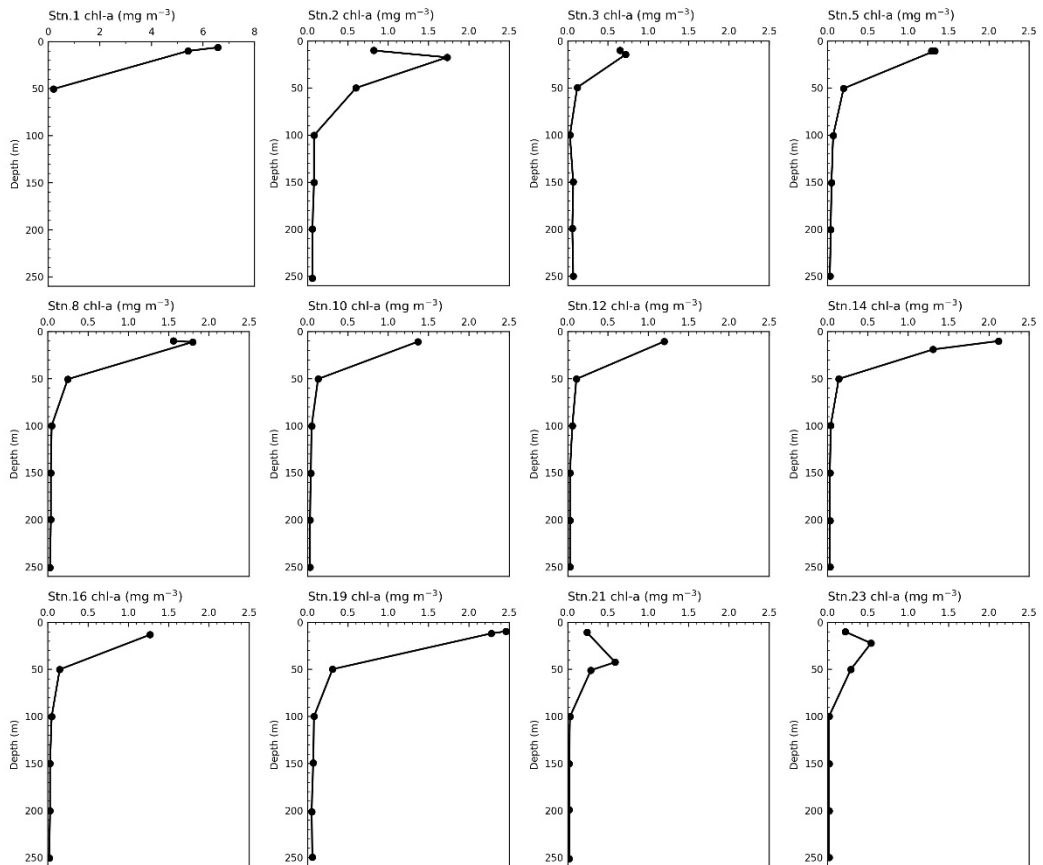


Figure 4.12.1 Relationships between pure chlorophyll *a* concentrations and fluorescence light intensity (n=10).



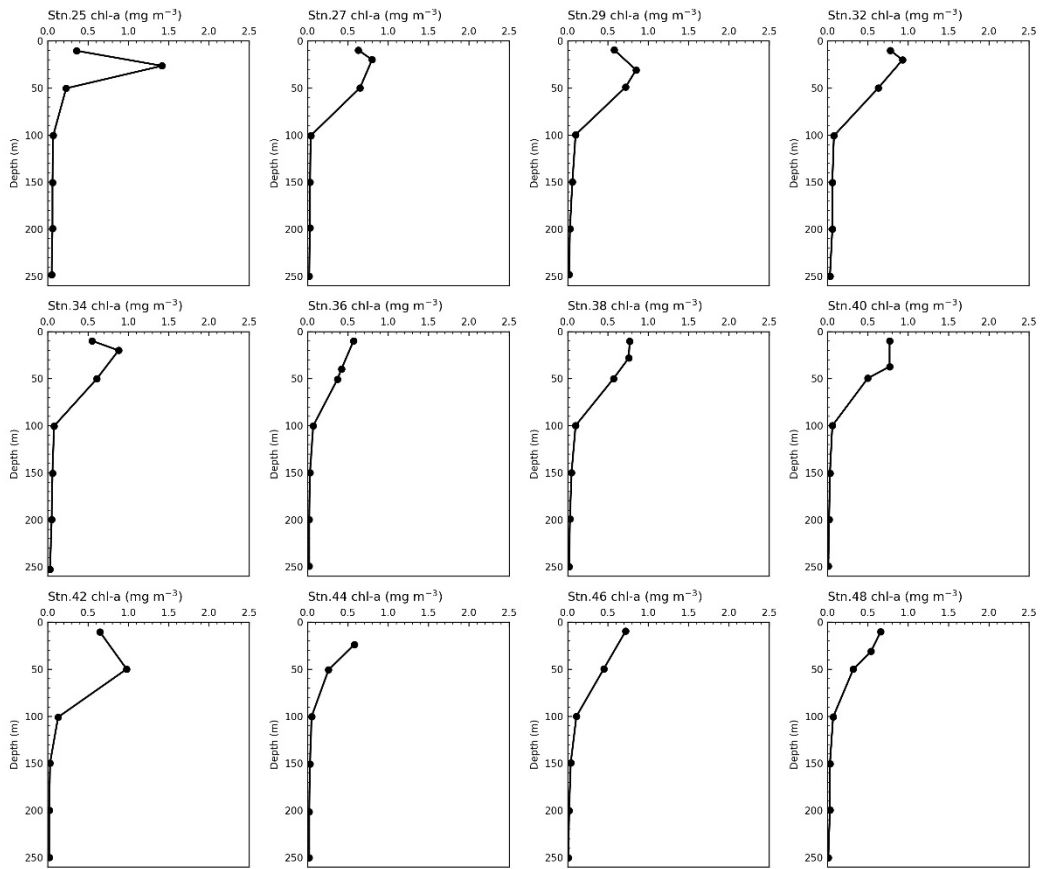


Figure 4.12.2 Vertical profiles of chlorophyll *a* concentration (46-stations) along the P01 section obtained from hydrographic casts.

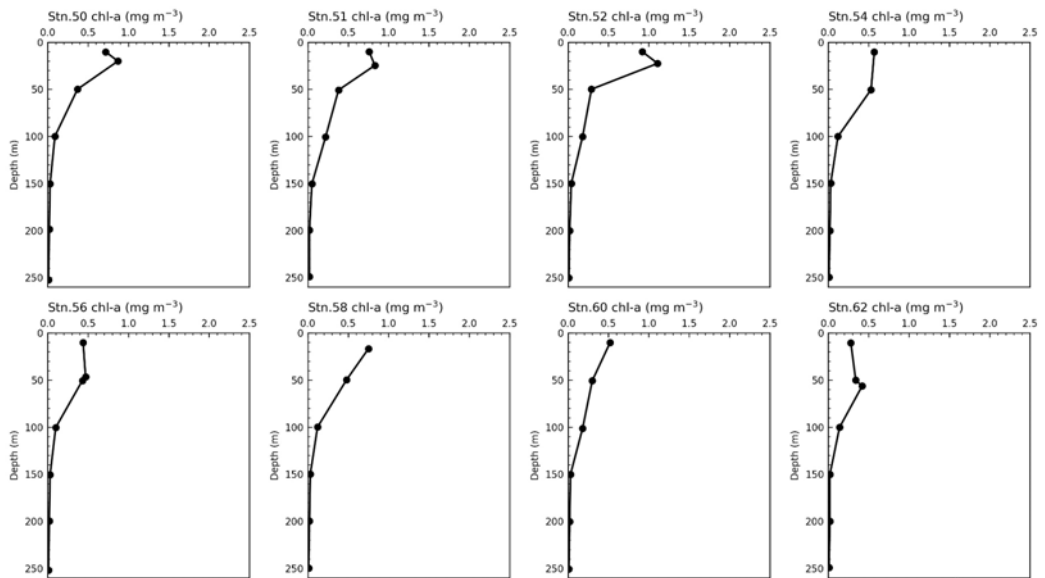


Figure 4.12.2 (Continued)

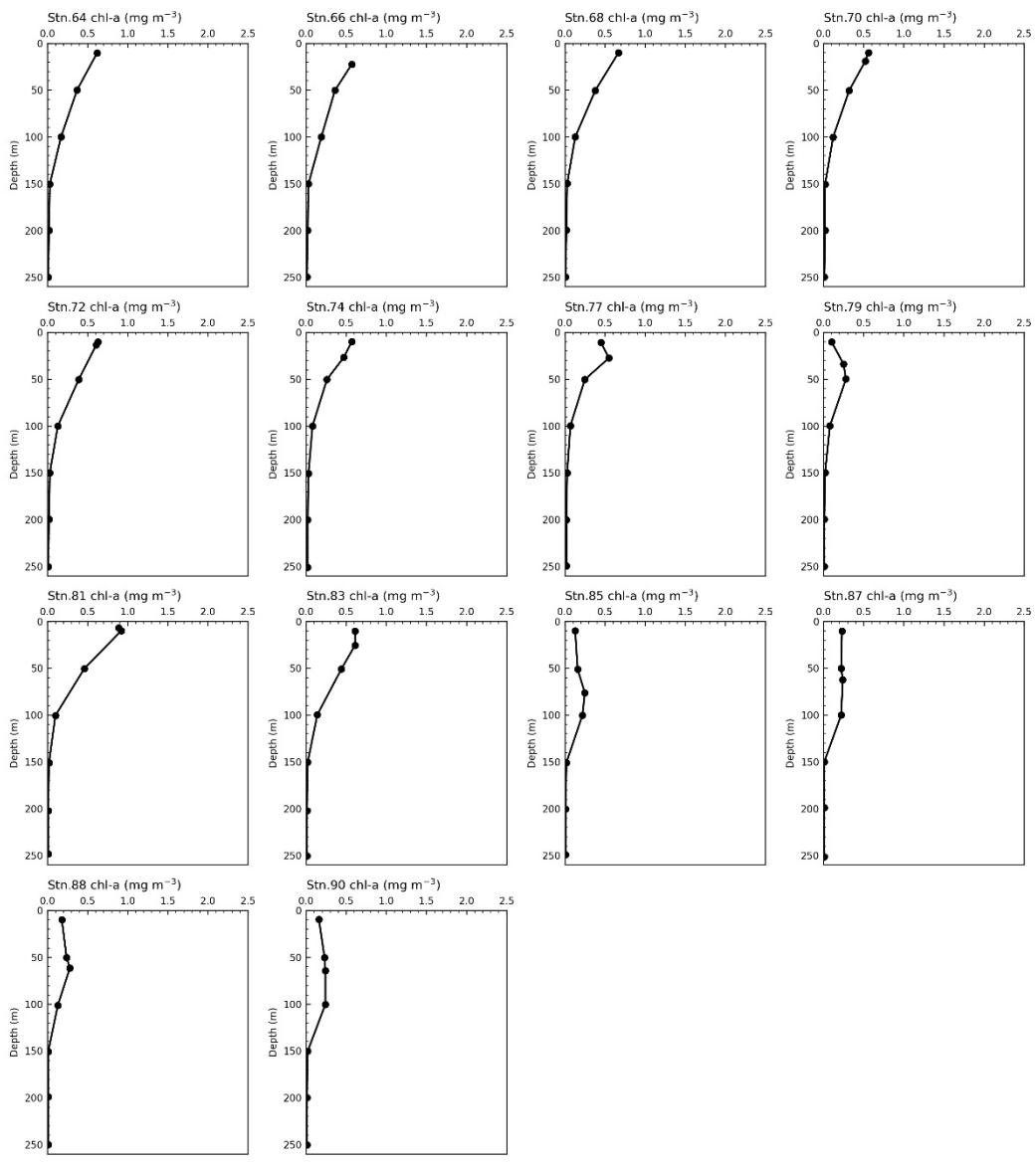


Figure 4.12.2 (Continued)

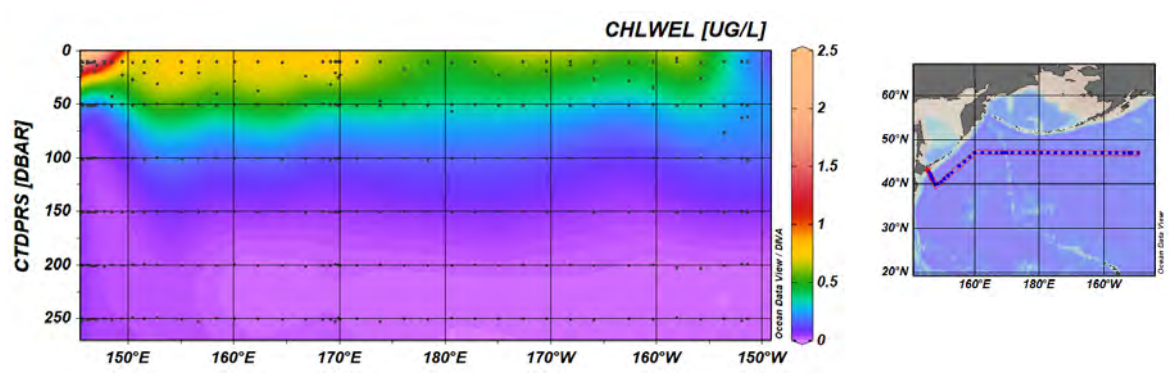


Figure 4.12.3 Cross section of chlorophyll *a* concentrations along the P01 section obtained from hydrographic casts.

## 4.13 Carbon isotopes

August 25, 2021

Yuichiro Kumamoto

Japan Agency for Marine-Earth Science and Technology (JAMSTEC)

### (1) Personnel

Yuichiro Kumamoto JAMSTEC

### (2) Objective

In order to investigate the water circulation and carbon cycle in the northern North Pacific Ocean, seawaters for measurements of carbon-14 (radiocarbon) and carbon-13 (stable carbon) ratios of dissolved inorganic carbon were collected by the hydrocasts from surface to near bottom.

### (3) Sample collection

The sampling stations and number of samples are summarized in Table 4.13.1. All samples for carbon isotope ratios (total 120 samples) were collected at 5 stations using the 12-liter bottles. The seawater sample was siphoned into a 250 cm<sup>3</sup> glass bottle with enough seawater to fill the glass bottle 2 times. Within a few hours after sampling, 10 cm<sup>3</sup> of seawater was removed from the bottle and poisoned by 0.1 cm<sup>3</sup>  $\mu$ l of saturated HgCl<sub>2</sub> solution. Then the bottle was sealed by a glass stopper with Apiezon grease M and stored in a dark space on board.

Table 4.13.1 Sampling stations and number of samples for carbon isotopic ratios.

Station	Lat. (N)	Long. (E)	Sampling Date (UTC)	Number of samples	Max. Pressure (dbar)
034	45.07	156.65	2021/07/23	24	4847.7
040	46.98	162.24	2021/07/26	24	5732.8
056	47.01	173.84	2021/07/31	24	5795.6
068	46.99	187.30	2021/08/05	24	5906.9
083	46.99	204.15	2021/08/12	24	5343.7
Total				120	

### (4) Sample preparation and measurements

In our laboratory, dissolved inorganic carbon in the seawater samples will be stripped as CO<sub>2</sub> gas cryogenically and split into three aliquots: radiocarbon measurement (about 200  $\mu$ mol), carbon-13 measurement (about 100  $\mu$ mol), and archive (about 200  $\mu$ mol). The extracted CO<sub>2</sub> gas for radiocarbon will be then converted to graphite catalytically on iron powder with pure hydrogen gas. The carbon-13 ratio (<sup>13</sup>C/<sup>12</sup>C) of the extracted CO<sub>2</sub> gas will be measured using a mass spectrometer (Finnigan MAT253). The carbon-14 ratio (<sup>14</sup>C/<sup>12</sup>C) in the graphite sample will be measured by Accelerator Mass Spectrometry.

### (5) Data archives

The data obtained in this cruise will be submitted to the Data Management Group of JAMSTEC and will be opened to the public via “Data Research System for Whole Cruise Information in JAMSTEC (DARWIN)” in the JAMSTEC web site.

## 4.14 Dissolved organic carbon (DOC) and Total Dissolved Nitrogen (TDN)

### (1) Personnel

Dennis A. Hansell University of Miami  
Masahito Shigemitsu JAMSTEC

### (2) Introduction

Marine dissolved organic matter (DOM) is known to be the largest ocean reservoir of reduced carbon, and huge amounts of the carbon exist as refractory DOM (RDOM) (Hansell et al., 2009). In the North Pacific, DOM in the deep ocean is largely introduced via the northward flowing bottom

waters. By unknown mechanisms, DOM then experiences a net removal in association with transformation of the water mass from bottom water to southward flowing Pacific Deep Water.

In this cruise, we try to gain insights into the loss mechanisms along the path of flow from the west to the east in the far North Pacific. To this end, we are determining the concentrations of dissolved organic carbon (DOC) and total dissolved nitrogen (TDN).

### (3) Instruments and methods

#### Bottle sampling

Discrete water samples for each station were collected using 12L Niskin bottles mounted on a CTD system. Each sample taken in the upper 250 m was filtered using a pre-combusted glass fiber filter (GF/F, Whatman). The filtration was carried out by connecting a spigot of Niskin bottle through silicone tube to an inline plastic filter holder.

Filtrates were collected for DOC and TDN measurements in acid-washed and pre-combusted 40 mL glass vials with acid-washed Teflon®-lined caps after triple rinsing. Other samples taken below 250 m were unfiltered. The samples for DOC and TDN were collected at Stations 1, 2, 3, 5, 8, 10, 11, 12, 14, 16, 19, 20, 21, 23, 24, 25, 27, 29, 30, 31, 32, 34, 36, 37, 38, 40, 41, 42, 44, 46, 47, 48, 50, 51, 52, 54, 55, 56, 58, 60, 61, 62, 63, 64, 66, 68, 69, 70, 72, 74, 75, 77, 78, 79, 81, 83, 84, 85, 87, 88, and 90. The water, once in the vials, was killed with 100 µL of 4N HCl, then stored under cool, dark conditions until analyzed in the shore-based laboratory.

#### DOC and TDN measurements

The samples will be analyzed by a Shimadzu TOC-L system coupled with a Shimadzu Total N analyzer at the University of Miami (Halewood et al., 2010). Standardization will be achieved using potassium hydrogen phthalate (KHP) made in low carbon water, and the analyses will be referenced against consensus reference material provided by the Hansell Laboratory, University of Miami (Hansell, 2005).

### (4) References

Halewood, E., Opalk, K., Custals, L., Carey, M., Hansell, D.A., and Carlson, C.A. 2010. GO-SHIP Repeat Hydrography: Determination of dissolved organic carbon (DOC) and total dissolved nitrogen (TDN) in seawater using High Temperature Combustion Analysis. In *The GO-SHIP Repeat Hydrography Manual: A Collection of Expert Reports and Guidelines*. Hood, E.M., C.L. Sabine, and B.M. Sloyan, eds. IOCCP Report Number 14, ICPO Publication Series Number 134. Available online at: <http://www.go-ship.org/HydroMan.html>.

Hansell, D.A. 2005. Dissolved organic carbon reference material program. *EOS* 86(35): 318.

Hansell, D.A., C.A. Carlson, D.J. Repeta, R. Schlitzer. 2009. Dissolved organic matter in the ocean: New insights stimulated by a controversy. *Oceanography* 22: 52-61

## 4.15 Fluorescent dissolved organic matter (FDOM)

### (1) Personnel

Masahito Shigemitsu	JAMSTEC
Kosei Sasaoka	JAMSTEC
Koki Miyakawa	JAMSTEC
Ayaka Tanaka	JAMSTEC

### (2) Introduction

Marine dissolved organic matter (DOM) is known to be the largest ocean reservoir of reduced carbon, and huge amounts of the carbon exist as refractory DOM (RDOM) (Hansell et al., 2009). RDOM is considered to be generated during microbial degradation of organic matter produced in the sunlit surface ocean, and is hypothesized to play an important role in the atmospheric CO<sub>2</sub> sequestration (Jiao et al., 2010). Some components of the RDOM can be detected as fluorescent DOM (FDOM). In the intermediate waters of the North Pacific, allochthonous FDOM is introduced

from the surrounding marginal seas and is mixed into the above-mentioned autochthonous FDOM (Yamashita et al., 2021).

In this cruise, we try to gain insights into the relative proportion of allochthonous and autochthonous FDOM in the intermediate waters of the North Pacific.

### (3) Instrument and method

#### Bottle sampling

Discrete water samples for each station were collected using 12L Niskin bottles mounted on a CTD system. Each sample taken in the upper 250 m was filtered using a pre-combusted glass fiber filter (GF/F, Whatman). The filtration was carried out by connecting a spigot of Niskin bottle through silicone tube to an inline plastic filter holder.

Filtrates were collected for FDOM measurements in acid-washed and pre-combusted glass vials with acid-washed Teflon®-lined caps after triple rinsing. Other samples taken below 250 m were unfiltered. The samples for FDOM were collected at Stations 1, 2, 3, 5, 8, 10, 11, 12, 14, 16, 19, 20, 21, 23, 24, 25, 27, 29, 30, 31, 32, 34, 36, 37, 38, 40, 41, 42, 44, 46, 47, 48, 50, 51, 52, 54, 55, 56, 58, 60, 61, 62, 63, 64, 66, 68, 69, 70, 72, 74, 75, 77, 78, 79, 81, 83, 84, 85, 87, 88, and 90.

#### FDOM measurement

Excitation-emission matrix (EEM) fluorescence spectra were measured onboard using the Horiba Scientific Aqualog after the samples were acclimated to laboratory temperature in the dark. Emission scans from 248 to 829 nm were obtained at 2.33 nm intervals for performing sequential excitation from 240 and 560 nm at 5 nm intervals by using an integration time of 12 s and employing the high charge-coupled device (CCD) gain mode. Blank subtraction and normalization of fluorescence intensities to Raman Units (RU) (Lawaetz and Stedmon, 2009) were carried out as post-measurement steps.

### (4) Preliminary results of FDOM

We measured EEMs of all samples onboard, but all data are still preliminary. Here, we show the results of FDOM (FDOM<sub>370/440</sub>) determined at the 370 nm excitation and 440 nm emission wavelengths (Figures 4.15.1).

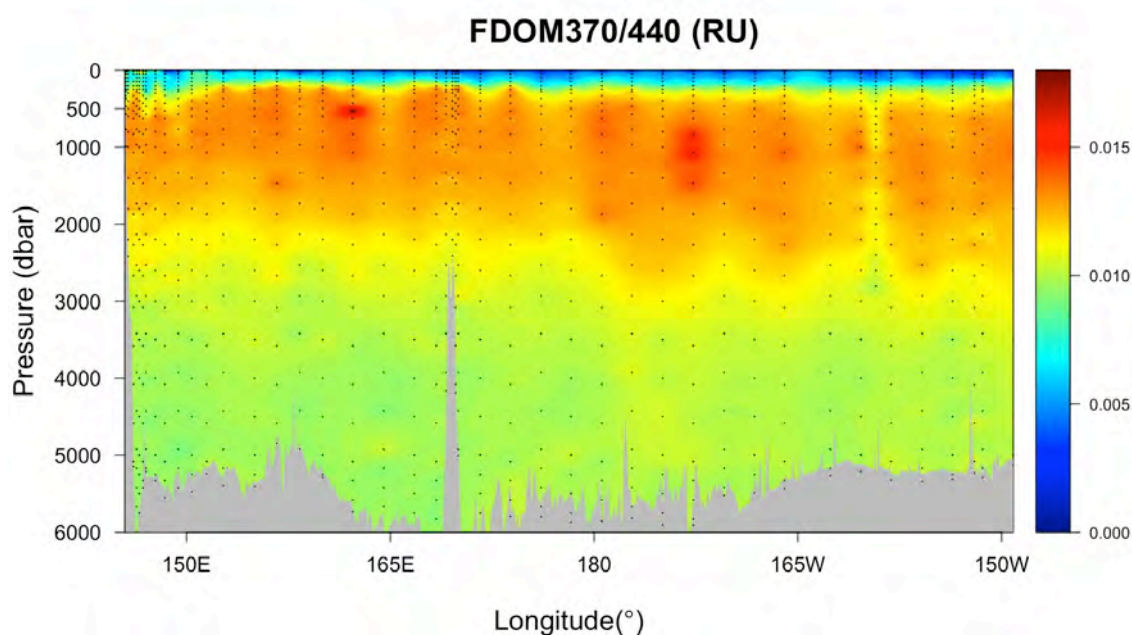


Fig. 4.15.1 Vertical section of FDOM<sub>370/440</sub> in RU

## (5) References

Hansell, D.A., C.A. Carlson, D.J. Repeta, R. Schlitzer (2009). Dissolved organic matter in the ocean: New insights stimulated by a controversy. *Oceanography* 22, 52-61.

Jiao, N., G. Herndl, D.A. Hansell, R. Benner, G. Kattner, S. Wilhelm, et al. (2010). Microbial production of recalcitrant dissolved organic matter: long-term carbon storage in the global ocean. *Nat. Rev. Microbiol.* 8, 593–599. doi:10.1038/nrmicro2386

Yamashita, Y., T. Tosaka, R. Bamba, R. Kamezaki, S. Goto, J. Nishioka, et al. (2021). Widespread distribution of allochthonous fluorescent dissolved organic matter in the intermediate water of the North Pacific. *Prog. Oceanogr.* 191, 102510.

Lawaetz, A.J., and C.A. Stedmon (2009). Fluorescence intensity calibration using the Raman scatter peak of water. *Appl. Spectrosc.* 63(8), 936-940.

## 4.16 Absorption coefficients of Chromophoric Dissolved Organic Matter (CDOM)

### (1) Personnel

Kosei Sasaoka	JAMSTEC
Masahito Shigemitsu	JAMSTEC
Koki Miyakawa	JAMSTEC
Ayaka Tanaka	JAMSTEC

### (2) Objectives

Oceanic dissolved organic matter (DOM) is the largest pool of reduced carbon, and its inventory in the ocean is approximately 660 Pg C (Hansell et al., 2009). Thus, investigating the behavior of oceanic DOM is important to exactly evaluate the carbon cycle in the ocean. Chromophoric Dissolved Organic Matter (CDOM) play an important role in determining the optical properties of seawater, and the global CDOM distribution appears regulated by a coupling of biological, photochemical, and physical oceanographic processes all acting on a local scale, and greater than 50% of blue light absorption is controlled by CDOM (Siegel et al., 2002). Additionally, some investigators have reported that CDOM emerges as useful tracers for diagnosing changes in the overturning circulation and evaluating DOC quality, similar to dissolved oxygen (e.g., Nelson et al., 2010; Catala et al., 2015). The objectives of this study are to clarify the spatial and vertical distributions of light absorption by CDOM along P01 section in the North Pacific.

### (3) Methods

Seawater samples for determination of the absorption coefficient of CDOM ( $a_{\text{cdom}(\lambda)}$ ) were filtered at the depths (above 250m) and not filtered (300m-bottom). All samples were collected in 60 ml pre-combusted glass vials with acid-washed Teflon-lined caps using the same way as DOC and FDOM. Optical densities of CDOM ( $\text{OD}_{\text{cdom}(\lambda)}$ ) in seawaters between 190 and 750 nm were measured at 0.5 nm intervals by an UV-VIS recording spectrophotometer (UV-2600, Shimadzu Co.) onboard, using 10-cm pathlength quartz cells. Milli-Q water was used as a reference and base line sample. The absorption coefficient of CDOM ( $a_{\text{cdom}(\lambda)}$  ( $\text{m}^{-1}$ )) was calculated from measured optical densities ( $\text{OD}_{\text{cdom}(\lambda)}$ ) as follows:

$$a_{\text{cdom}(\lambda)} = 2.303 \times \text{OD}_{\text{cdom}(\lambda)} / 0.1 \text{ (0.1 is the cuvette path-length (m))}.$$

### (4) Preliminary results

Vertical profiles of CDOM (as absorption coefficient at 325nm, unit =  $\text{m}^{-1}$ ) at 47-stations were shown in Fig. 4.16.1. Cross sections of CDOM (as absorption coefficient at 325 nm, unit =  $\text{m}^{-1}$ ) along P01 section were shown in Figure 4.16.2.

### (5) References

Catala, T. S., et al., 2015, Turnover time of fluorescent dissolved organic matter in the dark global ocean, *Nat. Com.*, 6, 1-8, doi:10.1038/ncomms6986.

Hansell, D. A., C. A. Carlson, D. J. Repeta, and R. Shlitzer, 2009, Dissolved organic matter in the ocean: A controversy stimulates new insight, *Oceanogr.*, 22, 202-211

Nelson, N. B., D. A. Siegel, C. A. Carlson, and C. M. Swan, 2010, Tracing global biogeochemical cycles and meridional overturning circulation using chromophoric dissolved organic matter, *Geophys. Res. Lett.*, *37*, L03610, doi:10.1029/2009GL042325.

Siegel, D.A., Maritorena, S., Nelson, N.B., Hansell, D.A., Lorenzi-Kayser, M., 2002, Global distribution and dynamics of colored dissolved and detrital organic materials. *J. Geophys. Res.*, *107*, C12, 3228, doi:10.1029/2001JC000965.

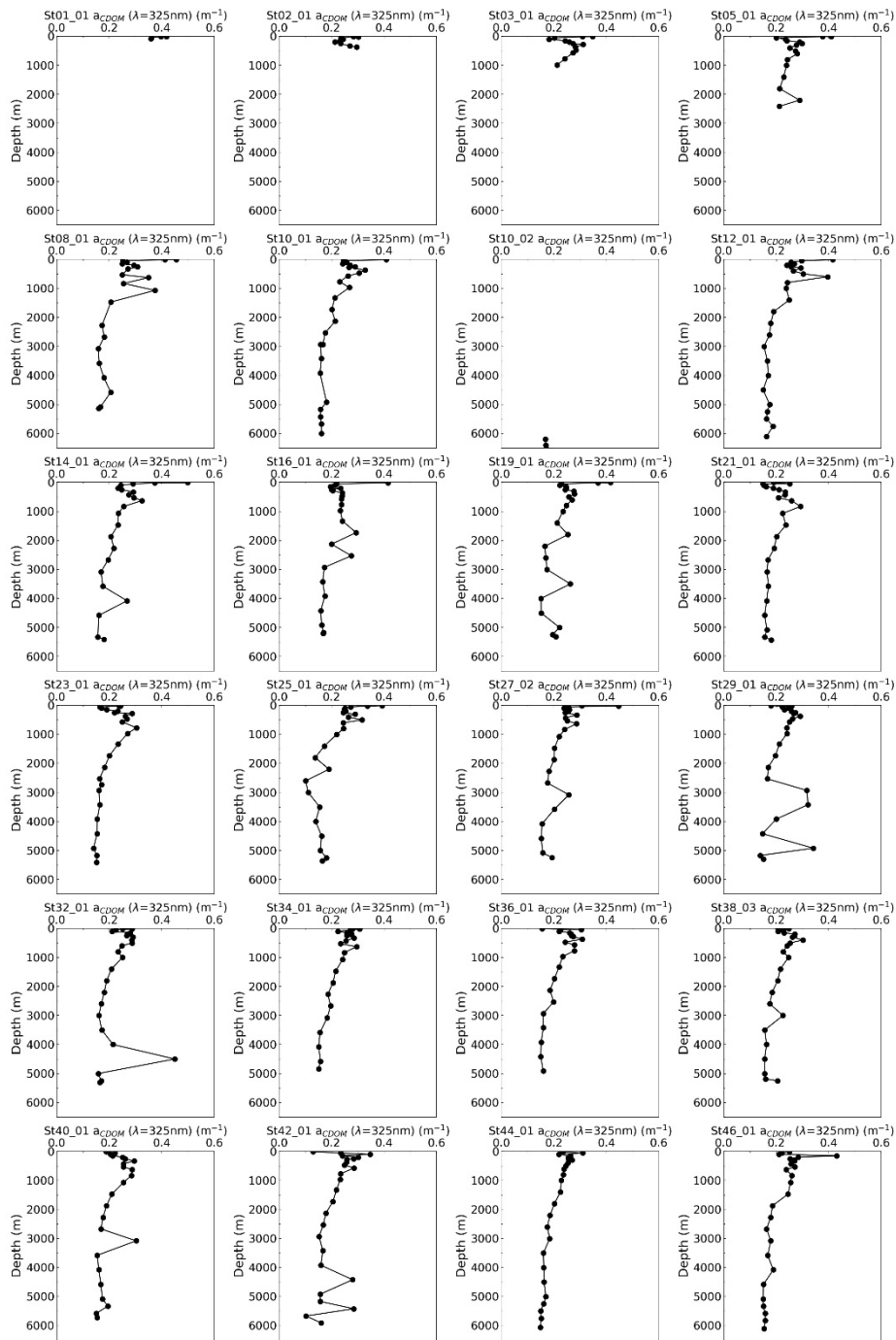


Fig.4.16.1 Vertical profiles of CDOM (as absorption coefficient at 325 nm, unit =  $m^{-1}$ ) at 47-stations.

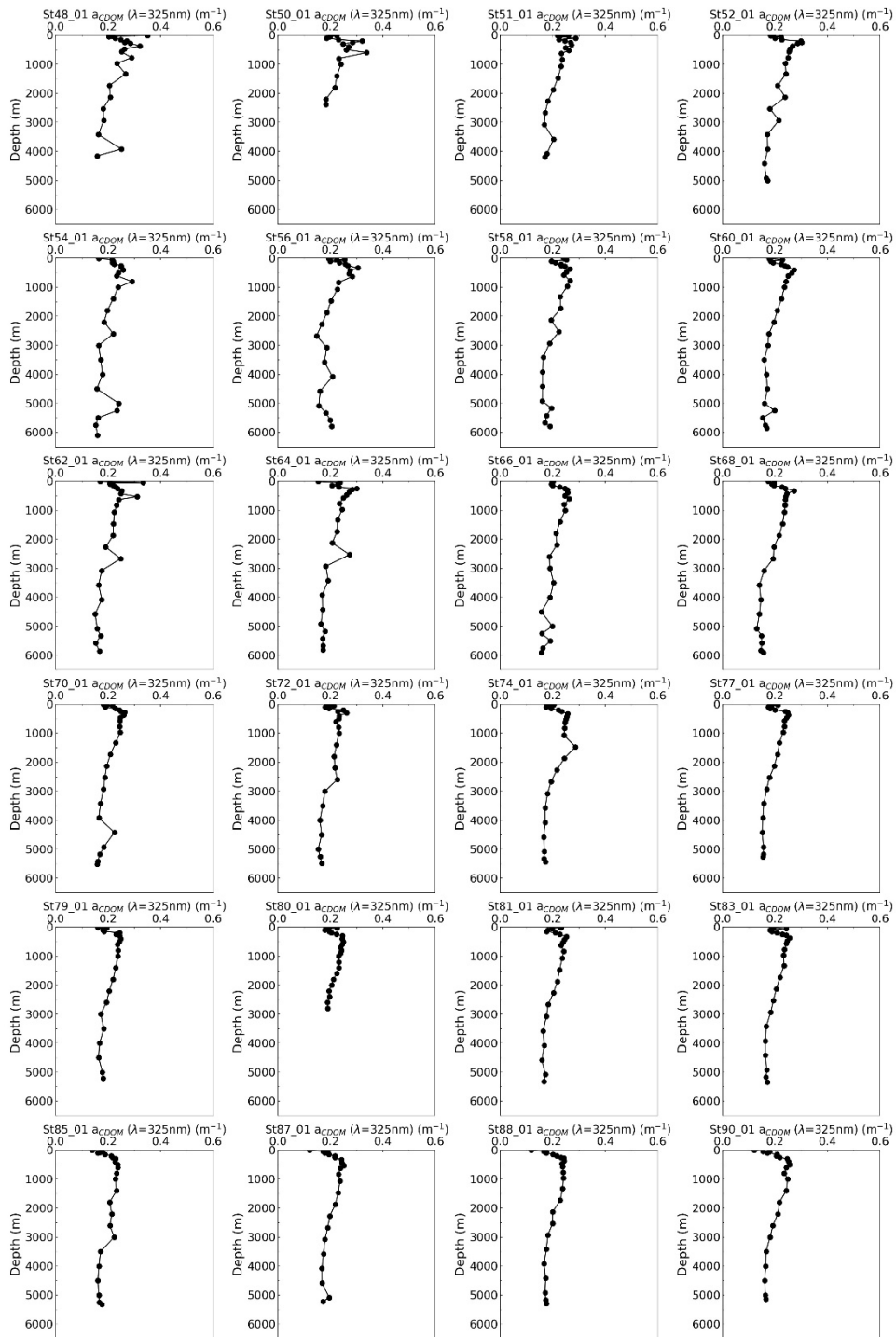


Fig.4.16.1 (Continued).

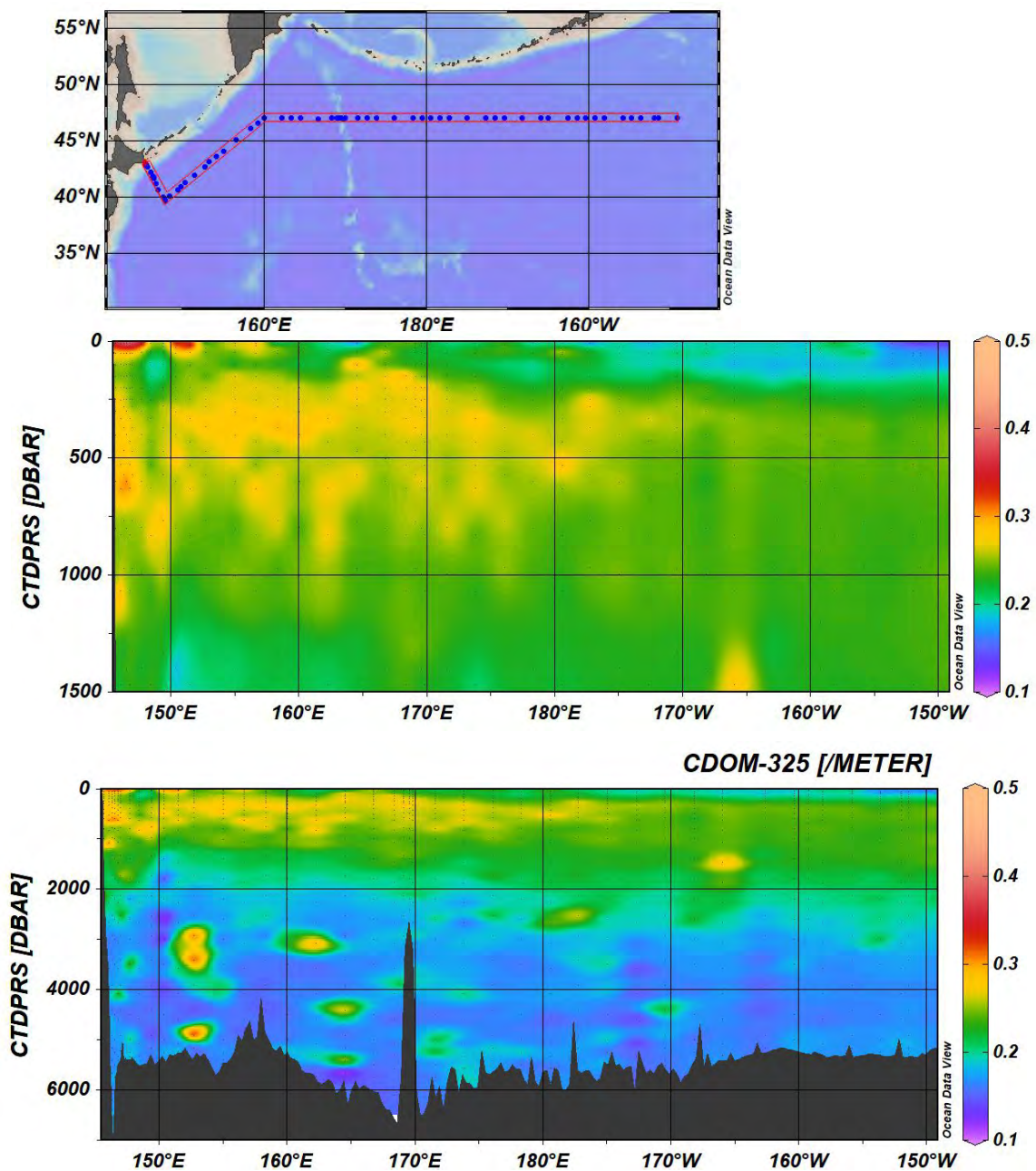


Fig.4.16.2 Sections of CDOM (as absorption coefficient at 325 nm, unit =  $\text{m}^{-1}$ ) along P01 section obtained from hydrographic casts. The top section covers surface to the bottom and the lower section covers the upper 1,500 m.

#### 4.17 Iodine isotopes

August 20, 2021

##### (1) Personnel

Yuanzhi Qi The University of Tokyo

##### (2) Objective

The objective of this study is to explore the cycling processes of both stable iodine ( $^{127}\text{I}$ ) and radioiodine ( $^{129}\text{I}$ ) in the North Pacific Ocean.

### (3) Parameters

We measured total iodine-127 ( $T^{127}I$ ), iodide-127 ( $^{127}I^-$ ), iodate-127 ( $^{127}IO_3^-$ ), dissolved organic iodine-127 ( $DO^{127}I$ ), total inorganic iodine-129 ( $TI^{129}I$ ), iodide-129 ( $^{129}I^-$ ), iodate-129 ( $^{129}IO_3^-$ ) and dissolved organic iodine-129 ( $DO^{129}I$ ).

### (4) Instruments and method

#### i) Instruments

- ICP-MS: Agilent 7500 with ChemStation (G1834B)
- IC: Thermo ICS-1100
- Solid Phase Extraction cartridge: Agilent, Bond Elut PPL, Strong barrel cartridge, Bed mass (5 g), Volume (60 ml), Particle size (125  $\mu$ m)
- Membrane filter: ADVANTEC, mixed cellulose ester, pore size (0.45  $\mu$ m), diameter (47 mm)

#### ii) Reagents

- Potassium iodide (KI): 1 M solution, FUJIFILM Wako Pure Chemical Corporation, JIS Reagent Grade
- $HNO_3$ : FUJIFILM Wako Pure Chemical Corporation, JIS Special Grade
- $Na_2SO_3$ : FUJIFILM Wako Pure Chemical Corporation, JIS Special Grade
- $KNO_3$ : FUJIFILM Wako Pure Chemical Corporation, JIS Special Grade
- $K_2S_2O_8$ : FUJIFILM Wako Pure Chemical Corporation, JIS Special Grade
- $AgNO_3$ : FUJIFILM Wako Pure Chemical Corporation, JIS Special Grade
- Anion exchange resin: FUJIFILM Wako Pure Chemical Corporation, Dowex 1x8, 100-200 mesh
- Woodward iodine: as “old iodine” from Woodward iodine cooperation, Oklahoma, USA
- Artificial seawater (all reagents used are JIS Special Grade from FUJIFILM Wako Pure Chemical Corporation):  
 $NaCl$ ,  $MgSO_4 \cdot 7H_2O$ ,  $MgCl_2 \cdot 6H_2O$ ,  $CaCl_2 \cdot 2H_2O$ ,  $NaHCO_3$ ,  $NaBr$ ,

#### iii) Sampling

Surface seawater samples were collected by bucket, and seawater samples of other depths were collected from Niskin bottles attached to the CTD/Carousel Water Sampling System (CTD system). Rainwater samples were collected by PP box on the top deck. All samples were filtered by mixed cellulose ester membrane filter immediately after sampling.

#### iv) Methods

##### a. $T^{127}I$

$T^{127}I$  of seawater was measured by Inductively Coupled Plasma Mass Spectrometry (ICP-MS) after 10-time dilution by ultrapure water. Iodine concentration was calibrated by a 6-point calibration curve generated from artificial seawater-based KI standard solution. Artificial seawater was made according to Kester et al. (1967). The instrument status and blank were checked by inner standard (5 ppb Cesium) and artificial seawater, respectively.

##### b. $^{127}I^-$

$^{127}I^-$  of seawater was measured by Ion Chromatography (IC) directly. Iodine concentration was calibrated by a 6-point calibration curve generated from ultrapure water-based KI standard solution. The instrument blank was checked by ultrapure water.

##### c. $DO^{127}I$

After adjusting the pH of 30 ml seawater sample to 1~2 by 60%  $HNO_3$ , 30  $\mu$ l 1 M  $Na_2SO_3$  was used to reduce all iodate to iodide. Then the reduced sample was loaded on anion exchange column ( $\phi$  1.0 cm x 5 cm) and passed through the column at 1~2 ml/min. 10 ml 0.2 M  $KNO_3$  was used to flush the remaining DOI on the column. All eluate was collected and measured by ICP-MS. The analysis of  $DO^{127}I$  was only for surface and 10 m depth seawater, because the DOI is negligible in

deep water of open sea (Wong and Cheng, 1998).

d.  $^{127}\text{IO}_3^-$

For surface and 10 m depth seawater,  $^{127}\text{IO}_3^-$  was calculated by the difference of  $\text{T}^{127}\text{I}$  and the sum of  $^{127}\text{I}^-$  and  $\text{DO}^{127}\text{I}$ :

$$^{127}\text{IO}_3^- = \text{T}^{127}\text{I} - ^{127}\text{I}^- - \text{DO}^{127}\text{I}$$

For deep seawater,  $^{127}\text{IO}_3^-$  was calculated by the difference of  $\text{T}^{127}\text{I}$  and  $^{127}\text{I}^-$ :

$$^{127}\text{IO}_3^- = \text{T}^{127}\text{I} - ^{127}\text{I}^-$$

e.  $\text{TI}^{129}\text{I}$ ,  $^{129}\text{I}^-$  and  $^{129}\text{IO}_3^-$

All iodine species were transferred to AgI form by modified coprecipitation method according to Luo et al. (2013) and Xing et al. (2017), and then measured by Accelerator Mass Spectrometry (AMS).

f.  $\text{DO}^{129}\text{I}$

DOI was preconcentrated by Solid Phase Extraction (SPE) cartridge and converted to  $\text{I}^-$  by  $\text{K}_2\text{S}_2\text{O}_8$  (Dang et al., 2013) and  $\text{Na}_2\text{SO}_3$ . 0.03 M  $\text{AgNO}_3$  is used to precipitate  $\text{I}^-$  as AgI, which can be measured by AMS.

g.  $^{129}\text{I}$ -AMS system in MALT (Micro Analysis Laboratory, Tandem accelerator, The University of Tokyo)

For  $^{129}\text{I}$  measurement, the terminal voltage of AMS was 3.48 MV and the charge state is 5+. The target material was AgI, mixed with Nb or Ag powder. At the injection magnet,  $^{129}\text{I}$  and  $^{127}\text{I}$  were sequentially injected into the accelerator.  $^{127}\text{I}^{5+}$  was measured at off-set Faraday cup (called MFC 04-2) after the analyzing magnet during the  $^{127}\text{I}$  injection timing.  $^{129}\text{I}^{5+}$  was detected at the end of AMS line by GIC (Gas Ionization Chamber). The blank subtraction was carried out using Woodward iodine that was analyzed with samples. From a series of chemical blank measurements, the  $^{129}\text{I}/^{127}\text{I}$  ratio of Woodward iodine was found to be  $1.5 \times 10^{-14}$ . The standard validation was checked against Z94-0596 ( $^{129}\text{I}/^{127}\text{I}$  ratio:  $6.54 \times 10^{-11}$ ) and Z94-0597 ( $^{129}\text{I}/^{127}\text{I}$  ratio:  $8.38 \times 10^{-12}$ ) provided by PRIME Lab., Purdue University.

**(5) Station list**

The sampling station list for iodine isotopes is shown in Table 4.17-1

Table 4.17-1 List of stations

Station	Date (UTC)	Position		Depth (m)
	(mmddyy)	Latitude	Longitude	
1	071521	42-58.41N	145-27.12E	86
3	071521	42-51.42N	145-32.37E	905
5*	071521	42-38.29N	145-42.37E	2493
10	071621	41-52.42N	146-19.16E	6890
19	071921	39-57.21N	147-41.80E	5329
25	072021	41-16.08N	150-23.20E	5481
29*	072221	42-40.67N	152-41.39E	5401
32	072321	44-05.16N	155-00.92E	5405
38	072421	47-00.56N	160-01.31E	5292
42	072721	46-59.93N	164-30.86E	6050
46*	072921	46-59.41N	168-22.75E	6100
48*	072921	47-00.11N	169-05.89E	4241
50*	073021	46-59.06N	169-34.46E	2409
52	073021	46-58.86N	169-59.75E	5006
58*	080121	46-59.81N	176-05.64E	5803
62	080221	46-59.15N	179-25.58W	5846

66*	080421	47-00.14N	174-57.24W	5901
70	080521	46-59.73N	170-25.49W	5530
74*	080721	47-00.59N	165-58.99W	5434
79	080821	46-59.66N	160-21.63W	5215
83*	081221	46-59.26N	155-51.09W	5344
90	081021	46-59.41N	149-08.60W	5141

\*: Only for iodine-127

#### (6) Data archive

These obtained data will be submitted to JAMSTEC Data Management Group (DMG).

#### (7) Reference

Dang, H., Hou, X., Roos, P., & Nielsen, S. P. (2012). Release of iodine from organic matter in natural water by  $K_2S_2O_8$  oxidation for  $^{129}I$  determination. *Analytical methods*, 5(2), 449-456.

Kester, D. R., Duedall, I. W., Connors, D. N., & Pytkowicz, R. M. (1967). Preparation of artificial seawater. *Limnology & Oceanography*, 12(1), 176-179.

Luo, M., Hou, X., He, C., Liu, Q., & Fan, Y. (2013). Speciation analysis of  $^{129}I$  in seawater by carrier-free  $AgI-AgCl$  coprecipitation and accelerator mass spectrometric measurement. *Analytical Chemistry*, 85(7).

Wong, G. T. F. & Cheng, X. H. (1998). Dissolved organic iodine in marine waters: Determination, occurrence and analytical implications. *Marine Chemistry*, doi:10.1016/S0304-4203(97)00078-9.

Xing, S., Hou, X., Aldahan, A. & Possnert, G. (2017). Speciation analysis of  $^{129}I$  in seawater using coprecipitation and accelerator mass spectrometry and its applications. *Journal of Radioanalytical and Nuclear Chemistry*, doi:10.1007/s10967-016-5060-6.

### 4.18 Spatial patterns of prokaryotic abundance, activity and community composition

#### (1) Personnel

Taichi Yokokawa            JAMSTEC  
Masahito Shigemitsu       JAMSTEC

#### (2) Introduction

Prokaryotes (Bacteria and Archaea) play a significant role in marine biogeochemical fluxes. Biogeochemical transformation rates and functional diversity of microbes are representative major topics in marine microbial ecology. However, the link between prokaryotes properties and biogeochemistry in the epipelagic layers has not been explained systematically despite recent studies highlighting microbes' role in the cycling of organic and inorganic matter.

The objectives of this study, which analyze the epipelagic layer of the North Pacific, were 1) to determine the abundance of microbes; 2) to assess the community composition of prokaryotes; 3) to know microbial diversity along the longitudinal transect.

#### (3) Methods

##### Microbial abundance

Samples for microbial abundances (prokaryotes, eukaryotes and viruses) were collected in Station#: 1, 10, 12, 16, 23, 25, 32, 42, 44, 48, 52, 54, 60, 64, 70, 72, 83, and 85 from 10m. And, Station#: 19, 38, 56, 66, and 81 from five sampling depths (10, 50, 100, 150, and 200 m). Samples were fixed with glutaraldehyde (final concentration 1%) and frozen at  $-80^{\circ}C$ . The abundance and relative size of microbes and viruses will be measured by a flow cytometry in JAMSTEC after nucleic acid staining with SYBR-Green I.

##### Microbial diversity

Microbial cells in water samples were filtrated on a cellulose acetate filter ( $0.2\mu m$ ) and stored at  $-80^{\circ}C$ . Environmental DNA or RNA will be extracted from the filtrated cells and used for 16S/18S

rRNA gene tag sequencing using MiSeq, quantitative PCR for genes for 16S rRNA, and/or metatranscriptomics. Samples for microbial diversity were taken at Station#: 1, 10, 12, 16, 23, 25, 32, 42, 44, 48, 52, 54, 60, 64, 70, 72, 83, and 85 from 10m; Station#: 19, 38, 56, 66, and 81 from five sampling depths (10, 50, 100, 150, and 200 m).

#### 4.19. NORPAC/Ring nets/VMPS/Surf. Water sampling

##### (1) Personnel

Atsushi Yamaguchi	Hokkaido University
Daiki Kojima	Hokkaido University
Takumi Teraoka	Hokkaido University

##### (2) Objective

The goals of this study are following:

- 1) Evaluate spatial and vertical distribution of zooplankton in the northern North Pacific (Yamaguchi)
- 2) Evaluate epibiont fauna on zooplankton in the northern North Pacific (Kojima)
- 3) Evaluate temperature effect on development of the dominant zooplankton in the northern North Pacific (Teraoka)

##### (3) Sampling

Zooplankton samples were collected by vertical hauls of Quad-NORPAC nets (45 cm mouth diameter, Hama et al., 2019) equipped 335 and 63  $\mu\text{m}$  meshes for quantitative sampling (Yamaguchi) and two 63  $\mu\text{m}$  mesh nets with bucket-cod ends for sorting (Kojima) and on board experiments (Teraoka). The Quad-NORPAC net was towed from 0-150 m and 0-50 m depths around midnight at 30 stations along the WOCE line (Table 4.19.1). Add to Quad-NORPAC net, vertical tows by 80-cm Ring net were made from 0-150 m or 0-500 m for sorting (Kojima). To evaluate vertical distribution of zooplankton, vertical stratified tows by VMPS (0.25 m<sup>2</sup> mouth opening, equipped 63  $\mu\text{m}$ ) were made at 3 stations along the WOCE line (Table 4.19.2). VMPS was lowered to desired depth and electrically open/close the net (Terazaki and Tomatsu, 1997). Three net samples were available by one cast. Filtered volume of each net sample was estimated from flowmeter reading. The flowmeter calibration was made at one station during the cruise (Table 4.19.3). All zooplankton sampling data (location, date, time, depth interval, and filtered volume) were summarized in Table 4.19.1-2. Zooplankton samples were preserved with 5% formalin (v/v) or 99.5% ethanol for later analyses in the land laboratory. Additional seawater sampling (1-L) was made from sea surface (bucket) and fluorescence maximum depth (Niskin-rosette) at stations made the plankton net samplings. For monitoring of microplankton fauna/flora, sea surface water samples were collected at interval of twice a day (noon and midnight) along the cruise track (Yamaguchi). All the sea water samples were preserved with 1% glutaraldehyde for the later analyses in the land laboratory.

##### References

- Hama, N., Y. Abe, K. Matsuno, A. Yamaguchi 2019. Study on effect of net mesh size on filtering efficiency and zooplankton sampling efficiency using Quad-NORPAC net. *Bulletin of Faculty of Fisheries, Hokkaido University* **69**: 47–56.
- Terazaki, M., Tomatsu, C., 1997. A vertical multiple opening and closing plankton sampler. *Journal of Advanced Marine Science Technological Society* **3**: 127–132.

Table 4.19.1. Data on plankton samples collected by vertical hauls with Quad-NORPAC net. For each tow, two samples collected by the 63 µm mesh equipped bucket-type cod end were used for on-board experiments.

Station no.	Position		UTC			Length of wire (m)	Angle of wire (°)	Depth estimated by wire angle (m)	Mesh size (µm)	Flowmeter		Estimated volume of water filtered (m <sup>3</sup> )	Bottle no.	
	Lat. (N)	Lon.	Date	Hour	No.					Reading				
3	42	51.42	145	32.37 E	15 July	15:20 - 15:29	152	10	150	335	3690	1401	19.94	N-1
										63	3996	1081	15.27	N-2
					15 July	15:38 - 15:45	50	8	50	335	3690	560	7.97	N-3
										63	3996	391	5.52	N-4
8	42	10.83	146	4.88 E	16 July	13:31 - 13:41	152	10	150	335	3690	1481	21.08	N-5
										63	3996	1003	14.17	N-6
					16 July	13:49 - 13:54	52	20	49	335	3690	518	7.37	N-7
										63	3996	330	4.66	N-8
11	41	43.08	146	26.67 E	17 July	13:10 - 13:19	155	15	150	335	3690	1502	21.37	N-9
										63	3996	882	12.46	N-10
					17 July	13:26 - 13:31	51	12	50	335	3690	409	5.82	N-11
										63	3996	301	4.25	N-12
16	40	38.11	147	1 E	18 July	13:40 - 13:51	156	15	151	335	3690	1480	21.06	N-13
										63	3996	997	14.09	N-14
					18 July	13:58 - 14:03	51	10	50	335	3690	551	7.84	N-15
										63	3996	372	5.26	N-16
20	39	41.58	147	54.82 E	19 July	13:29 - 13:38	156	16	150	335	3690	1522	21.66	N-17
										63	3996	932	13.17	N-18
					19 July	13:46 - 13:52	51	12	50	335	3690	540	7.68	N-19
										63	3996	260	3.67	N-20
24	40	55.74	149	51.92 E	20 July	14:13 - 14:23	151	7	150	335	3690	1485	21.13	N-21
										63	3996	920	13.00	N-22
					20 July	14:29 - 14:34	53	20	50	335	3690	479	6.82	N-23
										63	3996	340	4.80	N-24
27	41	56.3	151	28.67 E	21 July	11:50 - 11:59	151	5	150	335	3690	1428	20.32	N-25
										63	3996	982	13.88	N-26
					21 July	12:05 - 12:10	50	3	50	335	3690	480	6.83	N-27
										63	3996	318	4.49	N-28
30	43	4.88	153	19.45 E	22 July	12:06 - 12:15	160	20	150	335	3690	1574	22.40	N-29
										63	3996	1030	14.55	N-30
					22 July	12:24 - 12:29	51	10	50	335	3690	530	7.54	N-31
										63	3996	380	5.37	N-32
34	45	4.28	156	38.27 E	23 July	14:23 - 14:32	152	10	150	335	3690	1485	21.13	N-33
										63	3996	959	13.55	N-34
					23 July	14:40 - 14:44	50	5	50	335	3690	530	7.54	N-35
										63	3996	390	5.51	N-36
37	45	33.54	159	13.69 E	24 July	13:20 - 13:29	153	12	150	335	3690	1530	21.77	N-37
										63	3996	1023	14.45	N-38
					24 July	13:35 - 13:41	53	18	50	335	3690	615	8.75	N-39
										63	3996	403	5.69	N-40

38	47	0.56	160	1.31 E	25 July	12:54 - 13:03	156	15	151	335	3690	1530	21.77	N-41
										63	3996	905	12.79	N-42
					25 July	13:10 - 13:14	51	12	50	335	3690	530	7.54	N-43
										63	3996	210	2.97	N-44
40	46	59.14	162	14.97 E	26 July	11:06 - 11:15	158	18	150	335	3690	1520	21.63	N-45
										63	3996	940	13.28	N-46
					26 July	11:25 - 11:29	51	12	50	335	3690	571	8.13	N-47
										63	3996	356	5.03	N-48
41	46	59.23	163	22.79 E	27 July	12:00 - 12:10	153	12	150	335	3690	1500	21.35	N-49
										63	3996	1056	14.92	N-50
					27 July	12:17 - 12:22	50	1	50	335	3690	520	7.40	N-51
										63	3996	330	4.66	N-52
44	46	58.31	166	44.83 E	28 July	11:54 - 12:04	167	25	151	335	3690	1680	23.91	N-53
										63	3996	1094	15.46	N-54
					28 July	12:13 - 12:18	52	16	50	335	3690	581	8.27	N-55
										63	3996	355	5.02	N-56
47	46	59.22	168	59.73 E	29 July	13:19 - 13:28	156	15	151	335	3690	1490	21.20	N-57
										63	3996	980	13.85	N-58
					29 July	13:35 - 13:40	51	12	50	335	3690	545	7.76	N-59
										63	3996	375	5.30	N-60
52	46	58.86	169	59.75 E	30 July	13:00 - 13:10	155	14	150	335	3690	1570	22.34	N-61
										63	3996	996	14.07	N-62
					30 July	13:16 - 13:22	51	10	50	335	3690	570	8.11	N-63
										63	3996	382	5.40	N-64
55	47	0.2	172	43.23 E	31 July	12:10 - 12:19	151	5	150	335	3690	1432	20.38	N-65
										63	3996	882	12.46	N-66
					31 July	12:28 - 12:33	52	14	50	335	3690	518	7.37	N-67
										63	3996	296	4.18	N-68
58	46	59.81	176	5.64 E	1 Aug.	12:07 - 12:16	155	14	150	335	3690	1528	21.74	N-69
										63	3996	913	12.90	N-70
					1 Aug.	12:22 - 12:26	50	0	50	335	3690	545	7.76	N-71
										63	3996	320	4.52	N-72
61	47	0.65	179	26.96 E	2 Aug.	12:33 - 12:44	162	22	150	335	3690	1792	25.50	N-73
										63	3996	1306	18.45	N-74
					2 Aug.	12:50 - 12:54	52	15	50	335	3690	692	9.85	N-75
										63	3996	540	7.63	N-76
63	46	59.9	178	18.08 W	3 Aug.	12:52 - 13:02	151	6	150	335	3690	1640	23.34	N-77
										63	3996	1126	15.91	N-78
					3 Aug.	13:09 - 13:14	50	5	50	335	3690	702	9.99	N-79
										63	3996	505	7.14	N-80
66	47	0.14	174	57.24 W	4 Aug.	13:09 - 13:18	150	0	150	335	3690	1410	20.07	N-81
										63	3996	845	11.94	N-82
					4 Aug.	13:26 - 13:32	50	0	50	335	3690	552	7.86	N-83
										63	3996	318	4.49	N-84
69	47	0.5	171	33.55 W	5 Aug.	12:39 - 12:49	150	4	150	335	3690	1595	22.70	N-85
										63	3996	1042	14.72	N-86
					5 Aug.	12:56 - 13:02	51	10	50	335	3690	649	9.24	N-87
										63	3996	460	6.50	N-88
75	46	59.63	164	59.27 W	7 Aug.	11:24 - 11:35	155	14	150	335	3690	1660	23.62	N-89
										63	3996	1100	15.54	N-90
					7 Aug.	11:43 - 11:48	51	10	50	335	3690	600	8.54	N-91
										63	3996	348	4.92	N-92
78	46	59.77	161	28.98 W	8 Aug.	10:20 - 10:30	151	6	150	335	3690	1442	20.52	N-93
										63	3996	990	13.99	N-94
					8 Aug.	10:39 - 10:44	51	10	50	335	3690	574	8.17	N-95
										63	3996	426	6.02	N-96
88	47	0.21	151	24.29 W	11 Aug.	10:33 - 10:43	153	12	150	335	3690	2160	30.74	N-97
										63	3996	1675	23.67	N-98
					11 Aug.	10:52 - 10:57	52	14	50	335	3690	858	12.21	N-99
-	-	-	-	-						63	3996	703	9.93	N-100

84	46	59.51	154	44.93 W	12 Aug.	12:41 - 12:55	158	18	150	335	3690	2258	32.13	N-101
										63	3996	2015	28.47	N-102
					12 Aug.	13:02 - 13:10	52	14	50	335	3690	1076	15.31	N-103
										63	3996	880	12.43	N-104
81	47	0.00	158	8.21 W	13 Aug.	12:34 - 12:43	155	14	150	335	3690	1570	22.34	N-105
										63	3996	1072	15.15	N-106
					13 Aug.	12:49 - 12:53	51	10	50	335	3690	572	8.14	N-107
										63	3996	395	5.58	N-108
91	46	59.38	161	12.76 W	14 Aug.	11:33 - 11:43	155	14	150	335	3690	1680	23.91	N-109
										63	3996	1240	17.52	N-110
					14 Aug.	11:51 - 11:55	53	20	50	335	3690	790	11.24	N-111
										63	3996	426	6.02	N-112
92	46	59.33	167	43.08 W	15 Aug.	11:31 - 11:41	173	30	150	335	3690	1984	28.23	N-113
										63	3996	1725	24.37	N-114
					15 Aug.	11:49 - 11:53	51	10	50	335	3690	759	10.80	N-115
										63	3996	575	8.12	N-116
93	47	00.44	179	36.34 E	17 Aug.	11:33 - 11:42	151	5	150	335	3690	1553	22.10	N-117
										63	3996	988	13.96	N-118
					17 Aug.	11:49 - 11:53	50	8	50	335	3690	550	7.83	N-119
										63	3996	358	5.06	N-120

\*: omitted from mean calculation

Table 4.19.2. Data on plankton samples collected by vertical stratified hauls with VMPS.

Station	Position			Date	UTC		Depth (m) interval	Filtered water (m <sup>3</sup> )	Sample no.
	Lat. (N)	Lon.			Start	End			
38 (daytime)	47-00.56	160-01.31	E	25 July	07:51	7:52	0 - 25	5.64	V-1
					07:51	7:51	25 - 50	5.06	V-2
					07:50	7:51	50 - 75	6.62	V-3
					08:20	08:20	75 - 100	5.26	V-4
					08:19	08:20	100 - 150	11.10	V-5
					08:17	8:19	150 - 250	23.95	V-6
					09:12	9:23	250 - 500	82.17	V-7
					09:04	09:12	500 - 750	72.24	V-8
					07:56	09:04	750 - 1000	66.00	V-9
					06:36	6:46	1000 - 1500	113.9	V-10
					06:28	06:36	1500 - 2000	106.3	V-11
					06:06	6:28	2000 - 3000	223.3	V-12
62 (daytime)	46-59.15	179-25.58	W	3 Aug.	02:03	2:04	0 - 25	6.42	V-13
					02:03	02:03	25 - 50	5.45	V-14
					02:02	02:03	50 - 75	7.59	V-15
					02:29	3:29	75 - 100	5.45	V-16
					02:28	3:29	100 - 150	10.71	V-17
					02:26	2:28	150 - 250	25.70	V-18
					03:19	3:29	250 - 500	85.86	V-19
					03:09	3:19	500 - 750	110.20	V-20
					03:03	3:09	750 - 1000	42.45	V-21
					04:59	5:15	1000 - 2000	199.0	V-22
					04:37	4:59	2000 - 3000	256.0	V-23
					79 (daytime)	46-59.66	160-21.63	W	8 Aug.
19:56	19:57	25 - 50	5.60	V-25					
19:56	19:56	50 - 75	5.38	V-26					
20:24	20:24	75 - 100	8.19	V-27					
20:24	20:24	100 - 150	11.21	V-28					
20:21	20:24	150 - 250	27.80	V-29					
21:13	21:17	250 - 500	63.79	V-30					
21:09	21:13	500 - 750	60.34	V-31					
21:02	21:09	750 - 1000	77.16	V-32					

## 4.20 Radiocesium

August 25, 2021

Yuichiro Kumamoto

Japan Agency for Marine-Earth Science and Technology (JAMSTEC)

### (1) Personnel

Yuichiro Kumamoto JAMSTEC

### (2) Objective

In order to investigate the water circulation and ventilation process in the northern North Pacific Ocean, seawater samples were collected for measurements of radiocesium ( $^{137}\text{Cs}$  and  $^{134}\text{Cs}$ ), which was mainly released from the global fallout in the 1950s and 1960s and the Fukushima accident in 2011.

### (3) Sample collection

The sampling stations and number of samples are summarized in Table 4.20.1. The total 48 seawater samples for radiocesium measurement were collected at 12 stations from surface water that pumped up from about 4 m depth from the sea surface. The seawater sample was collected into four 20-L plastic containers (80 L each) after two time washing.

Table 4.20.1 Sampling stations and number of samples for radiocesium.

	Station	Latitude End time	Longitude End time	Sampling Date (UTC)	Sampling Time (UTC)	Sampling Lab.
1	001	42-58.37N	145-27.00E	2021/07/15	06:41-07:06	Wet Lab. 2
2	010	41-52.41N	146-09.16E	2021/07/17	06:15-06:47	Wet Lab. 2
3	019	39-57.22N	147-42.12E	2021/07/19	06:59-07:26	Wet Lab. 2
4	026	41-33.66N	150-53.03E	2021/07/21	04:35-05:06	Wet Lab. 2
5	029	42-40.48N	152-42.62E	2021/07/22	04:12-04:41	Wet Lab. 2
6	032	44-05.16N	155-00.94E	2021/07/23	02:16-02:46	Wet Lab. 2
7	038	47-01.07N	160-01.10E	2021/07/25	04:08-04:41	Wet Lab. 2
8	050	46-59.06N	169-34.48E	2021/07/30	02:21-02:55	Wet Lab. 2
9	062	46-59.14N	179-25.57W	2021/08/03	01:30-01:51	Wet Lab. 1
10	071	46-59.43N	169-20.66W	2021/08/06	01:36-01:56	Wet Lab. 1
11	081	46-59.94N	158-08.39W	2021/08/13	14:08-14:28	Wet Lab. 1
12	089	46-59.32N	150-17.62W	2021/08/11	00:46-01:05	Wet Lab. 1

### (4) Sample preparation and measurements

In our laboratory on shore, radiocesium in the seawater samples will be concentrated using ammonium phosphomolybdate (AMP) that forms insoluble compound with cesium. The radiocesium in AMP will be measured using Ge  $\gamma$ -ray spectrometers.

### (5) Data archives

The data obtained in this cruise will be submitted to the Data Management Group of JAMSTEC and will be opened to the public via “Data Research System for Whole Cruise Information in JAMSTEC (DARWIN)” in the JAMSTEC web site.

## 4.21 XCTD

### (1) Personnel

Shinya Kouketsu	JAMSTEC: Principal investigator
Katsuro Katsumata	JAMSTEC
Masanori Murakami	Nippon Marine Enterprises, Ltd (NME)
Wataru Tokunaga	NME
Fumine Okada	NME

Yoichi Inoue MIRAI crew

## (2) Objectives

To obtain vertical profiles of sea water temperature and salinity (calculated by the function of temperature, pressure (depth), and conductivity).

## (3) Parameters

Parameters of XCTD-4N (eXpendable Conductivity, Temperature & Depth profiler; Tsurumi-Seiki Co.) are as follows;

Parameter	Range	Accuracy
Conductivity	0 ~ 60 [mS/cm]	+/- 0.03 [mS/cm]
Temperature	-2 ~ 35 [deg-C]	+/- 0.02 [deg-C]
Depth	0 ~ 1850[m]	5 [m] or 2 [%] (whichever is greater)

## (4) Methods

We observed the vertical profiles of the sea water temperature and conductivity measured by XCTD system. We launched 10 XCTD-4N probes by using the automatic launcher, MK-150N digital converter (Tsurumi-Seiki Co.) and AL-12B software (Ver.1.6.3; Tsurumi-Seiki Co.). The summary of XCTD observations were shown in Table 4.21.1.

## (5) Calibration

At station 90, three XCTD probes were deployed at the moment the CTD sensor reached approximately 1000, 2000, and 3000 dbar downcast. These side-by-side casts provide data for calibrating XCTD with more accurate CTD data (Uchida *et al.*, 2011).

After smoothing and correcting the conductivity temporal delay, the comparison of fall rate from the side-by-side casts shows differences of about 5 to 10 m, which are not however systematic (Fig.4.21.1). We therefore decided to apply no fall rate bias correction. The temperature bias is of order of 0.01°C (Fig.4.21.2). We subtracted 0.0075°C (average of difference below 1000 dbar) from the measured temperature of XCTD. After the temperature correction, TS-diagram shows a salinity bias of XCTD compared to CTD (not yet corrected to bottle salinity though) of 0.007 PSU (XCTD salinity is lower) for temperature between 1.8 to 2.3°C. We added this bias to the measured salinity of XCTD.

## (6) Data archives

These data obtained in this cruise will be submitted to the Data Management Group of JAMSTEC, and will be opened to the public via “Data Research System for Whole Cruise Information in JAMSTEC (DARWIN)” in JAMSTEC web site.

Table 4.21.1 Summary of XCTD observation and launching log

No.	Station No.	Date [YYYY/MM/DD]	Time [hh:mm]	Latitude [deg]	Longitude [deg]	Depth [m]	SST [deg-C]	SSS [PSU]	Probe S/N
1	80	2021/08/09	04:25	46-59.2439N	159-15.3185W	5192	13.275	32.454	21032650
2	82	2021/08/09	11:53	47-00.4223N	157-01.2621W	5230	13.574	32.337	21032653
3	83	2021/08/09	15:40	46-59.2935N	155-51.0965W	5250	13.572	32.342	21032654
4	84	2021/08/09	19:18	46-59.6009N	154-44.9465W	5205	14.022	32.309	21032656
5	85	2021/08/09	23:02	46-59.8547N	153-37.0406W	5228	14.621	32.253	21032655
6	86	2021/08/10	02:36	46-59.2626N	152-31.7069W	5189	14.501	32.216	21032658
7	87	2021/08/10	04:29	47-00.0418N	152-00.0136W	5138	14.285	32.272	21032657
8	90	2021/08/10	15:25	46-59.3386N	149-08.5504W	5059	14.668	32.181	21032659
9	90	2021/08/10	15:40	46-59.3488N	149-08.6151W	5058	14.686	32.182	21032661
10	90	2021/08/10	15:53	46-59.3946N	149-08.6311W	5061	14.674	32.183	21032660

Depth: The depth of water [m]

SST: Sea Surface Temperature [deg-C] measured by TSG (ThermoSalinoGraph).

SSS: Sea Surface Salinity [PSU] measured by TSG.

References:

Uchida, H., K. Shimada, T. Kawano, 2011, A method for data processing to obtain high-quality XCTD data, *Journal of Atmospheric and Oceanic Technology*, **28**, 816 – 826, doi:10.1175/2011JTECHO795.1

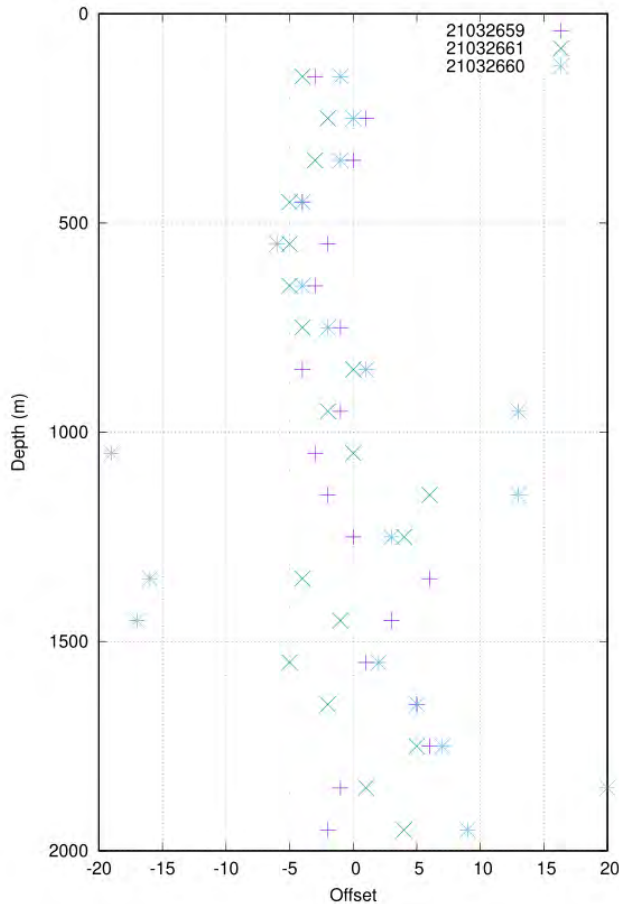


Fig.4.21.1: Offset in meters needed to maximize correlation between the band-pass-filtered XCTD and CTD temperature in side-by-side observations.

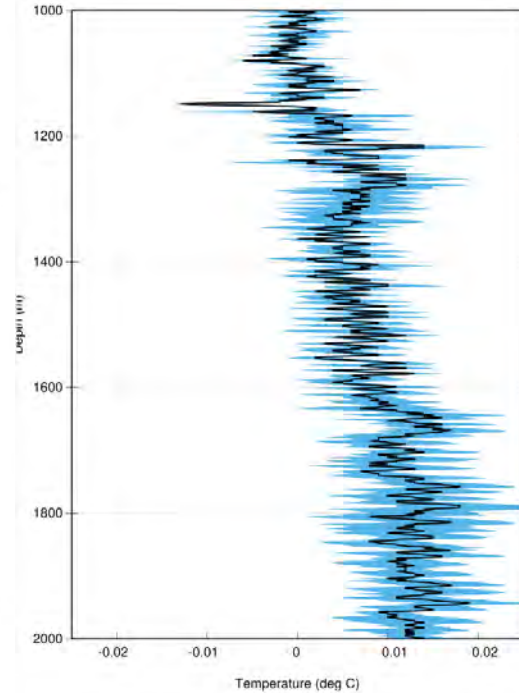


Fig.4.21.2: Mean (black) and standard deviation (blue) of difference between XCTD and CTD in temperature for 3 side-by-side observations.

## 4.22 In situ calibration of the Compact-TDs

August 10, 2021

### (1) Personnel

Hiroshi Uchida                      JAMSTEC

### (2) Objective

The objective of this study is to calibrate the Compact-TDs by comparing with the CTD data.

### (3) Instruments and method

The Compact-TD (model ATD-HR-Z23, JFE Advantech Co. Ltd., Nishinomiya, Hyogo, Japan) is self-contained temperature and pressure recorder. In situ calibration of eight Compact-TDs were conducted at station 55 by attaching the Compact-TDs to the CTD/water sampling frame to compare with the shipboard CTD temperature and pressure data. Atmospheric pressure data were also used to

compare with the data obtained on deck just before and after the CTD cast.

The Compact-TDs and CTD data were obtained at stops of the winch at 500-dbar intervals during the down and up cast. The Compact-TDs and CTD data at least 30 seconds after the stop were averaged over about 5 seconds and were used for the in situ calibration of the Compact-TDs (Fig. 4.22.1).

The pressure sensor of the Compact-TD was calibrated as follows:

$$P = c_0 + c_1 N + c_2 N^2$$

where P is the calibrated pressure (in dbar), N is the raw data (N-value) and  $c_0$ - $c_2$  are the calibration coefficients. The calibration coefficients were determined by a least square technique to minimize the deviation from the CTD pressure data. The calibration coefficients are listed in Table 4.22.1.

The temperature sensor of the Compact-TD was calibrated assuming that the difference is derived from a pressure dependency and time drift of the temperature sensor as follows:

$$T_{cor} = T - (d_0 + d_1 P)$$

where  $T_{cor}$  is calibrated temperature (in degrees C), T is the temperature before calibration, P is pressure (in dbar), and  $d_0$ - $d_1$  are the calibration coefficients. The calibration coefficients were determined by a least square technique to minimize the deviation from the CTD temperature data. The calibration coefficients are listed in Table 4.22.1.

The results of the in situ calibration are shown in Fig. 4.22.2.

#### (4) Data archive

These obtained data will be submitted to JAMSTEC Data Management Group (DMG).

Table 4.22.1. Calibration coefficients for the pressure and temperature sensor of the Compact-TDs.

Serial no. of TD	c0	c1	c2	d0	d1
198	-241.302	0.121712	-7.89780e-9	-1.38856e-2	2.18414e-6
199	-231.265	0.122689	-7.34542e-9	-6.66520e-3	1.25332e-6
200	-236.707	0.122602	-8.81759e-9	-1.62970e-2	4.01570e-6
201	-234.370	0.122997	-1.05126e-8	-1.51569e-2	3.63960e-6
202	-227.061	0.122025	-8.75352e-9	-2.00755e-2	3.30981e-6
203	-235.751	0.123112	-9.19141e-9	-6.45791e-3	2.07283e-6
204	-250.553	0.122874	-6.54361e-9	-1.09835e-2	3.11492e-6
205	-236.800	0.121333	-4.38125e-9	-1.11566e-2	4.20012e-6

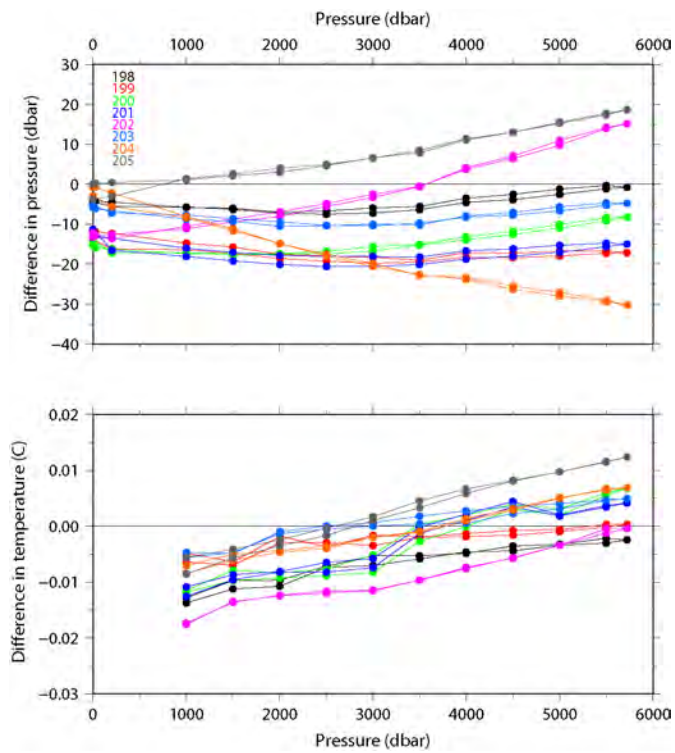


Figure 4.22.1. Difference in pressure and temperature between the eight Compact-TDs and CTD.

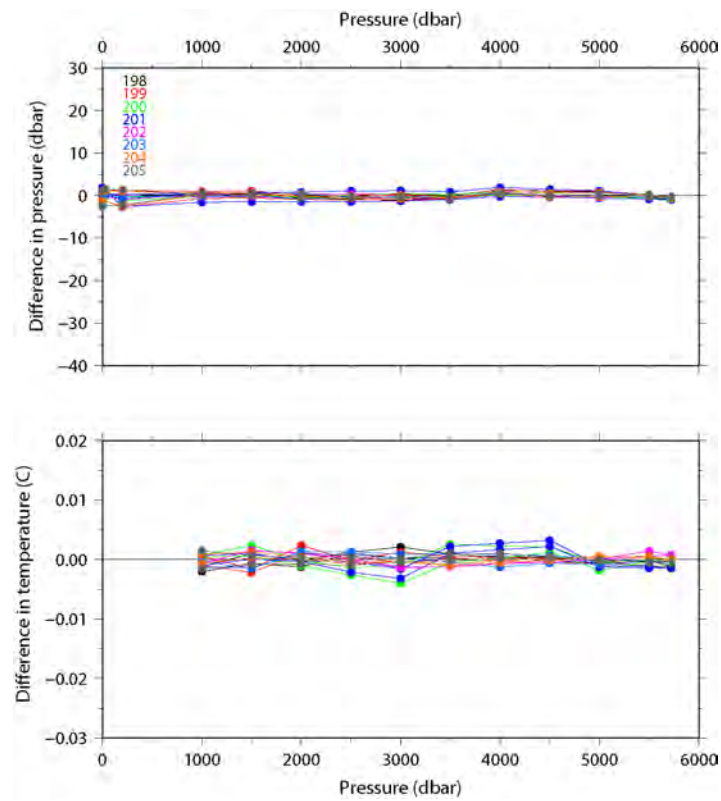


Figure 4.22.2. Same as Fig. 4.22.1, but for after the in situ calibration.

## 5. Float, Drifter and Mooring

### 5.1 Core/Deep Argo Floats

#### (1) Personnel

Shigeki Hosoda	JAMSTEC:Principal investigator
Kanako Sato	JAMSTEC
Mizue Hirano	JAMSTEC
Rei Ito	MWJ
Ko Morita	MWJ
Takayuki Hashimukai	MWJ

#### (2) Objective

The research objective is to clarify the mechanisms of climate and oceanic environment variability, and to understand changes of earth system through estimations of heat and material transports, within the framework of the Argo programme. To achieve the objective, two core Argo floats and one deep Argo float are deployed to carry out automatically measurements of long-term temperature, salinity, and dissolved oxygen variations in the North Pacific Ocean where the spatial density of the Argo floats is sparse due to a lack of float deployment opportunities for the Core Argo mission. The deep Argo float is deployed in the central North Pacific where the region is considerably at the upwelling area of the global deep ocean circulation and an enhancement of deep ocean observations is strongly required. Data accumulated from Argo floats also contribute to improve long-term forecasts of climate changes through data assimilation systems.

#### (3) Parameters

- Core Argo float :Water temperature, salinity and pressure.
- Deep Argo float :Water temperature, salinity, pressure and dissolved oxygen.

#### (4) Method

We launched APEX and Deep APEX floats manufactured by Teledyne Webb Research. Those floats are equipped with CTD sensor manufactured by Sea-Bird Electronics Inc. The float drifts at a depth of 1000dbar or 4500dbar (called the parking depth) during waiting measurement, then goes upward from a depth of 2000dbar or 5500dbar to the sea surface every 1-10 days. During the ascent, physical values are measured following depth table. During surfacing for approximately half an hour, the float sends all measured data to the land via the Iridium RUDICS telecommunication system. The lifetime of floats is expected to be about four-eight years. The status of float and its launching information is shown in Table 5.1. 1.

Table 5.1. 1 Specifications of floats and their launching positions

Float Type	Core	APEX float manufactured by Teledyne Webb Research.
CTD sensor	Deep	Deep APEX float manufactured by Teledyne Webb Research.
	Core	SBE41 manufactured by Sea-Bird Electronics Inc.
Dissolved oxygen sensor	Deep	SBE61 manufactured by Sea-Bird Electronics Inc.
	Core	AROD-FT manufactured by JFE Advantech Co., Ltd.
Cycle	Core	every 1-10 day (approximately 30minutes at the sea surface)
	Deep	every 2-10 day (approximately 30minutes at the sea surface)
Iridium transmit type	Deep	Router-Based Unrestricted Digital Internetworking Connectivity
	Core	Solutions (RUDICS)
Target Parking Pressure	Core	1000 dbar
Sampling layers	Deep	4500 dbar
	Core	2dbar interval from 2000 dbar to surface (approximately 1000 levels)

Deep physical parameters(water temperature, salinity, pressure)  
2dbar interval from 2000 dbar to surface (approximately 1000 levels) .

Biogeochemical parameter(dissolved oxygen)  
interval 50dbar from 5500 dbar to 2000 dbar  
interval 20dbar from 1980 dbar to 1000 dbar  
interval 10dbar from 990 dbar to 400 dbar  
interval 2dbar from 398 dbar to surface

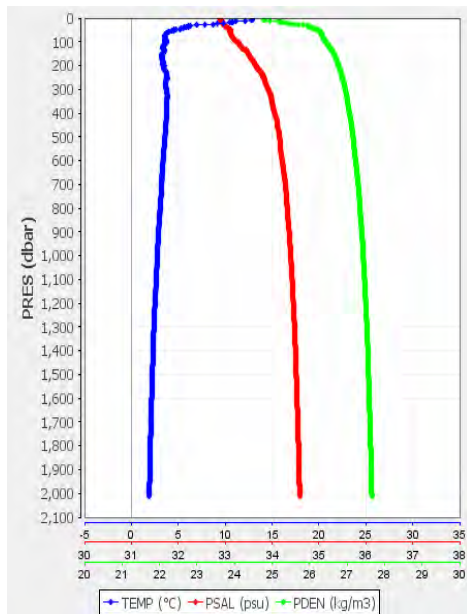
Table 5.1.2 Floats launching positions

Float S/N	WMO ID	Date and Time of Launch (UTC)	Location of Launch	Station
9304	2903662	2021/7/28 0:57	46° 59.83' N 164° 31.09'E	042
9305	2903663	2021/7/30 17:36	46° 59.31'N 170° 00.67'E	052
053	4902990	2021/8/3 1:30	46° 58.87'N 179°25.44' W	062

**(5) Data archive**

The Argo float data will be provided conducting the real-time quality control within 24 hours following the procedure decided by Argo data management team. Then the delayed mode quality control will be conducted within 6 months ~ 1 years, to satisfy their data accuracy for climate research use. Those quality-controlled data are freely available via internet and utilized for not only research but also weather forecasts and any other variable use through internet. Global Data Assembly Center (GDAC: <http://www.usgodae.org/argo/argo.html>, <http://www.coriolis.eu.org/>), Global Telecommunication System (GTS).

(a) S/N 9304



(b) S/N 9305

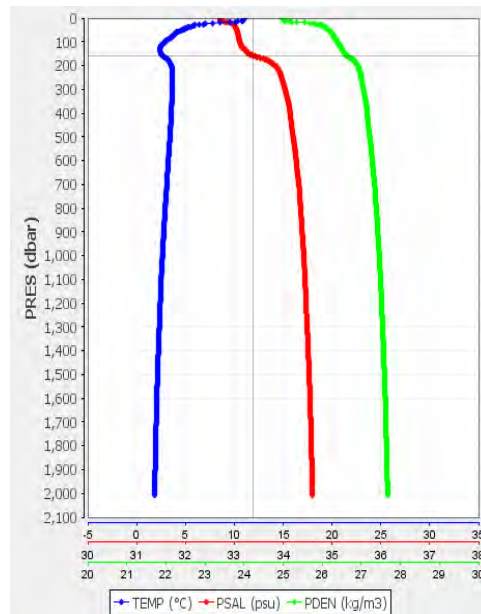


Fig. 5.1.1 (a and b). Vertical temperature, salinity and density profiles of their first measurements for two Core Argo floats (SN9304 and SN9305). Blue, red and light green lines show temperature, salinity and density profiles.

(c) S/N053

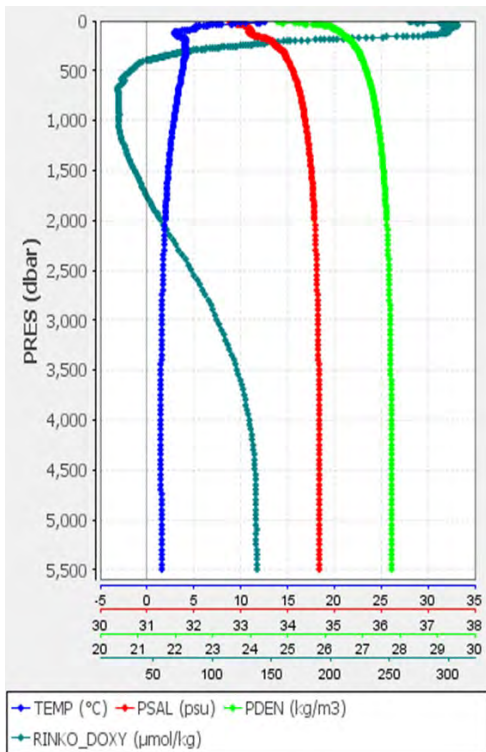


Fig. 5.1.2 (c). Vertical temperature, salinity, density and dissolved oxygen profile of third measurements for Deep Argo float (SN053). Blue and red lines show temperature and salinity profiles. And light green and dark green lines show density and dissolved oxygen profiles.

## 5.2 Deep Argo float

### (1) Personnel

Yusuke Sasaki	AORI (Principal investigator)
Ichiro Yasuda	AORI
Ryosuke Oyabu	AORI
Taku Niinuma	AORI

### (2) Objective

Deep Argo float equipped with microstructure probes was deployed to measure fine scale temperature, salinity and microstructure shear in horizontal velocity and temperature for a long period (~ 1year) while tracking subsurface water masses. The purpose of this study is to explore the relationship between vertical mixing and water mass formation in the western North Pacific Ocean.

### (3) Instruments and method

We deployed one Deep Argo float (Deep Ninja) manufactured by Tsurumi Seiki Co., Ltd. This Deep Argo float is equipped with a Sea-Bird Electronics (SBE) 41CP CTD sensor and microstructure probes manufactured by Rockland Scientific International (RSI) Inc. The RSI system records data from microstructure shear probe, fast thermistor temperature probe (FP07) and two accelerometers. The float drifts at the parking depth for 9 days. After drift, it sinks to the predetermined depth (which is called ‘max depth’), then ascends from the max depth to the sea surface every 10 days. For the first dive, the parking depth was set to 175dbar, and the max depth was set to 1000dbar. We plan to change these parameters depending on how the float is drifted. During the ascent, temperature, salinity, and pressure measurements are obtained from the CTD sensor at a 2dbar interval. Microstructure system is turned on when the float is rising, and microstructure shear and temperature profiles are measured at a 512Hz interval.

While at the surface, the float sends the measured CTD profile (temperature, conductivity and pressure) and its location to the land via the Iridium communication. Microstructure data are internally recorded in the internal recorder. We intend to download these microstructure data from the instruments after recovery, which is planned on another cruise in April 2022.

Table 5.2-1 Status of Deep Argo float and launch information

#### Status of Deep Argo float

Float type		Deep Ninja Tsurumi Seiki Co., Ltd		
CTD sensor		SBE41CP manufactured by Sea-Bird Electronics Inc.		
Microstructure probe S/N	Shear	M2249		
	Fast-response thermistor (FP07)	T2165		
Cycle		10 days		
Iridium transmit type		Short Burst Data Service (SBD)		
Parking pressure		175 dbar		
Max pressure		1000 dbar		
Sampling Interval for CTD profiles		2 dbar interval		

#### Launch information

Float S/N	Date	Time (UTC)	Lat	Lon
4317	2021/7/25	3:44:30	47-00.92N	160-01.35E

## 5.3 Subsurface Drifter

### (1) Personnel

Yusuke Sasaki	AORI (Principal investigator)
Ichiro Yasuda	AORI
Taku Niinuma	AORI
Ryosuke Oyabu	AORI

### (2) Objective

The objective of this study is to quantify the subsurface horizontal diffusivity by tracking the separation of two drifters.

### (3) Instruments and method

We deployed two drifters manufactured by Zeni Lite Buoy Co., Ltd. The drifters consist of a surface buoy and a holey-sock drogue attached by 150m-long tether. The drogues were deployed within minutes after the buoys were released. The details of the launch information are shown in table 5.3-1. The drifters report their location to the land via the Globalstar satellites every 30 minutes. We plan to estimate the subsurface horizontal diffusivity by analyzing the temporal variation in horizontal dispersion of the two drifters.

Table 5.3-1: Launch Information

Drifter S/N	Deployment of buoy				Deployment of drogue			
	Date	Time (UTC)	Lat	Lon	Date	Time (UTC)	Lat	Lon
0-4413666	2021/7/25	4:08	47-01.45 N	160-01.44 E	2021/7/25	4:13	47-01.60 N	160-01.47 E
0-4413723	2021/7/25	4:19	47-01.76 N	160-01.49 E	2021/7/25	4:26	47-01.96 N	160-01.52 E

## 6. Notice on Using

This cruise report is a preliminary documentation as of the end of cruise.

This report is not necessarily corrected even if there is any inaccurate description (i.e. taxonomic classifications). This report is subject to be revised without notice. Some data on this report may be raw or unprocessed. If you are going to use or refer the data on this report, it is recommended to ask the Chief Scientist for latest status.

Users of information on this report are requested to submit Publication Report to JAMSTEC.

<http://www.godac.jamstec.go.jp/darwin/explain/1/e#report>